Photonic Generation of Millimeter-Waves Using Two Cascaded Electro-Absorption Modulators in Radio-over-Fiber Systems

Liwen Wu

A Thesis

In the Department

of

Electrical and Computer Engineering

Presented in Partial Fulfillment of the Requirements

For the Degree of Master of Applied Science at

Concordia University

Montréal, Québec, Canada

August 2010

Your file Votre référence
ISBN: 978-0-494-71068-5
Our file Notre référence
ISBN: 978-0-494-71068-5

ABSTRACT

Photonic Generation of Millimeter-Waves Using Two Cascaded Electro-Absorption Modulators in Radio-over-Fiber Systems

Liwen Wu

The development of wireless communication services requires broader access bandwidth. To meet this requirement, unlicensed millimeter wave (mm-wave) band has been considered as a potential carrier for the next generation wireless communications. However, due to high attenuation loss in mm-wave signal transmission, the number of the picocell base station (BS) should be increased in the coverage area. Radio over fiber (RoF) transport scheme is a good option to face the challenge of mm-wave wireless distribution, because it takes advantages of long transmission distance, large bandwidth and immunity to electromagnetic interference.

In RoF technique, optical mm-wave signal generation is one of the crucial issues. There are two major schemes to generate optical mm-wave signals, optical heterodyning technique and optical frequency multiplication (OFM) technique, in which OFM technique can provide simpler BS configuration. One of the most popular OFM techniques is optical harmonic generation using optical external modulators. There are mainly two options of external modulator: one is Mach-Zehnder Modulator (MZM) and the other is Electro-Absorption Modulator (EAM).

The objective of this thesis is to propose a novel photonic frequency doubling and quadrupling technique for the generation of mm-wave signal using two cascaded EAMs. The two cascaded EAMs driven by a low frequency radio frequency (RF) signal and the phase shift between the two EAMs is 180 degree. Theory of techniques using two

cascaded EAMs with identical characteristics and two cascaded EAMs with different characteristics is investigated and verified by simulation based on VPI Transmission Maker. Good agreement is achieved between theory and simulation. It is shown that power of doubling and quadrupling signal is increasing with RF modulation index, and bias voltages of EAMs also have a great impact on the performance of the system. It is found that by using cascaded EAMs with identical characteristics, odd-order optical harmonics are perfectly suppressed while even-order harmonics are maximized, and as a result high quality frequency doubling and quadrupling signals can be generated; by using cascaded EAMs with different characteristics, good system performance still can be achieve when phase shift, RF modulation voltage and bias voltages are optimized. Power fading induced by fiber chromatic dispersions is also investigated and an optical filter is adopted in order to make the system immune to chromatic dispersions at frequency quadrupling.

Experiment is also carried out to verify the concept of the proposed technique. A low cost electro-absorption modulator integrated laser (EML) is used in experiment to achieve a cost-effective system. Good quality doubling signal and quadrupling signal are generated while noise level is reasonable. It suggests that the proposed technique is efficient for mm-wave generation using frequency doubling or quadrupling.

Acknowledgements

First of all, I would like to express my sincere gratitude to my supervisor Dr. X. Zhang for the opportunity he provided to me and for his considerate guidance, patient advice and financial support for me to finish this thesis.

I am really grateful to Bouchaib Hraimel and Mohmoud Mohamed, for their valuable time and help in my research and their suggestions on this thesis.

I have sincere appreciation to the Fonds de recherché sur la nature et les technologies (FQRNT), Quebec, Canada for supporting this research project.

Last but not least, I am very grateful to my father, mother and sister for their love and support throughout my life.

Table of Contents

List of Figures

List of Tables

List of Acronyms

AP	Access Point
BB	Baseband
BS	Base Station
BTS	Base Transceiver Station
CS	Central Station
CW	Continuous Wave
dB	Decibel
dBm	The measured power referenced to one milliwatt
DC	Direct Current
DCF	Dispersion Compensating Fiber
DWDM	Dense Wavelength Division Multiplexing
DPSK	Differential Phase Shift Keying
EAM	Electro-Absorption Modulator
EDFA	Erbium Doped Fiber Amplifier
EMI	Electromagnetic Interference
EML	Electro-Absorption Modulator Integrated Laser
E/O	Electrical to Optical Converter
EVM	Error Vector Magnitude
FBG	Fibre Bragg Grating
FCC	Federal Communications Commission
GVD	Group Velocity Dispersion
HD	Harmonics Distortions

IF	Intermediate Frequency
IMD	Intermodulation Distortion
IM/DD	Intensity Modulation/Direct-Detection
LAN	Local Access Network
LD	Laser Diode
LO	Local Oscillator
MAC	Multiple Access
MATB	Maximum transmission bias
MB	Multi-Band
MITB	Minimum transmission bias
MMF	Multi Mode Fiber
MZM	Mach-Zehnder Modulator
MZI	Mach-Zehnder interferometer
OCS	Optical Carrier Suppression
O/E	Optical to Electrical Converter
ODSB	Optical Double Side Band
OFDM	Orthogonal Frequency Division Multiplexing
OFM	Optical Frequency Multiplication
OIL	Optical Injection Locking
OPLL	Optical Phase Locked Loops
OSSB	Optical Single Side Band
OSA	Optical Spectrum Analyzer
OTDM	Optical Time Division Multiplexing

PD	Photo Detector
PHY	Physical Layer
PM	Phase Modulator
QB	Quadrature Bias
QoS	Quality of Service
RAU	Remote Antenna Units
RF	Radio Frequency
RHD	Remote Heterodyne Detection
RIN	Relative Intensity Noise
RoF	Radio over Fiber
RSA	RF Spectrum Analyzer
SCM	Subcarrier Modulation
SMF	Single Mode Fiber
SNR	Signal to Noise Ratio
TLS	Tunable Laser Source
UWB	Ultra wideband
WLAN	Wireless Access Networks

List of Principal Symbols

λ	Wavelength (nm)
ω	Frequency (TH_z)
α	Fiber loss (dB/km)
β_2	GVD coefficient (ps^2/km)
$T(\cdot)$	Transfer function of EAM
V_b	Bias voltage
f	RF frequency
V_0	RF modulation voltage
m	Modulation index
$\Re$	Responsivity
P_{out}	Output power
P_{in}	Input power
Ω	Radio frequency carrier
E_{in}	Average optical electric field input
E_{out}	Output optical electric field
ω	Optical angular frequency
c	Speed of light
D	Chromatic dispersion
L	Fiber length
$\Delta\omega$	RF angular frequency
$I(\ )$	Bessel function of the first kind
I	Received photocurrent

V_{rf}	RF driving voltage
ϕ	Phase shift

Chapter 1

Introduction

1.1 Preface

The availability of traditional wireless local access network (LAN) frequencies in the 2.4 and 5 GHz bands and the price reduction of radio technology result in wireless networks service expanding at an unprecedented pace, which causes severe congestion at those frequencies. Since too many systems in the same space (frequency), it is difficult to achieve very high data rate such as 100 Mb/s and beyond. Moreover, the traditional wireless networks are easily and cheaply intercepted, which is not good for security services. Fortunately, unlicensed millimeter-wave (mm-wave) band (57-64 GHz), which offers much more bandwidth, is available world-wide and with better efficiency and security than traditional wireless LAN frequencies. In addition, the antenna systems can be millimeter size since higher frequencies mean shorter wavelengths [35]. Therefore, mm-wave is one of good choices for future wireless communications.

When mm-wave band is used for future wireless communications, there are three transmission options: mm-wave over air, mm-wave over coaxial cable and mm-wave over fiber. Why choose mm-wave over fiber? mm-wave over air transmission is limited to tens of meter due to high transmission loss; mm-wave over coaxial cable transmission is limited by the coaxial cable bandwidth and high cost as well as high transmission loss. It is well-known that optical fiber has much broader bandwidth, low loss and very low cost. Moreover, broad-band wireless distribution based on mm-wave over fiber enables

transparent delivery of mm-wave radio signals to remote base stations without interferences existing in other two distribution methods [2].

Key improvements needed in communication system are capacity, bandwidth, security, mobility and flexibility. Optical fiber technology can provide tremendous bandwidth, but it does not support user mobility or flexible system reconfiguration. Wireless communication systems using traditional RF and microwave frequencies can provide user's mobility, but they do not support high data rates and security. However, when these two technologies are combined together, the bandwidth and mobility can be achieved at the same time.

To better access and manage networks, a central station (CS) will control a number of base stations (BSs) where mm-wave antennas radiate mm-wave signals to users. The connection between a CS and BSs can be realized with fiber ring, fiber tree or fiber star topologies that are used to distribute mm-wave wireless signals to remote base stations. However, the main drawback of mm-wave band is that the mm-wave wireless communications suffer from high transmission loss due to atmospheric conditions by GHz frequency. As a result, to maintain the Quality of Service (QoS), the distance between the BSs should be reduced and a larger number of the BSs are needed in mm-wireless networks than in traditional wireless LAN networks. Therefore, another reason why we choose mm-wave over fiber is that mm-wave over fiber can provide a system configuration with simple, small and cheap BSs.

Radio over fiber (RoF) system was first proposed in 1990 by A. J. Cooper [44]. In such systems, the radio signal is generated at a CS before distributed through a fiber link to a number of remote antenna base stations for wireless distribution. A basic RoF system

is shown in Fig. 1.1. When the signal is transmitted between the CS and the BS, electrical-to-optical (E/O) and optical-to-electrical (O/E) converters are needed before and after the signal distributed over an optical fiber, respectively.

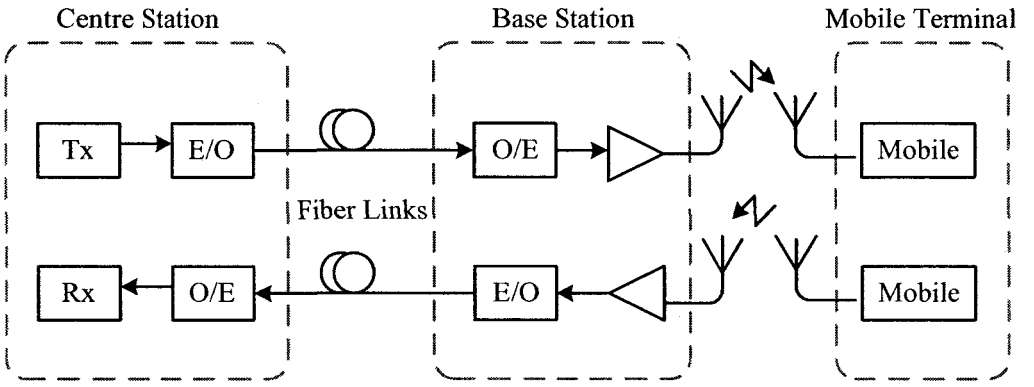

Figure 1.1 Basic RoF system

RoF technique has become a promising solution of mm-wave transmission nowadays thanks to its feasibility of the broadband wireless access network by facilitating the implementation of simple and compact BSs. This could be possible by generating a radio signal at the CS and delivering it to the simplified BSs. Complicated signal processing such as modulation, demodulation, up-conversion, coding, routing can be performed at the CS, while the BS simply consists by O/E and E/O converters, RF amplifiers and an antenna. In such transport scheme, the transmission distance between the CS and mobile users can be largely extended, compared to the direct RF free-space or coaxial cable transport scheme [45]. There are many possible applications for RoF technique. For instance, RoF technique can be used in the backbone of both outdoor and indoor wireless networks. Fig. 1.2 shows both indoor and outdoor RoF systems where the CS (the base transceiver station (BTS) or access point (AP)) and the BS (the remote antenna units (RAU)) are communicated through the single-mode fiber (SMF).

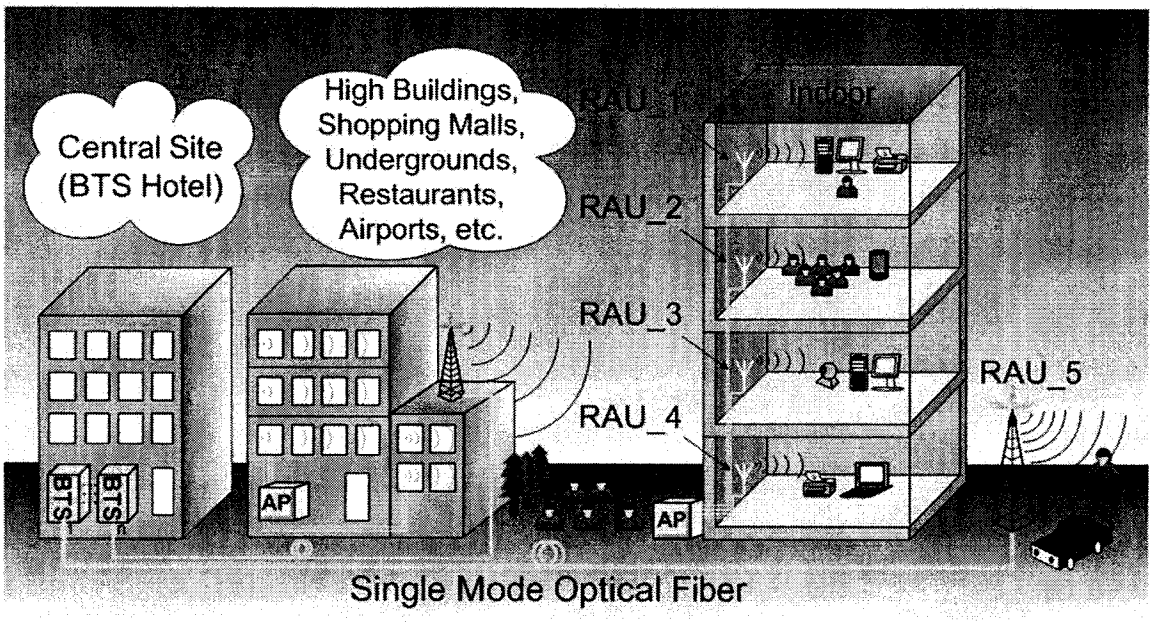

Figure 1.2 Application of the RoF technique in indoor and outdoor wireless networks [46].

1.2 Review of Related Technologies

With the rapid development of wireless communications, the techniques of mm-wave frequency range of 57-64GHz has attracted a growing interest in recent years because of limited bandwidth and spectral congestion at low microwave frequencies. When it comes to the transmission of mm-wave signals, RoF system is considered as a broad-bandwidth and cost-effective solution [1, 2]. As a result, how to generate mm-wave signals over RoF system has become an attractive topic recently. A number of techniques for mm-wave signals generation have been proposed, such as optical carrier suppression [2, 5, 4, 10, 11, 41], optical frequency multiplication (OFM) [2-5, 7, 10, 11, 18, 41], optical heterodyne detection with optical interleaving [1, 12], frequency up-conversions using optical amplifier [6, 9] and four-wave mixing [13-15], and so on.

The common objective of all techniques of mm-wave generation is to provide high frequency mm-wave signal at the BS by applying low frequency driving RF at the CS. One of the key issues of RoF system design is cost efficiency which means to maintain the required QoS by using lowest cost equipments. In industry, RF electrical components and equipment with frequency response of higher than 26 GHz are much more expensive than those of below 26 GHz. So if mm-wave signal can be generated by using RF driving signal lower than 26 GHz, the cost of system will be largely reduced.

One of the most cost-effective options for the mm-wave generation is to use external optical modulators (single one or cascaded ones) driven by a low RF signal to generate high-order optical harmonic sidebands [2-5, 7, 10, 11, 18, 41], which is called optical harmonic generation technique or OFM technique. An external optical modulator restrains the light and allows the amount of light passed to vary from some maximum amount to some minimum amount according to its transfer function. When the light source is injected into the external modulator driven by an RF signal at frequency f, the harmonic sidebands will be generated at $\pm f, \pm 2f, ..., \pm nf$ relative to the optical carrier. At the photodetector, these optical sidebands will beat with each other and generate RF signals at $f, 2f, ..., nf$. In this way, the mm-wave signals doubling, quadrupling or even sextupling of the low driving RF signal can be produced. For example, RF power at $2f$ (frequency doubling of f) mainly consists of two parts, beating between the second-order optical sideband and the optical carrier, and the other beating between the two first-order optical sidebands; RF power at $4f$ (frequency quadrupling of f) is also constituted by two parts, beating between the two second-order optical sidebands, and the other beating

between the forth-order optical sideband and the optical carrier. Therefore, to achieve high quality desired mm-wave signal, optical sidebands contributing in the generation of the mm-wave signals should be maximized while the undesired optical sidebands should be minimized. There are two commonly used types of external optical modulators: the Electro Absorption modulator (EAM) and the Mach-Zehnder modulator (MZM). The normalized power transfer functions for the two popular external optical modulators are shown in Fig. 1.3 (a) and (b), respectively.

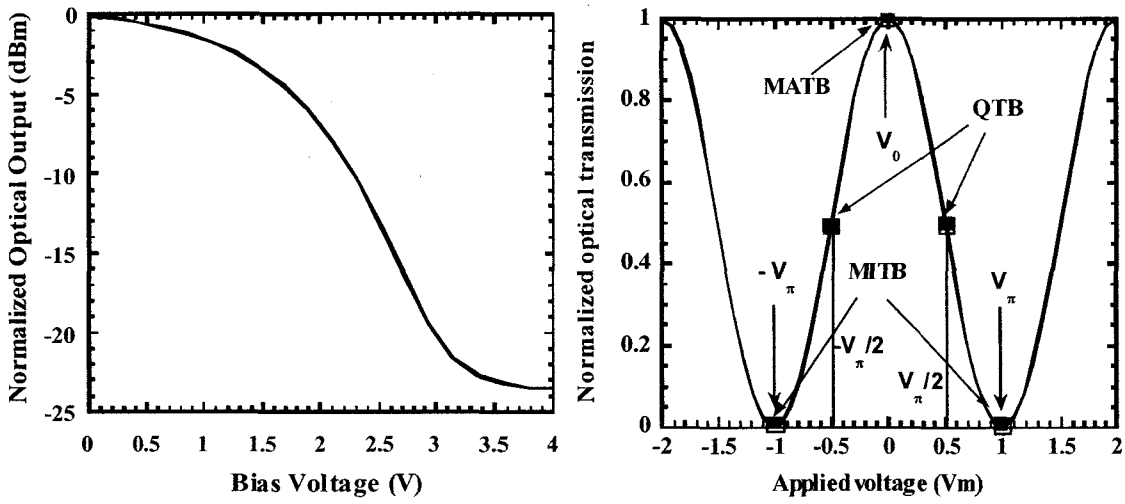

(a) (b)

Figure 1.3 Transfer functions for the external optical modulators: (a) EAM and (b) MZM.

A number of techniques for mm-wave generation using MZM as external modulator have been reported [3-5, 7]. The transfer function of MZM shown in Fig. 1.3 (b) can be expressed as $I_{out}(t) = \mu I_{in} \cos^2\left(\pi V_m(t) / 2V_\pi\right)$, where $I_{out}(t)$ is the transmitted intensity, μ is the insertion loss, I_{in} is the input intensity, and V_π is a specified driving voltage needed to obtain a π phase shift between the MZM arms. The modulation voltage $V_m(t)$ that is applied to the MZM can be divided into a constant bias and a time

varying modulation. According to the dc bias, three bias points are available as shown in Fig. 1.3 (b), which are minimum transmission bias (MITB) point (biased at $\pm V_{\pi}$), quadrature bias (QB) point (biased at $\pm V_{\pi}/2$), and maximum transmission bias (MATB) point (biased at V_0), respectively.

Mohmoud Mohamed et al. have investigated the photonic generation of mm-waves using OFM technique with dualelectrode MZM, considering the three bias cases of the MZM in [7]. The system setup for the technique in [7] is shown in Fig. 1.4. The continuous wave (CW) light is injected into a MZM driven by an RF signal at 7.5 GHz. The RF signal is applied to both electrodes of the MZM with a 180° phase-shifter. The output signal from the MZM is amplified by an EDFA before distributed over a single mode fiber with attenuation loss of α = 0.21 dB/km and chromatic dispersion of 16 ps/(nm.km). The optical signal is transmitted through 24 km fiber and detected by a high-speed PD with a 3 dB bandwidth of 40 GHz and a responsivity of 0.62 A/W. The biasing of the MZM at MATB, MITB and QB was placed under consideration. Beating between the optical harmonic sidebands at the photodetector generates RF signals at frequency doubling (15 GHz), quadrupling (30 GHz) and sextupling (45 GHz) of the driving RF signal at 7.5 GHz. It has been found that MATB is the best bias for frequency quadrupling and MITB is the best for frequency doubling and sextupling. However, when the MZM is biased at the either minimum or maximum point of transfer function, and the bias drifting would happen so that the desired optical sidebands are not maximized any more, introducing poor system robustness [16].

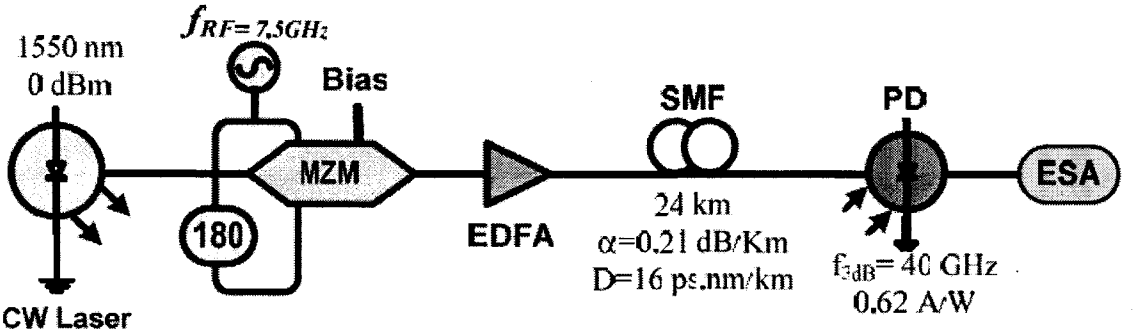

Figure 1.4 System setup for the mm-wave generation using OFM with a dual-electrode MZM [7]. EDFA: erbium-doped fiber amplifier, RSA: RF spectrum analyzer, PD: photodiode, and SMF: single-mode-fiber.

Besides MZMs, electro-absorption modulators (EAMs) have also been extensively studied as a low-power-consumption and low-cost external modulator. An EAM has many advantages, such as low drive voltage, high extinction ratio, polarization independence and monolithic integration capability with other optical components compared to an MZM. A comparison photograph of EAM and MZM is shown in Fig. 1.5. It is seen that the EAM has much smaller size than the MZM. Moreover, the EAM in the Fig. 1.5 is an electro-absorption modulator integrated laser (EML) which is much cheaper than an MZM and an individual EAM. An EML consists of a CW DFB laser followed by an EAM. Both the DFB laser and the EAM can be integrated monolithically on the same InP substrate as shown in Fig. 1.6, and a compact design and low coupling losses between the two devices can be achieved [47]. The transfer function of EAM shown in Fig. 1.3 (a) can be given as

$$T(V) = \exp\left(a_0 + a_1 V + a_2 V^2 + ... + a_m V^m\right) \tag{1.1}$$

where the voltage $V = V_b + V_{rf}$ denotes the driving voltages to the EAM, where V_b is bias voltage. The coefficients a_k ($k = 0,1,2...m$) are related to the transfer function of the EAM.

Suppose that the RF signal is given by $V_{rf} = V_0 \cos(2\pi ft)$ for the EAM, where f and V_0 are the radio frequency (RF), modulation voltage, respectively. Before this thesis, no technique for mm-wave generation using EAMs was proposed.

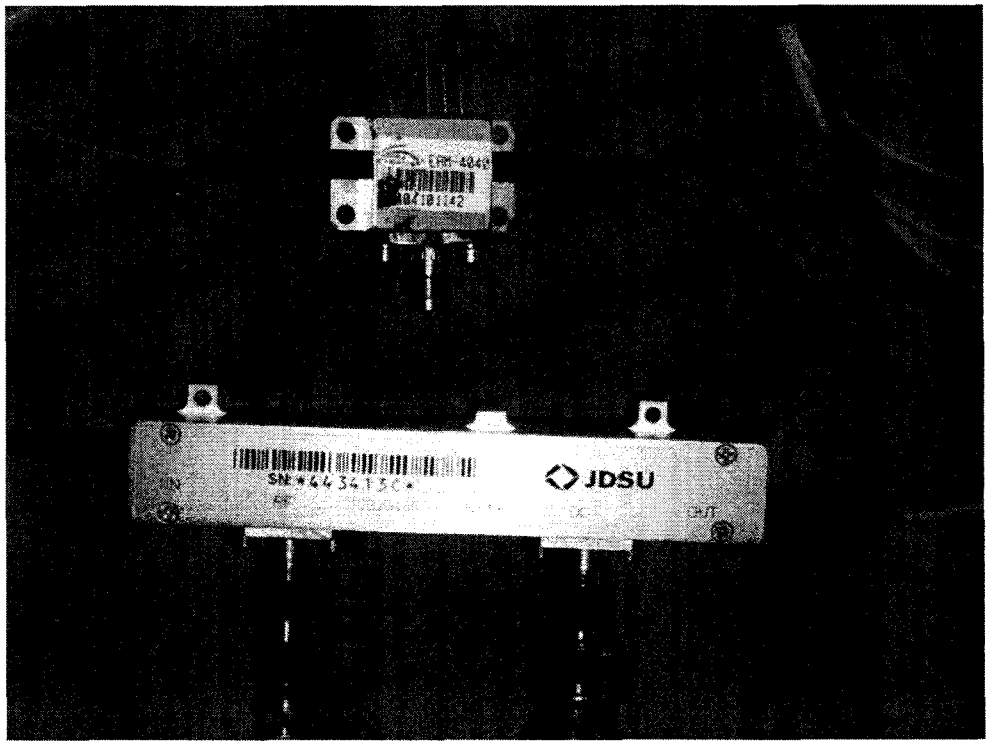

Figure 1.5 Photograph of EAM (up) and MZM (down).

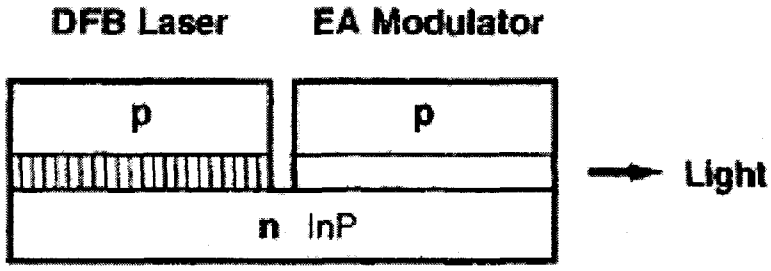

Figure 1.6 Integrated laser and EAM [47].

1.3 Motivation

Wireless communication systems using mm-wave bands provide broadband and secure data transmission platforms and have brought considerable benefits to telecommunication industry. However, the cost of the electrical equipments using for transmission of mm-wave signals is extremely high. Moreover, high transmission loss of the mm-wave transmission suggests that for applications of mm-wave spectrum, only short distance communications links will be supported [36]. Fortunately, RoF technology offers a potential solution to this issue. In RoF systems, mm-wave signal is transferred from electrical domain to optical domain at the CS and transported over an optical fiber to the BS. Compared to electrical cables, optical fibers have many economic advantages such as lower price, broader bandwidth, lower transmission loss and higher security. Furthermore, development of optical up-conversion techniques provides another cost-efficient benefit because only low RF equipment is need at the CS (while high frequency electrical equipment is very expensive).

However, there are still many challenges to the research of mm-wave systems in the near future.

- Nowadays, the number of BSs needed in a wireless service network increases with rising requirement for the amount and quality of customer service. On the other hands, though mm-wave band is a promising candidate for future broadband wireless communication systems, the free space-propagation attenuation of mm-wave band is very high. As a result, the key issue of cost efficiency of the RoF

system design is to reduce cost and size of the BS. The structure of the BS should be as simple as possible and cheap equipment should be used at the BS.

- Since the BSs should be kept simple and cheap, the complexity and expensive devices are shift to the CS. Generally, signal generation, processing and modulation are completed at the CS. Therefore, another important issue of the RoF system design is to generate high quality mm-wave signal using low cost equipments at the CS.
- In wireless communications using RoF technique, one of the most important limitations to the system performance is fiber chromatic dispersion which could cause serious power fading after signal is transported over fiber. Therefore, the techniques used to deal with fiber chromatic dispersion effect should be provided to improve system performance.
- There are two popular options for mm-wave generation based on OFM technique, one is frequency doubling method and the other is frequency quadrupling method as defined in previous sections. By using frequency doubling method, high quality mm-wave signal can be generated; however, this method is not suitable for the mm-wave generation higher than 60 GHz because the cost of the system will be very high. As a result, frequency quadrupling method becomes a better choice for 60 GHz mm-wave generation since RF devices lower than 20 GHz can be used at the CS. Therefore, frequency quadrupling technique which can generate high quality mm-wave signal should be investigated.

1.4 Thesis Scope and Contributions

The objective of this thesis is to develop novel modulation techniques for the generation and distribution of mm-wave signal based on optical frequency multiplication (OFM). Effective solutions are investigated for the two most importance design goals for RoF system: mitigate chromatic dispersion effect and low-cost BS configuration. In this thesis for the first time to our knowledge, the structure of two cascaded EAMs is used to generate mm-wave signals. The main contributions of this thesis are:

1. A novel technique for the optical mm-wave signal generation using frequency doubling and quadrupling technique is proposed. The mathematical model of the OFM technique based on two cascaded EAMs is introduced and then verified using Matlab and VPI Transmission Maker [48].
2. The performance of the mm-wave generation system using two cascaded EAMs is investigated in details. Theoretical analysis of back-to-back transmission and transmission over optical fiber is carried out considering phase shift, bias voltages of the cascaded EAMs and RF modulation index. In addition, experiments are conducted and verified by our theoretical analysis and good agreement is achieved.
3. The effect of fiber chromatic dispersion on the proposed system performance is investigated. Also, the robustness to bias and phase drifting of the proposed system is investigated, since the drifting problems are very normal to a reality RoF system.

1.5 Thesis Outline

This thesis is composed of seven chapters. The rest of the thesis is organized as follows:

In Chapter 2, an overview of RoF technology and a review of the techniques of optical mm-wave signal generation and distribution over optical fiber links are introduced. Advantages and disadvantages of presented techniques are investigated.

In Chapter 3, theoretical analyses of OFM technique based on two cascaded EAMs are given. Both systems of cascaded EAMs with identical characteristics and cascaded EAMs with different characteristics are investigated. The mathematical model of method by using a filter to remove fiber chromatic dispersion is also induced. The theoretical analysis is then verified by simulation. The comparison of effects of fiber chromatic dispersion to system performance before and after using filter is presented. Also, robustness of the system relative to bias drifting and phasing drifting is investigated.

In Chapter 4, experimental setup for the system using a low cost EML cascaded with an isolate EAM is introduced.

In Chapter 5, the conclusion of this thesis with the potential benefits of the proposed novel technique is presented. The continued work of this research in future is also discussed.

Chapter 2

Background Knowledge of RoF Technology

2.1 Introduction

As previously presented in Chapter 1, mm-wave band can offer broad bandwidth and high security to the future wireless access networks. Moreover, RoF techniques are considered as a cost-efficient option for the distribution of the future mm-wave wireless access networks to reduce high attenuation loss and provide simple BSs. As a consequence, much research has focused intensively on mm-wave over fiber systems in which generation of optical mm-wave signals is one of the key technologies.

This chapter is organized as follows. Three typical RoF link configurations and the advantages of RoF techniques are given in Section 2.1. Section 2.3 gives a review of techniques of optical mm-wave signal generation and transmission over fiber, also the advantages and disadvantages of all presented generation techniques are given. Finally, the main conclusions of the chapter are given in Section 2.4.

2.2 Radio over Fiber Technology

Radio-over-Fiber (RoF) technology refers to the use of optical fiber links to distribute RF signals from a central station (CS) to remote controlled base stations (BSs). In RoF systems, the light modulated by a RF signal is transmitted over optical fibers between a CS and a set of BSs before being radiated through the air. Recently, RoF technology has

been considered as one of the most potential solutions for the distribution of the future wireless access networks due to its cost-effectivity and reliability. Such a technology can be used for millimeter-wave signal distribution in cellular systems or for the "last mile" delivery of broadband data, since it provides an end user with a truly broadband access to the network while guaranteeing the increasing requirement for mobility. Furthermore, RoF technology enables efficient provisioning of broadband wireless services in particular when combined with flexible optical routing and dispersion-robust RoF transport techniques, such as optical frequency multiplying (OFM), to improve the network's throughput and operational efficiency [22].

2.2.1 RoF link configurations

We have several possible approaches to transporting radio signals over optical fiber in RoF systems, which is usually classified into three main categories (Intermediate frequency (IF) transmission over fiber, Baseband (BB) transmission over fiber, and RF transmission over fiber) depending on the frequency range of the radio signal to be transported [23, 24]. The three fundamental techniques are shown in Fig. 2.1 [23].

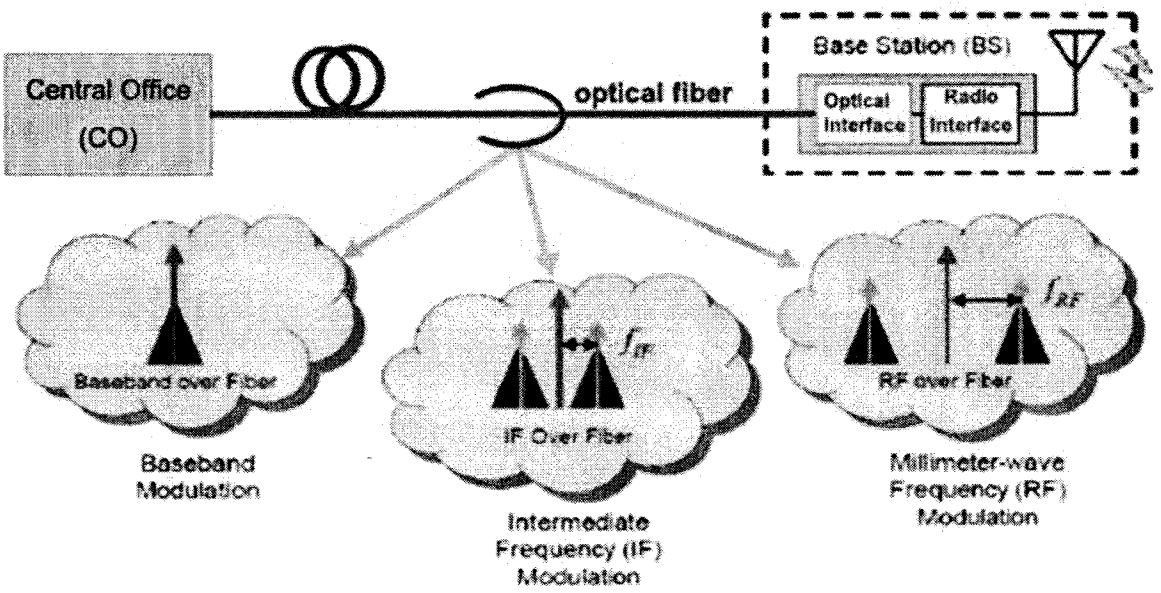

Figure 2.1 Radio signal transport schemes for RoF systems [23].

- ***IF transmission over fiber*** –Fig. 2.2(a) shows shows a scheme required for downstream signal transmission in an RoF system based on the distribution of the radio signal at an IF (Intermediate Frequency) radio signal with a lower frequency (less than 10 GHz). In the scheme, the data is directly modulated onto an optical carrier in the IF band at the CS, while at the BS, the modulated signal is detected by a photodetector (PD) and then up-converted to the desired RF band. IF-over-fiber scheme offers the advantage that the effect of fiber chromatic dispersion on the distribution of IF signals is really small. However, the requirement for frequency conversion at the BS increases the complexity and cost of the BS architecture particularly at the applications in the millimeter wave frequency region since expensive mm-wave band oscillators and mixers are needed for remote frequency conversion. In addition, when there is a system upgrade required changes in RF frequency, the up-conversion circuitry at all BSs should be upgraded.

- ***Baseband transmission over fiber*** – A RoF system based on baseband over fiber transport is shown in Fig. 2.2(b). The radio information is transported to the BS as a digital data stream. At the BS, after detected by a PD, the modulated signal is recovered and then up-converted to an RF band directly or through an IF band, and transmitted to the user. As with IF over fiber, influence of the fiber dispersion effect is negligible for this scheme and however unfortunately it also has disadvantages of increasing cost and complexity of the BS and limiting the upgradeability of the overall fiber radio system since expensive electrical mm-wave oscillators and mixers are needed at all BSs and an upgrade in RoF system leads to the change of signal modulation circuitry at each BS.
- ***RF transmission over fiber*** – In RF-over-Fiber configuration shown as Fig. 2.1(c), a data-carrying RF (Radio Frequency) signal is carried by the optical mm-wave generated at the CS and converted to electrical mm-wave signal using a low-cost O/E converter at the BS. Consequently, the wireless signals are transmitted directly over the fiber at the radio carrier transmission frequency without the need for any frequency up or down conversion at the remote antenna BS, thereby resulting in simple and cost-effective implementation enabled at the BS. However, the RF-signal-fading effect induced by chromatic dispersion in optical fiber seriously limits the transmission distance [25, 26].

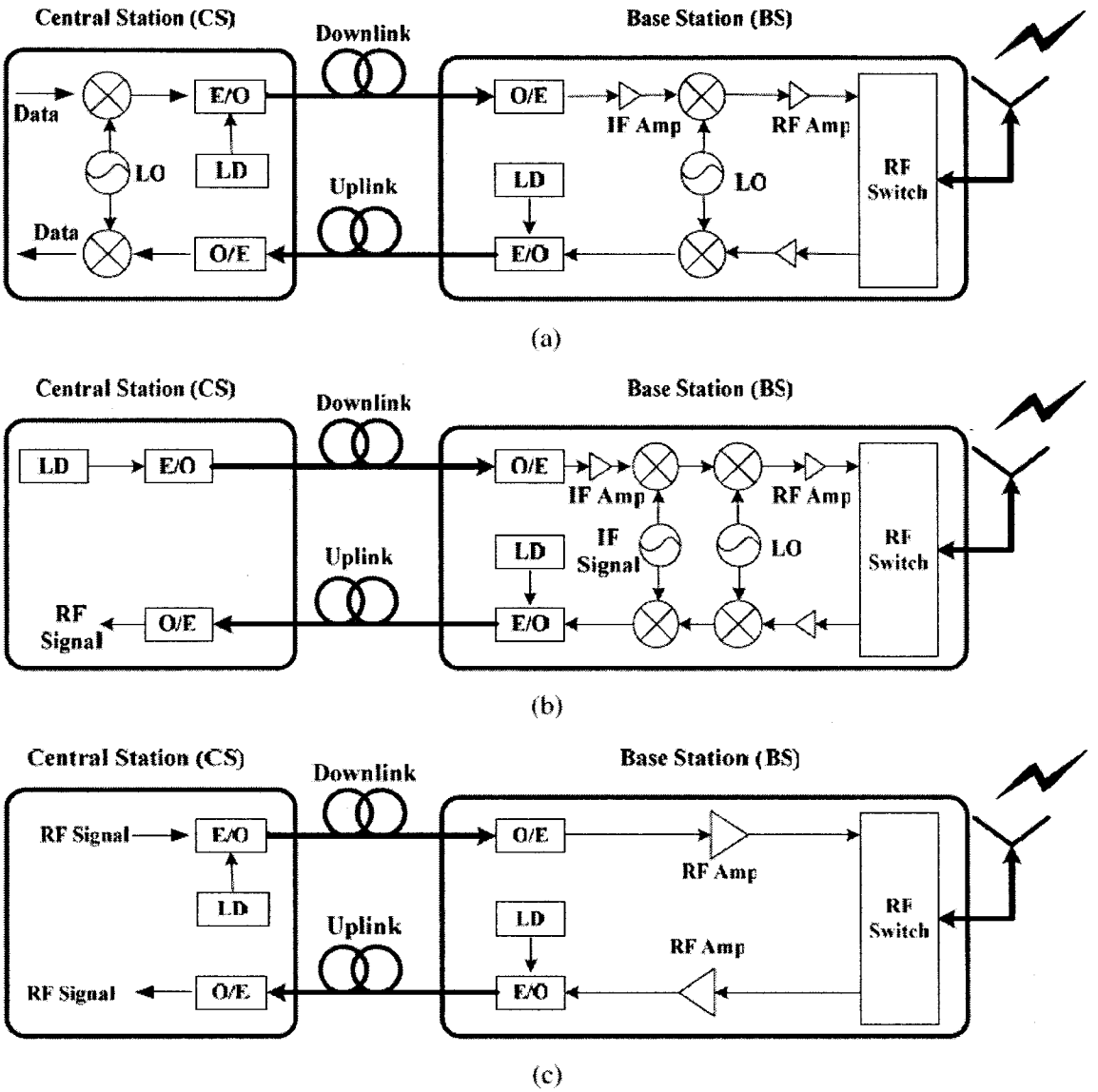

Figure 2.2 RoF links configuration. (a) IF modulated signal, (b) baseband modulated signal and (c) RF modulated signal. LD: Laser diode, E/O: electrical-to-optical conversion, O/E: optical-toelectrical conversion, LO: local oscillator and Amp: amplifier [24].

2.2.2 Advantages of RoF Systems

Some of the benefits of the RoF technology compared with electronic signal distribution are given below [27].

- ***Low attenuation*** – Signals transported on optical fiber attenuate much less than other medium. For instance, commercially available standard Single Mode Fibers (SMFs) made from glass (silica) have attenuation losses below 0.2dB/km and 0.5dB/km in the 1550nm and the 1300 nm windows, respectively. These losses are much lower than those encountered in coaxial cable, whose losses are higher by three orders of magnitude at higher frequencies. For example, the attenuation of a ½ inch coaxial cable (RG-214) is >500 dB/km for frequencies above 5 GHz [28]. Therefore, by transmitting microwaves over fiber, transmission distances are increased and the required transmission powers are reduced.
- ***Large bandwidth*** – Optical fiber communication provides enormous bandwidth. Three main transmission windows offered by optical fiber, namely the 850 nm, 1310 nm, and 1550 nm wavelengths, which offers low attenuation. For a single SMF optical fiber, the combined bandwidth of the three windows is in the excess of 50 THz which is extremely wide [29].
- ***Immunity to radio frequency interference*** – Since transmitted information is modulated by the light with RF signal, RoF system is immune to electromagnetic interference (EMI), which is a very attractive property of optical fiber communications, especially for microwave and mm-wave transmissions. Because of the EMI immunity, optical fiber communications is the immunity to eavesdropping too, which provides privacy and security for the communication system. Furthermore, RoF is free from multipath interference which is a common problem in normal wireless communications.

- ***Reduced power consumption*** – Reduced power consumption is a consequence of having simple equipment at the BS while most of the complex equipment is kept at the CS. In some applications, the BSs are even operated in passive mode which is largely reducing power consumption [30]. Moreover, low RF power antennas are required if fiber is used for distribution, which leads to reduction of interference and radiation.
- ***Lower cost*** – It is well known that optical fiber is very cheap and RoF can provide a very economic solution for broadband access networks if low cost lasers and photodetectors are used. On the other hand, in RoF systems, complex and expensive equipment is kept at the CS shared by several BSs. In such cases, a BS simply consists of a photodetector, an RF amplifier, and an antenna. Simpler structure of remote BSs means lower cost of construction, lower power consumption and simpler maintenance at BSs leading to lowering the overall installation and maintenance cost.

2.3 Millimeter-Wave Signal Generation Techniques

As mentioned in before, RoF technology is one of the most potential solutions in wireless communications for guaranteeing both the capacity and mobility as well as lessening costs of the BSs. Most complex equipment for the signal processing such as RF generation, coding, multiplexing and modulation is setup at the CS shared by several BSs. There are several optical techniques for generating and transporting RF signals over fiber, in which, intensity modulation/direct-detection (IM/DD) is the simplest technique optically generating and distributing RF signal over optical links. In the application of

IM/DD, the intensity of the light source is directly modulated by the RF signal and transmitted over fiber to the BS where it is directly detected by a photodetector. There are two ways of modulating the light source at the CS in the IM/DD technique. One way is to let the RF signal directly modulate the laser diode's current. The second method is to operate the laser in continuous wave (CW) mode and then use an external modulator such as a Mach-Zehnder Modulator (MZM) or an Electro-absorption modulator (EAM), to modulate the intensity of the light. The two options are shown in Fig. 2.3(a) and (b) respectively.

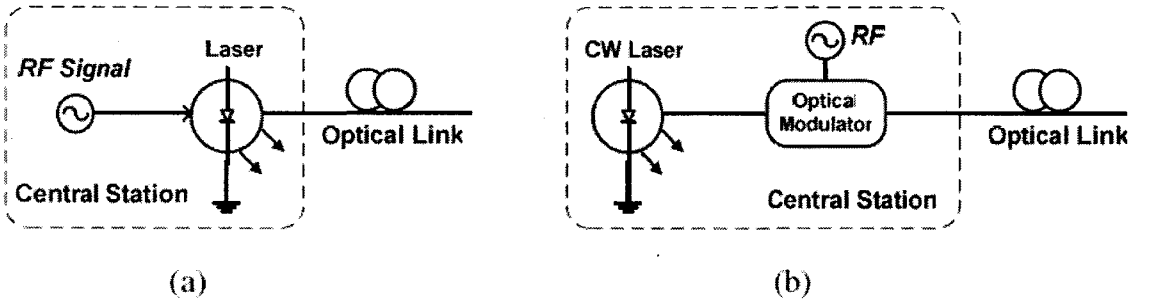

Figure 2.3 RF signal generation by (a) direct laser modulator and (b) an external modulator [24].

Although IM/DD is the simplest scheme, due to the limited modulation bandwidth of the laser and laser non-linearity, it is difficult to use for high frequency mm-wave applications which have been expected as a result of limited availability of the RF bands [31]. Much research up-to-date has been carried out in the optical mm-wave signal generation. The most popular methods to generate an mm-wave signal are to use optical heterodyne technique [1, 12, 32] and techniques based on optical harmonics generation [2-5, 7, 10, 11, 18].

2.3.1 Optical Heterodyning Technique

Remote Heterodyne Detection (RHD) technique relies on the principle of coherent mixing in the photodiode to generate the RF signal (see Fig. 2.4 and Fig. 2.5). In this technique, there are two lasers, of which one is master laser and other one is slave laser, are used to generate two optical carriers. The frequency offset between the two optical carriers is equal to the desired mm-wave frequency. One of these two signals is intensity-modulated with data while the other one is unmodulated. Then, both optical carriers are transported over fiber link from the CS to the BS; the electrical mm-wave signal is generated by beating two optical carriers in a PD at the BS. Assume that there are two optical fields is given by

$$E_1(t) = E_{01}\cos(\omega_1 t) \tag{2.1}$$

$$E_2(t) = E_{02}\cos(\omega_2 t) \tag{2.2}$$

where E_{01}, E_{02} are the amplitude terms, and ω_1, ω_2 are the angular frequency terms of the two optical fields. Then, after square-law photodetection, the generated photocurrent $I_{PD}(t)$ can be expressed as [39, 40]

$$I_{PD}(t) = \left|E_1 + E_2\right|^2 = \left|E_{01}\cos(2\omega_1 t) + E_{02}\cos(2\omega_2 t)\right|^2, \tag{2.3}$$

$$\begin{aligned} I_{PD}(t) = {} & \frac{1}{2}\left(E_{01}^2 + E_{02}^2\right) + \frac{E_{01}}{2}\cos(2\omega_1 t) + \frac{E_{02}}{2}\cos(2\omega_2 t) \\ & + E_{01}E_{02}\cos(\omega_1 - \omega_2)t + E_{01}E_{02}\cos(\omega_1 + \omega_2)t \end{aligned} \tag{2.4}$$

The term of interest is $E_{01}E_{02}\cos(\omega_1-\omega_2)t$ which shows that an electrical signal with a frequency equal to the frequency difference of the two optical fields is generated.

One important attribute of RHD technique is that very high frequencies can be generated, limited only by the bandwidth of the photodetector. Furthermore, since only one of the two optical carriers is modulated with data, system sensitivity to chromatic dispersion can be greatly reduced. Another benefit of RHD is that it permits low-frequency data modulation at the CS since high-frequency electro-optical components are not required. However, using two different laser sources for heterodyne signal generation will result in the strong influence of laser phase noise and optical frequency variations on the purity and stability of the generated mm-wave. To achieve a high quality carrier, phase control mechanisms need to be applied, which leads to more complex systems. Techniques used to reduce phase noise sensitivity include Optical Injection Locking (OIL) and Optical Phase Locked Loops (OPLL). The principles of OIL technique and OPLL technique are shown in Fig. 2.4 and Fig. 2.5 respectively.

For OIL technique, it consists of a master and slave laser source, PD, and a microwave reference oscillator. OIL is a technique that involves modulating the master laser with a low-frequency signal, and then part of the output of the master laser is fed into the slave laser resulting in the slave laser to lock onto the master's sidebands frequency and resonate there. By using OIL, cheaper broad-linewidth lasers can still be used to generate stable narrow electrical linewidth signals and OIL exhibits good phase noise suppression.

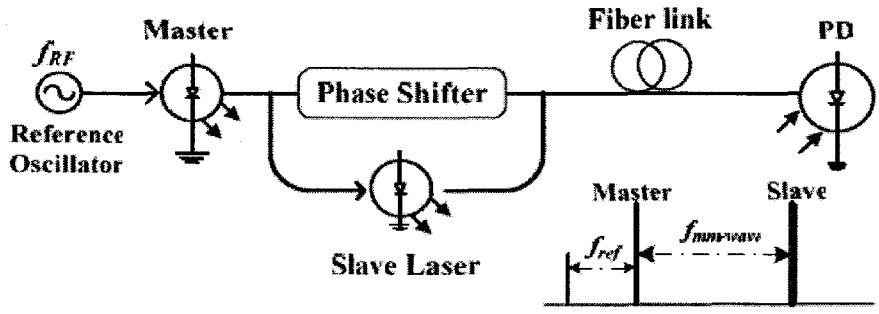

Figure 2.4 Principle of optical injection locking (OIL) technique [33].

For OPLL technique, it consists of a free running master laser, a PIN photodiode, a microwave amplifier, a frequency or phase detector, a loop filter, a slave laser and a microwave reference oscillator as shown in Fig. 2.5. The combined outputs of the master and slave lasers are split into two parts. Part of the optical signal is used in the OPLL system at the CS while the other part is transmitted to the BS. The optical signal at the CS is heterodyned on a photodiode to generate a microwave signal which is compared to the reference signal. Then a phase error signal of OPLL is fed back to the slave laser. In this way, the slave laser is forced to track the master laser at a frequency offset corresponding to the frequency of the microwave reference oscillator. It does not suppress small-scale frequency variations caused by phase noise. [27]

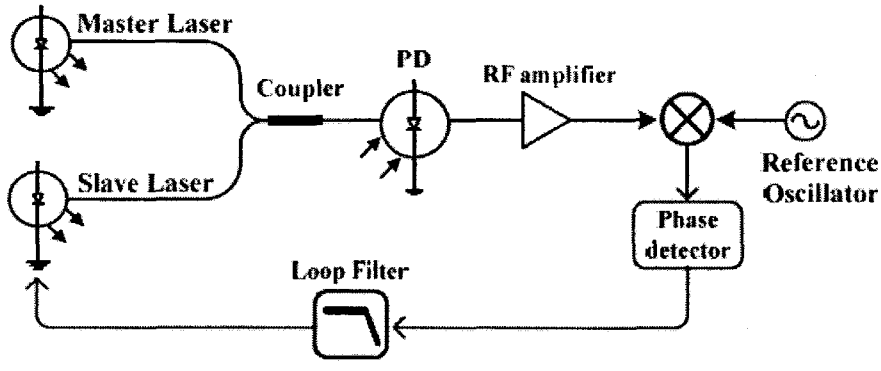

Figure 2.5 Principle of optical phase-looked loop (OPLL) technique [34].

2.3.2 Optical Harmonics Generation Techniques

Optical harmonics generation or optical frequency multiplication (OFM) technique is reported as a cost-effective technique which can generate high-purity and high-frequency mm-wave signals [3-5, 7]. The principle of OFM technique is to generate high-order optical harmonics using laser with another electrical to optical (E/O) converter, an external optical modulator, which is driven by a low RF signal, and nonlinear response of the E/O converter may generate higher-order optical harmonics. At the BS, by beating any two high-order optical harmonics or/and beating any high-order optical harmonics with the optical carrier in the PD, many mm-wave signals may be generated. In OFM technique, low-cost frequency electrical components and low-bandwidth optical external modulator can be used at the CS to generate mm-wave beyond 40 GHz, because RF electrical components and equipment with frequency response of higher than 26 GHz are much more expensive than those of below 26 GHz. However, the disadvantage of OFM is that the transmission distance is limited by fiber chromatic dispersion.

RoF systems used for generation of mm-wave signals based on OFM techniques can be generally classified into three categories:

- Harmonic generation using single MZM
- Harmonic generation using two cascaded MZMs
- Harmonic generation with optical phase modulator (PM) and
- Harmonic frequency generation with optical carrier suppression (OCS)

2.3.2.1 Harmonic Generation with single MZM

This subject has been very popular in the research of optical mm-wave generation recent years. A method to generate an mm-wave signal using an optical MZM is first proposed in 1992 by J. J. O'Reilly et al. [37]. This frequency doubling method is shown in Fig. 2.6. The applied voltage of the sinusoidal RF signal modulated by the MZM can be described by [37]

$$\upsilon(t) = V_{\pi}(1+\varepsilon) + \alpha V_{\pi}\cos(\omega_{RF}t)\ , \tag{2.5}$$

where ε is the normalized bias point of the MZM, α is the normalized amplitude of the drive voltage and the frequency of drive voltage is $\omega_{RF} = 2\pi f$ where f is the modulation frequency. The optical output field from the MZM can be written as

$$E(t) = \cos\left\{\frac{\pi}{2}\left[(1+\varepsilon) + \alpha\cos(\omega_{RF}t)\right]\right\}\cos(2\pi\omega_0 t)\ , \tag{2.6}$$

where ω_0 is the optical carrier frequency. Bessel function expansion of Eq. (2.6) leads to an expression for the output field as

$$\begin{aligned} E(t) = {} & \frac{1}{2}J_0\left(\alpha\frac{\pi}{2}\right)\cos\left[\frac{\pi}{2}(1+\varepsilon)\right]\cos(2\pi\omega_0 t) \\ & -J_1\left(\alpha\frac{\pi}{2}\right)\sin\left[\frac{\pi}{2}(1+\varepsilon)\right]\cos(2\pi\omega_0 t \pm \omega_{RF}t) \\ & -J_2\left(\alpha\frac{\pi}{2}\right)\cos\left[\frac{\pi}{2}(1+\varepsilon)\right]\cos(2\pi\omega_0 t \pm 2\omega_{RF}t) \\ & +J_3\left(\alpha\frac{\pi}{2}\right)\sin\left[\frac{\pi}{2}(1+\varepsilon)\right]\cos(2\pi\omega_0 t \pm 3\omega_{RF}t) + \ldots \end{aligned}\ , \tag{2.7}$$

where J_k is the kth Bessel function of the first kind. From the Eq. (2.7), we can see that when the MZM is biased at V_π ($\varepsilon = 0$) named as minimum transmission bias (MITB) point, the optical carrier is suppressed together with the even modulation sidebands at $\omega_0 \pm 2\omega_{RF}$, $\omega_0 \pm 4\omega_{RF}$ and etc. Therefore, two strong components (first-order harmonics) result centered at ω_0 and separated by $2\omega_{RF}$. Other odd-order terms higher than first-order harmonics have lower amplitudes and can be reduced to 15dB below the two major components by careful control of the bias point of the MZM [43]. As shown in Fig. 2.6, after MZM, an erbium-doped fiber amplifier (EDFA) was used to increase the level of the optical components produced by the MZM and these components are transmitted through a length of fiber. Then, the light is injected into the photodiode and the required doubling mm-wave signal at $2f$ is generated by photodetection. This technique is immune to fiber chromatic dispersion [37], since the generated mm-wave signal is mainly due to the beating between the two first-order harmonics.

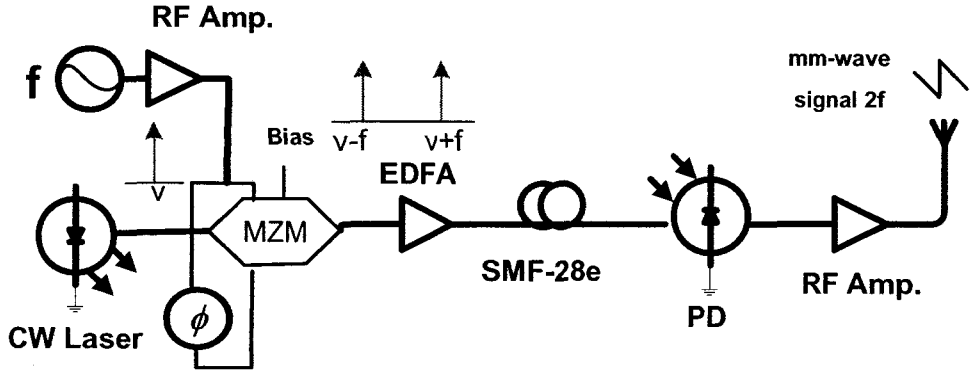

Figure 2.6 Frequency doubling technique for generating mm-wave signal using a MZM.

EDFA: Erbium-Doped Fiber Amplifier, PD: Photo Detector, CW: Continuous Wave, SMF: Single Mode Fiber.

In 1994, J. J. O'Reilly et al. proposed another method to generate a frequency-quadrupled electrical signal [38]. In this method, the MZM is driven with a RF signal at quarter the required mm-frequency. By biasing the MZM at maximum transmission bias (MATB) when $\varepsilon = 1$, the odd-order optical sidebands were suppressed. Then, a Mach-Zehnder interferometer (MZI) filter was used to suppress the optical carrier. After enhanced by an EDFA, those optical sidebands were propagated through the fiber. By beating the two second-order sidebands at photodetector, an electrical signal that has four times of the LO frequency was generated. However, the main disadvantage of this technique is the needs of a MZI filter which increases the complexity the system. Additionally, since the optical power of second-order harmonics is lower than first-order harmonics, the efficiency of this technique is lower that the frequency doubling technique. Therefore, these years many other Frequency quadrupling techniques have been proposed to deal with these problems [3-5, 24].

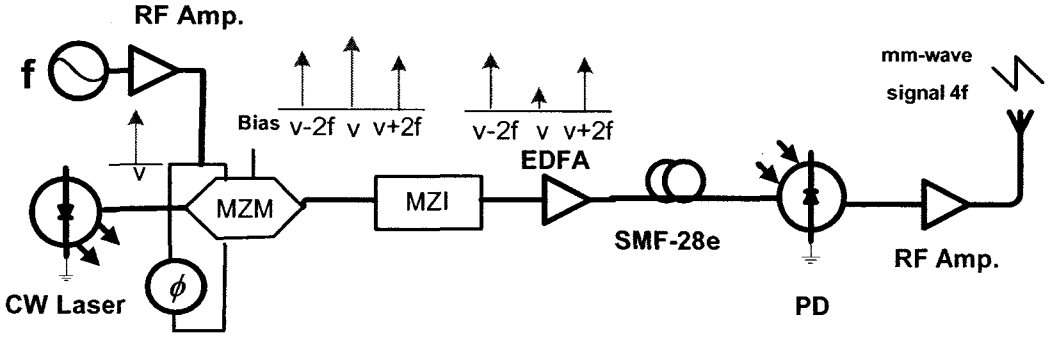

Figure 2.7 Frequency quadrupling technique for generating mm-wave signal using a MZM.

2.3.2.2 Harmonic Generation with two Cascaded MZMs

In the thesis [24], a frequency quadrupler and a frequency sixupler based on two cascaded MZMs are investigated and used to generate mm-wave signals respectively. For

the frequency quadrupler shown in Fig. 2.8, both MZMs are biased at the QB point with a 180 degree phase shift between the two MZMs. When the light passes the First MZM, one of the two first-order harmonics is suppressed. Then after another MZM, another first-order harmonic gets suppressed too. At the PD, two strong second-order sidebands are beating with each other and then the required quadrupling mm-wave signal is generated.

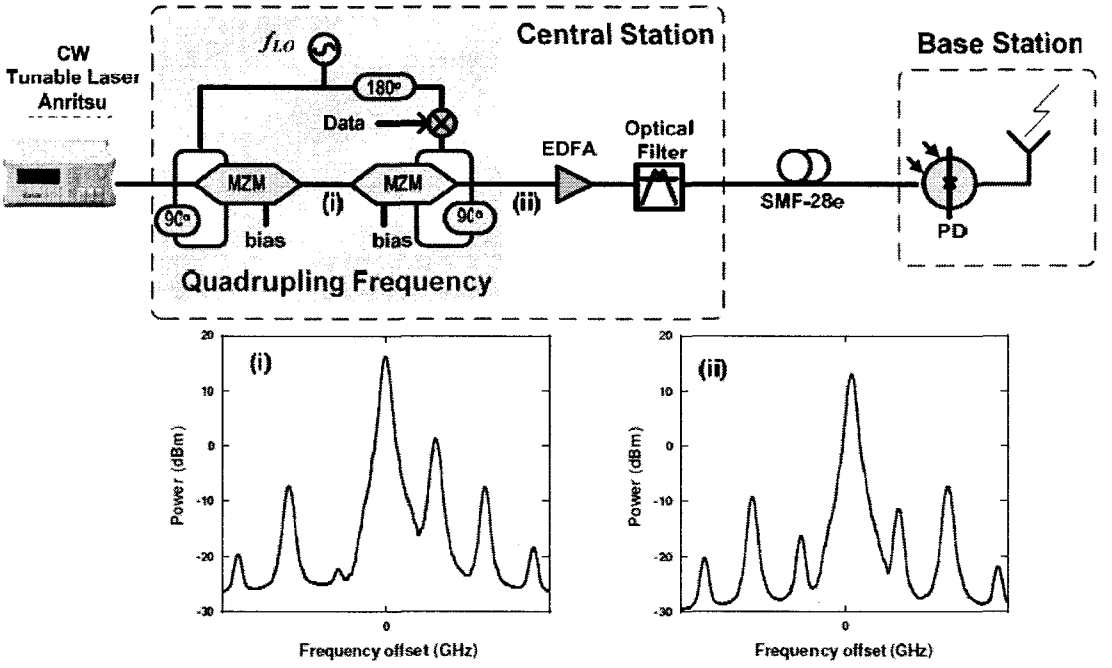

Figure 2.8 Frequency quadrupling technique for generating mm-wave signal using two cascaded MZMs. Measured optical spectrum in insets (i) and (ii) are obtained using an RF of 7.5 GHz that drive the MZM, and after second MZM, respectively [24].

In the frequency sextupling technique shown in Fig. 2.9, [24], the first MZM is biased at MATB and the second MZM is biased at MITB. A CW light injects in the first MZM and then all odd-order harmonics are suppressed while only even-order harmonics are generated. Then the optical carrier and even-order harmonics pass the second MZM,

resulting six optical sidebands at $\pm\omega_{RF}$, $\pm 3\omega_{RF}$, and $\pm 5\omega_{RF}$ as shown in Fig. 2.9 (ii). An EDFA is used to enhance the generated sidebands and then an optical filter is used to filter out other harmonics higher than third-order harmonics. As shown in Fig. 2.9(iii), two strong third-order harmonics are generated before transported through fiber to the BS where the two third-order harmonics are beating with each other at the PD and the required sextupling signal is generated. It means that to generated 60GHz signal, only 10GHz RF driving signal is needed at the CS. By using two cascaded MZMs, desired optical harmonics are maximized and non-desired optical harmonics are greatly suppressed, so that high frequency up-conversion efficiency is obtained with less nonlinear distortion impact [24].

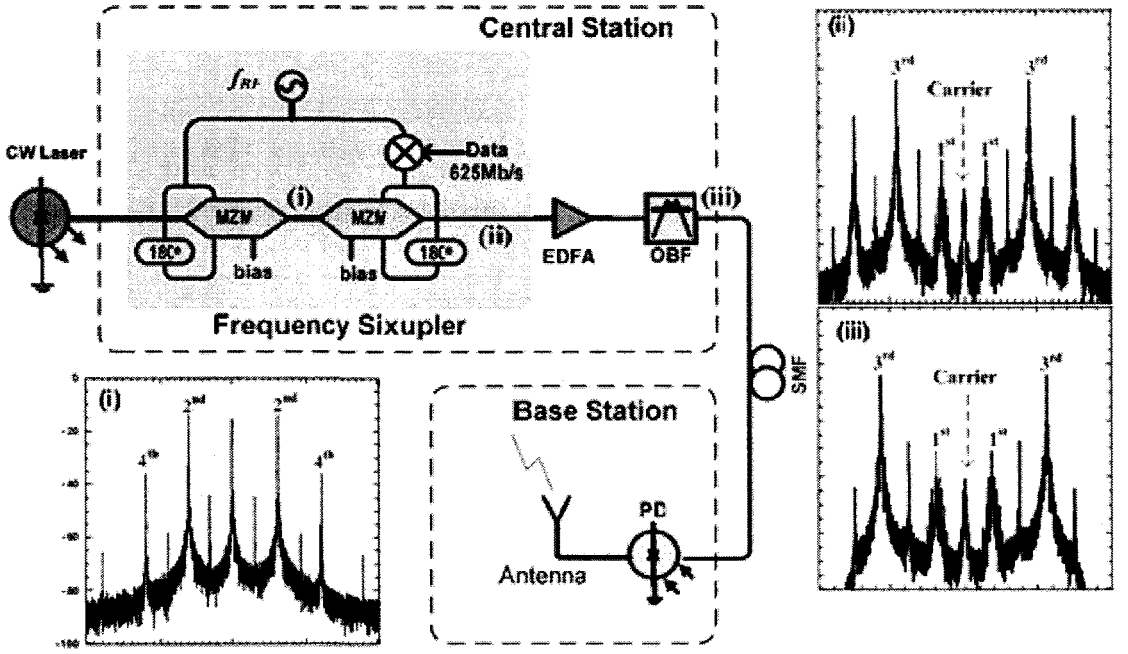

Figure 2.9 A frequency sixupler for generating mm-wave signal using two cascaded MZMs. OBF: Optical band-pass filter, ELPF: Electrical low pass filter and ESA: Electrical signal analyzer. The simulated optical spectra in insets (i), (ii) and (iii) are obtained after the first MZM,

after the two cascaded MZMs, and after optical filtering, respectively. An RF of 10 GHz that drives the two cascaded dual-electrode MZMs is used [24].

The approach using a MZM or cascaded MZMs to mm-wave generation, as discussed above, can produce a high-quality frequency quadrupling or sextupling mm-wave signal with a simple system structure. However, to suppress the odd- or even-order optical sidebands, the MZM should be biased at the minimum or maximum bias point, which would result in the bias-drifting problem, leading to poor system robustness or a sophisticated control circuit has to be employed to minimize the bias drift [16].

2.3.2.3 Harmonic Generation with optical phase modulator

In the method of using a MZM as external an optical modulator discussed in Section 2.3.2.1, biasing the MZM to suppress the even-order optical sidebands suffers from a dc bias-drifting problem, which reduces the robustness of the system. A simple solution of this problem is to replace the MZM by an optical phase modulator (PM). The key advantage of using an optical phase modulator is that frequency doubling or quadrupling of the electrical drive signal can be achieved without specific dc bias adjustment, which eliminates the bias drifting problem [42]. The setup for the generation of mm-wave signal using an optical phase modulator in [42] is shown in Fig. 2.10.

The use of a PM will generate all sidebands including the optical carrier. Therefore, a fixed optical notch filter is used to filter out the optical carrier. In the technique of Fig. 2.10, a fiber Bragg grating (FBG) is used as the fixed optical notch filter. The optical source is a tunable laser and the wavelength of the optical carrier generated by the tunable laser source (TLS) was tuned to match the maximum attenuation wavelength of the FBG. The output optical sidebands of the FBG were amplified by an

EDFA, and then distributed over fiber. Before detected by the PD, a dispersion compensating fiber (DCF) is used to eliminate the power fluctuation of the generated electrical signal caused by the fiber chromatic dispersion in order to maintain the electrical odd-order harmonic suppression. Then the beating of optical sidebands at a PD generates the required mm-wave signal.

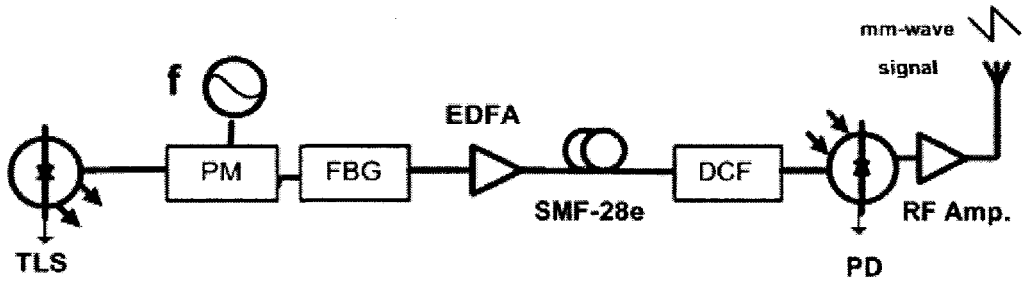

Figure 2.10 mm-wave signal generation using a phase modulator [42]. TLS: Tunable Laser Source, PM: Phase Modulator, FBG: Fibre Bragg Grating, DCM: Dispersion Compensating Fiber.

2.3.2.4 Harmonic Generation with optical carrier suppression

A millimeter-wave signal generation based on optical carrier suppression (OCS) technique was proposed in [43]. This is a frequency doubling technique and the experimental setup of the system is shown in Fig. 2.11. At the CS, a CW lightwave is generated by a tunable laser and injected into a MZM. The MZM was biased at MITB and driven by two complementary 20-GHz clocks in order to realize OCS. As a result, optical carrier is suppressed and two optical first-order sidebands are generated with a 40GHz frequency spacing that is two times of the driving radio frequency to the MZM. Then a PM is used to generate a 2.5-Gb/s differential phase-shift-keyed (DPSK) signal. After amplified by an EDFA, optical sidebands carrying with the 2.5-Gb/s DPSK data

were transmitted over the fiber. At the BS, a MZI was used to convert from phase-to-intensity modulation, since the PD is phase insensitive.

The key advantage of this technique is that optical carrier is suppressed without using an optical notch filter. Furthermore, for the 40-GHz mm-wave generation, this technique shows unique advantages in terms of system simplicity and transmission performance [43]. However, for 60 GHz mm-wave up-conversion in the downlink, a high-frequency MZM and 30 GHz RF driving signal generator should be used in this method, which will greatly increase the cost of the system. Therefore, cost-efficient methods using the main concept of OCS should be discussed in the future development of RoF system.

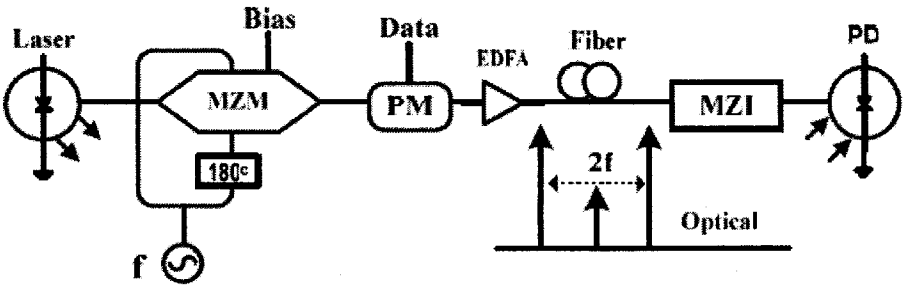

Figure 2.11 mm-wave signal generation using the OCS technique [43]

2.4 Summary

In this chapter, an extensive review of RoF technology for mm-wave frequency band has been presented. The discussion of three main schemes for RoF link based on the mm-wave RoF architectures is provided, including RF transmission over fiber, IF transmission over fiber, and BB transmission over fiber. A summary comparison among these three configurations for transporting radio signal over fiber is shown in Table 2.1.

Furthermore, two main categories of techniques for mm-wave generation and transportation using RoF systems were investigated: Optical heterodyning and harmonics generation. The advantages and disadvantages of the mm-wave generation techniques described in this chapter are summarized in Tables 2.2.

Table 2.1 Comparison of transporting RF signal configurations

Configurations	Advantages	Disadvantages
BB over fiber	▪ Not suffering from fiber chromatic dispersion	▪ Expensive and complicated BS; ▪ Limiting the upgradeability.
IF over fiber	▪ Not suffering from fiber chromatic dispersion	▪ Expensive and complicated BS; ▪ Limiting the upgradeability.
RF over fiber	▪ Simple and cheap BS; ▪ Easy to upgrade	▪ Suffering from fiber chromatic dispersion

Table 2.2 Comparison of mm-wave generation techniques

Techniques	Advantages	Disadvantages
Intensity Modulation/Direct-Detection	▪ The simplest scheme.	▪ Not suitable for mm-wave band because of the limited modulation bandwidth of the laser.
Optical Heterodyne	▪ High frequency generation; ▪ No fiber chromatic dispersion effect; ▪ Low-frequency data modulation at the CS.	▪ Phase control mechanisms need to be applied resulting in more complex system and additional cost.
Single MZM	▪ Simple configuration; ▪ Cost-effective technique; ▪ Driving RF at half or quarter the required mm-wave frequency.	▪ Optical filter needed; ▪ Bias drifting problem.

Cascaded MZMs	▪ High frequency up-conversion efficiency obtained with less nonlinear distortion impact; ▪ Driving RF at quarter or sixupler the required mm-wave frequency.	▪ Optical filter needed; ▪ Bias drifting problem; ▪ Limited transmission distance due to fiber chromatic dispersion effect; ▪ More complicated.
Phase Modulator	▪ No dc bias.	▪ MZI needed; ▪ High modulation index; ▪ DCF needed due to fiber chromatic dispersion effect.
OCS	▪ Optical carrier suppressed without using an optical notch filter	▪ High cost for 60GHz mm-wave up-coversion

Chapter 3

Proposed Millimeter-Waves Generation Technique

3.1 Introduction

As previously mentioned in Chapter 2, optical mm-wave signals generation using frequency doubling and quadrupling based on MZM has been reported [3-5, 7]. MZM can be used to generate high-purity mm-wave signal with a simple system structure. However, to suppress even-order or odd-order optical sidebands, MZM should be biased at the minimum or maximum point of transfer function and the bias drifting would happen which may affect the system performance [16].

Except for MZMs, EAM has also been extensively studied as a low-power-consumption and low-cost external modulator. An EAM has many advantages such as, low drive voltage, high extinction ratio, and monolithic integration capability with other optical components compared to the MZM. Moreover, since the EAM has a more complicated nonlinear transfer function, more high-order optical harmonics may be generated due to nonlinearity of the EAM [8, 17]. Two cascaded EAMs have been used in optical linearization scheme to suppress intermodulation distortion (IMD) products and harmonic distortion products generated by nonlinearity of EAM in [8, 17].

In order to generate high quality mm-wave signal while guarantying the cost-efficiency and system robustness, we shall propose and investigate the photonic generation of mm-wave signal using two cascaded EAMs. This technique uses a low RF signal to drive the two cascaded EAMs with a certain phase shift. The electrical phase

shift can be optimized to suppress the first-order optical harmonics and maximize the second-order harmonics. Two strong second-order optical sidebands are generated and have a frequency spacing of four times of the driving RF. By beating the optical carrier with the two strong second-order sidebands, frequency doubling of a low RF signal can be obtained. Similarly, beating of the two strong second-order sidebands results in a frequency quadrupling of a low RF signal. The performance of mm-wave signal generated with frequency doubling and quadrupling is investigated in an RoF system considering the impact of phase shift, and voltage of the RF signal and bias that drives the EAMs.

This chapter is organized as follows. Section 3.2 will introduce the configuration of the mm-wave generation technique using two cascaded EAMs. Section 3.3 will present the theoretical analysis of the mm-wave generation. The theoretical analysis is then verified by simulation in Section 3.4, considering the impact of phase shift, modulation voltage and bias voltages on the two cascaded EAMs. The discussion further explores, the impact of the fiber dispersion and drifting effect on the proposed system will be investigated. Finally, the conclusions are drawn in Section 3.5.

3.2 Proposed Millimeter-Waves Generation Technique

An EAM transfer function may have more pronounced nonlinearities, so the EAM may lead to stronger nonlinear effects than an MZM. As a result, strong high-order harmonics may be generated due to the pronounced nonlinearities of the EAM [8, 17]. When two cascaded EAMs are used for the mm-wave generation, to maximize the desired optical sidebands and minimize the undesired ones can be obtained by optimizing the bias and

RF modulation voltage [8]. The mechanism of the proposed technique is to suppress first-order optical sidebands and maximize the second-order sidebands, in order to efficiently generate mm-wave signal for frequency doubling and quadrupling.

The configuration of the cascaded EAMs is shown in Fig. 3.1, where a light is injected to the first EAM that is connected to a second EAM. A low RF signal is split equally and drives the two EAMs. A phase shifter is inserted in one arm of the RF splitter. In fact, this electrical phase shift can be replaced by an optical phase shift. Extending transfer function of EAM in [8], the transfer function of the EAM can be expressed as

$$T(V) = \frac{P_{out}}{P_{in}} = \exp\left(a_0 + a_1 V + a_2 V^2 + ... + a_n V^n\right). \tag{3.1}$$

The transfer function of the cascaded EAM structure can be given as

$$\begin{aligned} T(V_1, V_2) = T_1(V_1) T_2(V_2) = \exp\left(a_0 + a_1 V_1 + a_2 V_1^2 + ... + a_m V_1^m\right) \\ \times \exp\left(b_0 + b_1 V_2 + b_2 V_2^2 + ... + b_m V_2^m\right) \end{aligned} \tag{3.2}$$

where $T_1(\cdot)$ and $T_2(\cdot)$ are the transfer functions of the first and second EAM. The voltage $V_1 = V_{b1} + V_{rf1}$, and $V_2 = V_{b2} + V_{rf2}$ denote the driving voltages to the first and second EAM, where V_{b1} and V_{b2} are bias voltages. The coefficients a_k and b_k ($k = 0,1,2...m$) are related to the transfer function of the first and second EAM, respectively. Suppose that the RF signal is given by $V_{rf1} = V_0 \cos(2\pi ft)$ for the first EAM and thus $V_{rf2} = V_0 \cos(2\pi ft + \phi)$ for the second EAM, where f, V_0 and ϕ are the RF, modulation voltage and phase shift between the two cascaded EAMs.

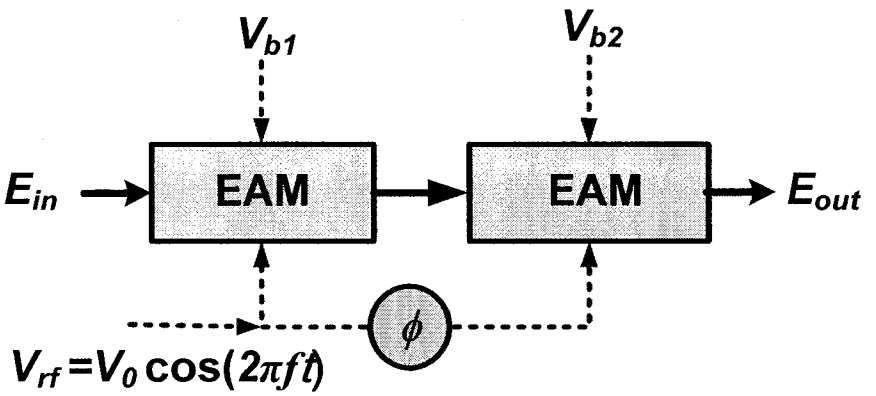

Figure 3.1 Configuration of two cascaded EAMs

3.3 Theoretical Analysis

In this section, a theoretical analysis of the proposed OFM technique using two cascaded EAMs is presented. Both use of two cascaded EAMs with identical characteristics and use of two cascaded EAMs with different characteristics will be investigated.

3.3.1 Use of Two Cascaded EAMs with Identical Characteristics

With the same transfer function, the two cascaded EAMs are also applied by the same bias voltage V_b and input RF modulation voltage V_0. The phase shift between the two EAMs is 180°. By assuming that the highest order of transfer function of the EAM is 7, then the transfer function of the two-cascaded EAMs structure can be written as

$$T(V)=\exp\left(a_0+a_1V_1+a_2V_1^2+\ldots+a_7V_1^7+a_0+a_1V_2 +a_2V_2^2+\ldots+a_7V_2^7\right), \tag{3.3}$$

where

$$V_1=V_b\left(1+m\cos 2\pi ft\right), \tag{3.4}$$

$$V_2=V_b\left(1-m\cos 2\pi ft\right), \tag{3.5}$$

where $m = V_0 / V_b$ is the RF modulation index and $a_i (i = 1,2,...,7)$ are the coefficient of the transfer function. In order to avoid clipping, we should have $V_b \le V_{b\max} / (1+m)$. Substituting Eqs. (3.4) and (3.5) into Eq. (3.3), then we can get the optical power

$$\begin{aligned} P_{out}(t) = P_{in} \exp\big[& a_0 + a_1 V_b (1 + m\cos 2\pi ft) + ... + a_7 V_b^7 (1 + m\cos 2\pi ft)^7 \\ & + a_0 + a_1 V_b (1 - m\cos 2\pi ft) + ... + a_7 V_b^7 (1 - m\cos 2\pi ft)^7 \big] \end{aligned}, \tag{3.6}$$

and Eq. (3.6) can reduces to

$$P_{out}(t) = P_{in} \exp(\gamma_0) \exp(\gamma_1 \cos 4\pi ft + \gamma_2 \cos 8\pi ft + \gamma_3 \cos 12\pi ft), \tag{3.7}$$

where $\gamma_i (i = 0,1,2,3)$ are expressions depended on V_b , a_i and m . The expressions of $\gamma_i (i = 0,1,2,3)$ are written as follows.

$$\begin{aligned} \gamma_0 = {} & 2a_0 + 2a_1 V_b + V_b^2 a_2 (2 + m^2) + V_b^3 a_3 (2 + 3m^2) \\ & + V_b^4 a_4 \left(2 + 6m^2 + \frac{3}{4} m^4\right) + V_b^5 a_5 \left(2 + 10m^2 + \frac{15}{4} m^4\right) \\ & + V_b^6 a_6 \left(2 + 15m^2 + \frac{45}{4} m^4 + \frac{5}{8} m^6\right) + V_b^7 a_7 \left(2 + 21m^2 + \frac{105}{4} m^4 + \frac{35}{8} m^6\right) \end{aligned}, \tag{3.8}$$

$$\begin{aligned} \gamma_1 = {} & V_b^2 a_2 m^2 + 3V_b^3 a_3 m^2 + V_b^4 a_4 (6m^2 + m^4) + V_b^5 a_5 (10m^2 + 5m^4) \\ & + V_b^6 a_6 \left(15m^2 + 15m^4 + \frac{15}{16} m^6\right) + V_b^7 a_7 \left(21m^2 + 35m^4 + \frac{105}{16} m^6\right) \end{aligned}, \tag{3.9}$$

$$\gamma_2 = \tfrac{1}{4} V_b^4 a_4 m^4 + \frac{5}{4} V_b^5 a_5 m^4 + V_b^6 a_6 \left(\frac{15}{4} m^4 + \tfrac{3}{8} m^6\right) + V_b^7 a_7 \left(\frac{35}{4} m^4 + \frac{21}{8} m^6\right), \tag{3.10}$$

$$\gamma_3 = \frac{1}{16} V_b^6 a_6 m^6 + \frac{7}{16} V_b^7 a_7 m^6 . \tag{3.11}$$

From Eq. (3.7), we can see that odd-order harmonics are suppressed in this case. We wrote the Eq. (3.7) as

$$P_{out}(t) = P_{in} \exp(\gamma_0) \exp(\gamma_1 \cos \Omega_1 t + \gamma_2 \cos \Omega_2 t + \gamma_3 \cos \Omega_3 t), \tag{3.12}$$

where $\Omega_1 = 4\pi f, \Omega_2 = 8\pi f, \Omega_3 = 12\pi f$.

It is known that

$$\exp(\gamma_i \cos\Omega_i t) = \sum_{n_i=-\infty}^{\infty} I_{n_i}(\gamma_i)\exp(jn_i\Omega_i t), \tag{3.13}$$

where $I_{n_i}(\gamma_i)$ is the Bessel function of the first kind of order n_i. So the Eq. (3.12) can be expressed as

$$\begin{aligned} P_{out}(t) &= P_{in}\exp(\gamma_0)\times\left[\sum_{n_1=-\infty}^{\infty} I_{n_1}(\gamma_1)\exp(jn_1\Omega_1 t)\right]\times\left[\sum_{n_2=-\infty}^{\infty} I_{n_2}(\gamma_2)\exp(jn_2\Omega_2 t)\right] \\ &\times\left[\sum_{n_3=-\infty}^{\infty} I_{n_3}(\gamma_3)\exp(jn_3\Omega_3 t)\right] \\ &= \exp(2a_0)\exp(\gamma_0)\sum_{n_1,n_2,n_3=-\infty}^{\infty} I_{n_1}(\gamma_1)I_{n_2}(\gamma_2)I_{n_3}(\gamma_3)\exp\left[j(n_1\Omega_1 + n_2\Omega_2 + n_3\Omega_3)t\right] \end{aligned} \tag{3.14}$$

where

$$n_1\Omega_1 + n_2\Omega_2 + n_3\Omega_3 = 4(n_1 + 2n_2 + 3n_3)\pi f = 4n\pi f, \tag{3.15}$$

then

$$n = n_1 + 2n_2 + 3n_3 . \tag{3.16}$$

From Eq. (3.15), we can get $2(n_2 + n - n_1) = 3(n - n_1 - n_3)$, then

$$\begin{cases} n_2 = 3k + n_1 - n \\ n_3 = n - n_1 - 2k \end{cases} \quad k \in Z . \tag{3.17}$$

Substituting Eqs. (3.15)-(3.17) into Eq. (3.14), the transfer function can be expressed by

$$\begin{aligned} P_{out}(t) = P_{in}\exp(\gamma_0)\sum_{n=-\infty}^{\infty}\left[\sum_{n_1=-\infty}^{\infty}\sum_{k=-\infty}^{\infty} I_{n_1}(\gamma_1)I_{3k+n_1-n}(\gamma_2)I_{n-n_1-2k}(\gamma_3)\right]. \\ \times\exp(j4n\pi ft) \end{aligned} \tag{3.18}$$

Then we can get the output power at $2n$ times of driving RF frequency:

$$P_{out}(2nf) = 2P_{in}\exp(\gamma_0)\sum_{n_1=-\infty}^{\infty}\sum_{k=-\infty}^{\infty} I_{n_1}(\gamma_1) I_{3k+n_1-n}(\gamma_2) I_{n-n_1-2k}(\gamma_3). \tag{3.19}$$

Then electrical current and the electrical power after photodetector can be calculated through $I = \Re P_{out}$ and $P_{rf} = \frac{1}{2} I^2$, where $\Re$ is responsibility of photodetector.

3.3.2 Use of Two Cascaded EAMs with Different Characteristics

When the two cascaded EAMs have different transfer functions, it is still possible that the first order harmonic is suppressed at certain sets of bias voltages, RF modulation voltage and phase shift. In this case, the transfer function shown in Eq. (3.2) should be used. Assume that $m = n = 7$, and substituting $V_{rf1} = V_0\cos(2\pi ft)$ and $V_{rf2} = V_0\cos(2\pi ft + \phi)$ into Eq. (3.2) and the output optical field can be written by

$$\begin{aligned}
\frac{E_{out}(t)}{E_{in}(t)} &= \exp\left\{\frac{1}{2}a_0 + \frac{1}{2}a_1\left(V_{b1} + V_0\cos(2\pi ft)\right) + \cdots + \frac{1}{2}a_m\left(V_{b1} + V_0\cos(2\pi ft)\right)^m \right. \\
&\left. + \frac{1}{2}b_0 + \frac{1}{2}b_1\left[V_{b2} + V_0\cos(2\pi ft + \phi)\right] + \cdots + \frac{1}{2}b_m\left[V_{b2} + V_0\cos(2\pi ft + \phi)\right]^m\right\} \\
&= \exp\left[\alpha_0 + \alpha_1\cos(2\pi ft) + \alpha_2\cos(4\pi ft) + \ldots + \alpha_m\cos(2m\pi ft)\right. \\
&\left. \beta_0 + \beta_1\cos(2\pi ft + \phi) + \beta_2\cos 2(2\pi ft + \phi) + \ldots + \beta_m\cos m(2\pi ft + \phi)\right] \\
&= \exp(\gamma_0)\exp\left[\gamma_1\cos(2\pi ft + \phi_1) + \gamma_2\cos(4\pi ft + \phi_2) + \ldots + \gamma_m\cos(2m\pi ft + \phi_m)\right]
\end{aligned} \tag{3.20}$$

where $E_{in}(t)$ is the input optical field, α_k $(k = 0,1,...,m)$ and β_k $(k = 1,...,m)$ are dependent on V_{b1}, V_{b2}, a_k, b_k, V_0 and ϕ. $\gamma_k = \sqrt{\alpha_k^2 + \beta_k^2 + 2\alpha_k\beta_k\cos k\phi}$, $\phi_k = \tan^{-1}\left(\frac{\beta_k\sin\phi}{\alpha_k + \beta_k\cos\phi}\right)$. The expressions of α_k and β_k are changed with different m. Assuming that $m = 7$ as before, α_k and β_k $(k = 0,1,...,7)$ can be given as

$$\alpha_0 = \frac{1}{2}V_0^2 a_2 + \frac{3}{8}V_0^4 a_4 + \frac{5}{16}V_0^6 a_6 + V_{b1}\left(a_1 + \frac{3}{2}V_0^2 a_3 + \frac{15}{8}V_0^4 a_5 + \frac{35}{16}V_0^6 a_7\right)$$
$$+V_{b1}^2\left(a_2 + 3V_0^2 a_4 + \frac{45}{8}V_0^4 a_6\right) + V_{b1}^3\left(a_3 + 5V_0^2 a_5 + \frac{105}{8}V_0^4 a_7\right) \quad , \qquad (3.21)$$
$$+V_{b1}^4\left(a_4 + \frac{15}{2}V_0^2 a_6\right) + V_{b1}^5\left(a_5 + \frac{21}{2}V_0^2 a_7\right) + V_{b1}^6 a_6 + V_{b1}^7 a_7$$

$$\alpha_1 = V_0 a_1 + \frac{3}{4}V_0^3 a_3 + \frac{5}{8}V_0^5 a_5 + \frac{35}{64}V_0^7 a_7 + V_{b1}\left(2V_0 a_2 + 3V_0^3 a_4 + \frac{15}{4}V_0^5 a_6\right)$$
$$+V_{b1}^2\left(3V_0 a_3 + \frac{15}{2}V_0^3 a_5 + \frac{105}{8}V_0^5 a_7\right) + V_{b1}^3\left(4V_0 a_4 + 15V_0^3 a_6\right) \quad , \qquad (3.22)$$
$$+V_{b1}^4\left(5V_0 a_5 + \frac{105}{4}V_0^3 a_7\right) + 6V_{b1}^5 V_0 a_6 + 7V_{b1}^6 V_0 a_7$$

$$\alpha_2 = \frac{1}{2}V_0^2 a_2 + \frac{1}{2}V_0^4 a_4 + \frac{15}{32}V_0^6 a_6 + V_{b1}\left(a_1 + \frac{3}{2}V_0^2 a_3 + \frac{5}{2}V_0^4 a_5 + \frac{105}{32}V_0^6 a_7\right)$$
$$+V_{b1}^2\left(3V_0^2 a_4 + \frac{15}{2}V_0^4 a_6\right) + V_{b1}^3\left(5V_0^2 a_5 + \frac{35}{2}V_0^4 a_7\right) \quad , \qquad (3.23)$$
$$+\frac{15}{2}V_{b1}^4 V_0^2 a_6 + \frac{21}{2}V_{b1}^5 V_0^2 a_7$$

$$\alpha_3 = \frac{1}{4}V_0^3 a_3 + \frac{5}{16}V_0^5 a_5 + \frac{21}{64}V_0^7 a_7 + V_{b1}\left(V_0^3 a_4 + \frac{15}{8}V_0^5 a_6\right)$$
$$+V_{b1}^2\left(\frac{5}{2}V_0^3 a_5 + \frac{105}{16}V_0^5 a_7\right) + 5V_{b1}^3 V_0^3 a_6 + \frac{35}{4}V_{b1}^4 V_0^3 a_7 \quad , \qquad (3.24)$$

$$\alpha_4 = \frac{1}{8}V_0^4 a_4 + \frac{3}{16}V_0^6 a_6 + V_{b1}\left(\frac{5}{8}V_0^4 a_5 + \frac{21}{16}V_0^6 a_7\right) + \frac{15}{8}V_{b1}^2 V_0^4 a_6 + \frac{35}{8}V_{b1}^3 V_0^4 a_7 , \qquad (3.25)$$

$$\alpha_5 = \frac{1}{16}V_0^5 a_5 + \frac{7}{64}V_0^7 a_7 + \frac{3}{8}V_1 V_0^5 a_6 + \frac{21}{16}V_{b1}^2 V_0^5 a_7 , \qquad (3.26)$$

$$\alpha_6 = \frac{1}{32}V_0^6 a_6 + \frac{7}{32}V_{b1} V_0^6 a_7 , \qquad (3.27)$$

$$\alpha_7 = \frac{1}{64} V_0^7 a_7 , \tag{3.28}$$

$$\begin{aligned}\beta_0 = {} & \frac{1}{2} V_0^2 b_2 + \frac{3}{8} V_0^4 b_4 + \frac{5}{16} V_0^6 b_6 + V_{b2}\left(b_1 + \frac{3}{2} V_0^2 b_3 + \frac{15}{8} V_0^4 b_5 + \frac{35}{16} V_0^6 b_7 \right) \\ & + V_{b2}^2 \left(b_2 + 3V_0^2 b_4 + \frac{45}{8} V_0^4 b_6 \right) + V_{b2}^3 \left(b_3 + 5V_0^2 b_5 + \frac{105}{8} V_0^4 b_7 \right) \\ & + V_{b2}^4 \left(b_4 + \frac{15}{2} V_0^2 b_6 \right) + V_{b2}^5 \left(b_5 + \frac{21}{2} V_0^2 b_7 \right) + V_{b2}^6 b_6 + V_{b2}^7 b_7 \end{aligned} , \tag{3.29}$$

$$\begin{aligned}\beta_1 = {} & V_0 b_1 + \frac{3}{4} V_0^3 b_3 + \frac{5}{8} V_0^5 b_5 + \frac{35}{64} V_0^7 b_7 + V_{b2}\left(2V_0 b_2 + 3V_0^3 b_4 + \frac{15}{4} V_0^5 b_6 \right) \\ & + V_{b2}^2 \left(3V_0 b_3 + \frac{15}{2} V_0^3 b_5 + \frac{105}{8} V_0^5 b_7 \right) + V_{b2}^3 \left(4V_0 b_4 + 15V_0^3 b_6 \right) \\ & + V_{b2}^4 \left(5V_0 b_5 + \frac{105}{4} V_0^3 b_7 \right) + 6V_{b2}^5 V_0 b_6 + 7V_{b2}^6 V_0 b_7 \end{aligned} , \tag{3.30}$$

$$\begin{aligned}\beta_2 = {} & \frac{1}{2} V_0^2 b_2 + \frac{1}{2} V_0^4 b_4 + \frac{15}{32} V_0^6 b_6 + V_{b2}\left(b_1 + \frac{3}{2} V_0^2 b_3 + \frac{5}{2} V_0^4 b_5 + \frac{105}{32} V_0^6 b_7 \right) \\ & + V_{b2}^2 \left(3V_0^2 b_4 + \frac{15}{2} V_0^4 b_6 \right) + V_{b2}^3 \left(5V_0^2 b_5 + \frac{35}{2} V_0^4 b_7 \right) \\ & + \frac{15}{2} V_{b2}^4 V_0^2 b_6 + \frac{21}{2} V_{b2}^5 V_0^2 b_7 \end{aligned} , \tag{3.31}$$

$$\begin{aligned}\beta_3 = {} & \frac{1}{4} V_0^3 b_3 + \frac{5}{16} V_0^5 b_5 + \frac{21}{64} V_0^7 b_7 + V_{b2}\left(V_0^3 b_4 + \frac{15}{8} V_0^5 b_6 \right) \\ & + V_{b2}^2 \left(\frac{5}{2} V_0^3 b_5 + \frac{105}{16} V_0^5 b_7 \right) + 5V_{b2}^3 V_0^3 a_6 + \frac{35}{4} V_{b2}^4 V_0^3 a_7 \end{aligned} , \tag{3.32}$$

$$\beta_4 = \frac{1}{8} V_0^4 b_4 + \frac{3}{16} V_0^6 b_6 + V_{b2}\left(\frac{5}{8} V_0^4 b_5 + \frac{21}{16} V_0^6 b_7 \right) + \frac{15}{8} V_{b2}^2 V_0^4 b_6 + \frac{35}{8} V_{b2}^3 V_0^4 b_7 , \tag{3.33}$$

$$\beta_5 = \frac{1}{16} V_0^5 b_5 + \frac{7}{64} V_0^7 b_7 + \frac{3}{8} V_{b2} V_0^5 b_6 + \frac{21}{16} V_{b2}^2 V_0^5 b_7 , \tag{3.34}$$

$$\beta_6 = \frac{1}{32}V_0^6 b_6 + \frac{7}{32}V_{b2}V_0^6 b_7, \tag{3.35}$$

$$\beta_7 = \frac{1}{64}V_0^7 b_7. \tag{3.36}$$

Using Sonine's expansion $\exp(z\cos\theta) = \sum_{n=-\infty}^{\infty} I_n(z)\exp(jn\theta)$ where $I_n(\cdot)$ is the modified Bessel function of the first kind of order n, Eq. (3.20) can be rewritten as

$$E_{out}(t) = E_{in}(t)\sum_{n=-\infty}^{\infty}\eta_n \exp\left[jn\left(2\pi ft + \phi_1\right)\right], \tag{3.37}$$

where η_n is the relative amplitude of the optical field component at frequency nf with respect to the optical carrier given by

$$\begin{aligned}\eta_n = \exp(\gamma_0) &\sum_{n_2,\ldots n_m=-\infty}^{\infty} I_{n-2n_2-\ldots-mn_m}(\gamma_1) \\ &\times\prod_{k=2}^{m} I_{n_k}(\gamma_k)\exp\left[j\sum_{k=2}^{m} n_k(\phi_k - k\phi_1)\right].\end{aligned} \tag{3.38}$$

Then the optical power of each sideband at frequency nf can be expressed by

$$P_{opt}(nf) = P_{in}|\eta_n|^2, \tag{3.39}$$

where P_{in} is the input optical power to the cascaded EAMs.

When it comes to the calculation of the RF power at nf, the optical power should be used instead of optical field. The output optical power can be written by

$$\begin{aligned}\frac{P_{out}(t)}{P_{in}(t)} &= \exp\Big\{a_0 + a_1\left(V_{b1} + V_0\cos(2\pi ft)\right) + \cdots + a_m\left(V_{b1} + V_0\cos(2\pi ft)\right)^m \\ &\quad + b_0 + b_1\left[V_{b2} + V_0\cos(2\pi ft + \phi)\right] + \cdots + b_m\left[V_{b2} + V_0\cos(2\pi ft + \phi)\right]^m\Big\} \\ &= \exp\Big[\alpha_0' + \alpha_1'\cos(2\pi ft) + \alpha_2'\cos(4\pi ft) + \ldots + \alpha_m'\cos(2m\pi ft) \\ &\quad \beta_0' + \beta_1'\cos(2\pi ft + \phi) + \beta_2'\cos 2(2\pi ft + \phi) + \ldots + \beta_m'\cos m(2\pi ft + \phi)\Big] \\ &= \exp(\gamma_0')\exp\Big[\gamma_1'\cos(2\pi ft + \phi_1') + \gamma_2'\cos(4\pi ft + \phi_2') + \ldots + \gamma_m'\cos(2m\pi ft + \phi_m')\Big]\end{aligned} \tag{3.40}$$

where $\alpha_k' = 2\alpha_k$, $\beta_k' = 2\beta_k$, $\gamma_k' = \sqrt{\alpha_k'^2 + \beta_k'^2 + 2\alpha_k'\beta_k'\cos k\phi}$, and $\phi_k' = \tan^{-1}\left(\frac{\beta_k'\sin\phi}{\alpha_k' + \beta_k'\cos\phi}\right)$.

Using Sonine's expansion as before, Eq. (3.40) can be rewritten as

$$P_{out}(t) = P_{in}(t)\sum_{n=-\infty}^{\infty}\delta_n\exp\left[jn\left(2\pi ft + \phi_1'\right)\right] \tag{3.41}$$

where δ_n is the relative amplitude of the optical power component at frequency nf with respect to the optical carrier given by

$$\begin{aligned}\eta_n' &= \exp(\gamma_0')\sum_{n_2,\ldots n_m=-\infty}^{\infty} I_{n-2n_2-\ldots-mn_m}(\gamma_1') \\ &\quad \times\prod_{k=2}^{m} I_{n_k}(\gamma_k')\exp\left[j\sum_{k=2}^{m} n_k\left(\phi_k' - k\phi_1'\right)\right].\end{aligned} \tag{3.42}$$

The photocurrent can be calculated through

$$I = \tfrac{1}{2}\Re\times\left|E_{out}(t)\right|^2 = \Re P_{in}\sum_{n=-\infty}^{\infty}\delta_n\exp\left[jn\left(2\pi ft + \varphi_1\right)\right] \tag{3.43}$$

where $\Re$ is responsibility of photodetector. Then the RF power at nf can be computed by

$$P_{rf}(nf) = 2\times 50\times\Re^2 P_{in}^2\left|\delta_n\right|^2. \tag{3.44}$$

To avoid clipping, for each of EAMs, the RF modulation voltage V_0 should satisfy:

$$V_0 \le \min\left(V_b, V_{b\max} - V_b\right). \tag{3.45}$$

3.3.3 Impact of Fiber Chromatic Dispersion

When the fiber dispersion is considered, by rewriting Eq. (3.40), the optical field can be expressed as

$$E_{out}(t) = E_{in}(t)\exp(-\alpha L/2)\sum_{n=-\infty}^{\infty}\eta_n \exp\left[j\frac{1}{2}\beta_2 L(2n\pi f)^2\right]\exp\left[jn(2\pi ft+\phi_1+\beta_1 L)\right] \quad (3.46)$$

where L and α are the length and loss of the fiber, respectively. β_1 is group velocity delay coefficient of the fiber. $\beta_2 = -\lambda^2 D/(2\pi c)$ is group velocity dispersion coefficient of the fiber and D is fiber dispersion.

Assuming that first-order sidebands are suppressed by technique proposed in Sections 3.31 and 3.32, an optical filter should be used to filter out all of optical harmonics higher than second harmonic before the optical signal is transmitted on the fiber. When the filter is used, the optical field can be expressed by

$$E_{out}(t) = E_{in}(t)\exp(-\alpha L/2)\sum_{k=-1}^{1}\eta_{2k} \exp\left[j\frac{1}{2}\beta_2 L(4k\pi f)^2\right]\exp\left[j2k(2\pi ft+\phi_1+\beta_1 L)\right]. \quad (3.47)$$

Then optical field at each sideband can be written as

$$E(2k) = E_{in}\exp(-\alpha L/2)\eta_{2k}\exp\left[j\frac{1}{2}\beta_2 L(4k\pi f)^2\right] \quad (3.48)$$

where $k = 0,\pm 1$, $E(0)$ is optical field at optical carrier and $E(2)$ and $E(-2)$ are optical field at two second-order sidebands.

At the base station, the photodetector converts the optical signal to electrical signal. Optical components will experience different phase shift due to chromatic dispersion as they propagate through the optical fiber. At the photodetetor these components will beat each other and generate different RF currents at $2f$ and $4f$. When the first-order sidebands are suppressed and higher-order sidebands are filtered out, only

optical carrier and two second-order sidebands are left. Therefore, the main contribution of RF currents at $2f$ is the beating between the optical carrier and the second-order optical sidebands, while RF current at $4f$ mainly consists of beating between the two second-order optical sidebands. Therefore, the current and RF power at $2f$ can be expressed as

$$\begin{aligned} i_{2f}(t) &= \Re 2\,\mathrm{Re}\left\{\left[E(2)E^*(0)+E(0)E^*(-2)\right]\exp(j4\pi ft)\right\} \\ &= 2\Re\left|E(2)E^*(0)+E(0)E^*(-2)\right|\cos(4\pi ft+\varphi) \end{aligned}, \tag{3.49}$$

$$\begin{aligned} P_{rf}(2f) &= \Re^2 R_L{}^2\left\langle i_{2f}^2(t)\right\rangle = 2\Re R_L{}^2\left|E(2)E^*(0)+E(0)E^*(-2)\right|^2 \\ &= 2\Re^2 R_L{}^2 P_{in}^2\exp(-2\alpha L)\left|\eta_0\eta_2\right|^2\times 4\cos^2\left(\frac{1}{2}\beta_2 L(4\pi f)^2\right) \end{aligned}, \tag{3.50}$$

where $\Re$ is responsibility of photodetector and R_L is resistance of circuit. The same as $2f$, the current and RF power at $4f$ can be presented by

$$\begin{aligned} i_{4f}(t) &= 2\Re\,\mathrm{Re}\left\{\left[E(2)E^*(-2)\right]\exp(j8\pi ft)\right\} \\ &= 2\Re\left|E(2)E^*(-2)\right|\cos\left(8\pi ft+\beta_2 L(4\pi f)^2\right) \end{aligned}, \tag{3.51}$$

$$\begin{aligned} P_{rf}(4f) &= \Re^2 R_L{}^2\left\langle i_{4f}^2(t)\right\rangle = 2\Re^2 R_L{}^2\left|E(2)E^*(-2)\right|^2 \\ &= 2\Re^2 R_L{}^2 P_{in}^2\exp(-2\alpha L)\left|\eta_2\right|^4 \end{aligned}. \tag{3.52}$$

From Eq. (3.52), we can see that the RF power fading caused by fiber dispersion is cancelled at $4f$ in this case, because RF power at $4f$ does not depend on fiber chromatic dispersion factor.

3.4 Analysis by Simulation

In this section, VPI Transmission Maker and Matlab have been used to verify the theory of the proposed technique. On the one hand, analysis based on Matlab is provided to prove the module of theories shown in Section 3.3; on the other hand, the proposed RoF

system is setup and simulated on VPI Transmission Maker to measure the performance of the system. The simulation system of mm-wave generation over fiber system using proposed technique is shown in Fig.3.2.

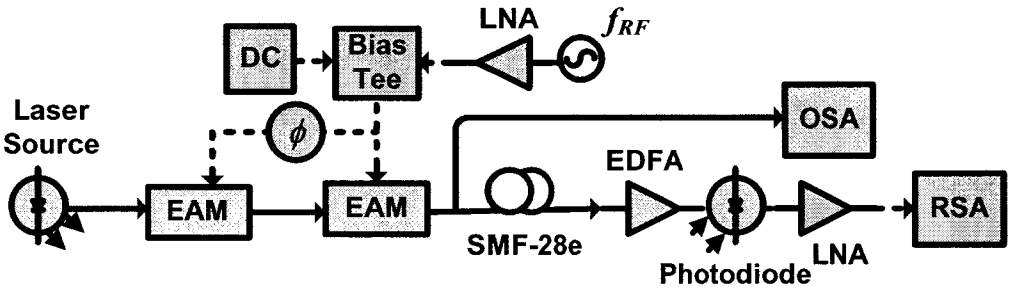

Figure 3.2 System setup for the mm-wave generation using proposed technique. DC: direct current, EDFA: erbium-doped fiber amplifier, RSA: RF spectrum analyzer, OSA: optical spectrum analyzer, LNA: low-noise amplifier and SMF: single-mode-fiber.

Three cases will be investigated. In the first two cases, the ideal situation is considered as follows. A continuous wave light from a laser source is assumed to have a wavelength of 1550 nm, output power of 0 dBm, and relative intensity noise (RIN) of -110 dB/Hz. The continuous wave light is injected into two cascaded EAMs, driven by an RF signal at frequency f =10 GHz. The phase shift between the cascaded EAMs is 180 degree. The output signal from the EAMs is injected into a single mode fiber (SMF), with chromatic dispersion of 16 ps/(nm.km). The optical signal is transmitted through fiber and detected by a high-speed PD with a 3 dB bandwidth of 40 GHz and a responsivity of 0.62 A/W. The bias voltages of the two cascaded EAMs and RF input power were placed under consideration, in order to compare 40 GHz mm-wave generation using the fourth harmonics. The mm-wave power at 40 GHz consists mainly of two beatings, one beating between the optical carrier and the fourth-order harmonic at

40 GHz, and the other beating between the two second-order harmonics at -20 and 20 GHz with respect to the optical carrier.

3.4.1 Case I: Use of Two Cascaded EAMs with Identical Characteristics

In this case, the parameters of the cascaded EAMs used in the simulation are as follows: $V_{b1} = V_{b2} = 1.7\,\mathrm{V}$, maximum bias $V_{b\max}$=4 V, average input power of the laser P_{in}= 1 mw and characteristics curve of the two EAMs are the same as shown in Fig.3.3, where the wavelength we used is 1553.5 nm and the insertion loss at 0 volt is -6.33 dB, and the parameters of the curve in Fig.3.3 is given by Eq. (3.53).

$$\begin{bmatrix} a_0 \\ a_1 \\ a_2 \\ a_3 \\ a_4 \\ a_5 \\ a_6 \\ a_7 \end{bmatrix} = \begin{bmatrix} 1.3544\text{e-}004 \\ -0.7044 \\ 2.6376 \\ -4.4730 \\ 3.5817 \\ -1.4969 \\ 0.3023 \\ -0.0232 \end{bmatrix}. \tag{3.53}$$

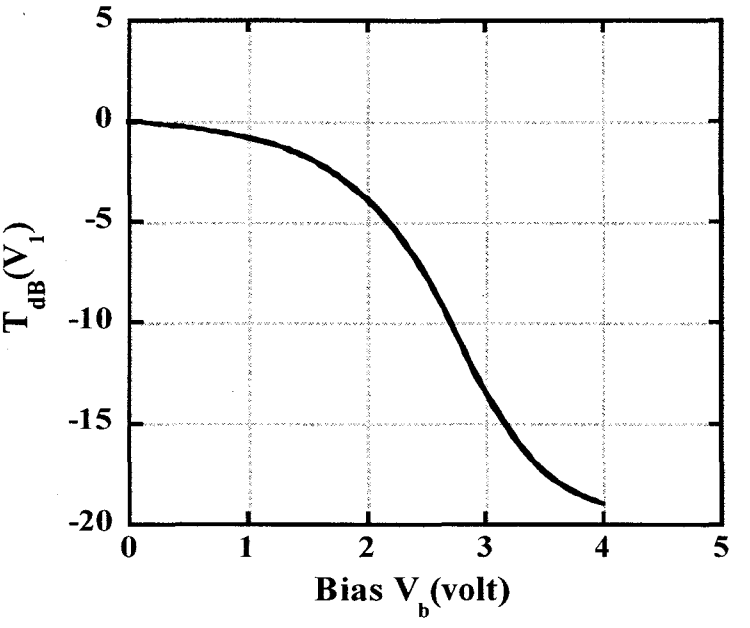

Figure 3.3 Characteristics of EAM Used in Simulation

3.4.1.1 Impact of RF Modulation Index and Bias Voltage

Firstly, how the electrical power at $2f$ and $4f$ changed with modulation index and bias voltage using two cascaded identical EAMs is investigated. At the photodetector, RF power at $2f$ mainly consists of current from the beating between optical carrier and the second-order optical sidebands since first-order sideband is suppressed. RF power at $4f$ is mainly contributed from two parts—beating between the two second-order harmonics and the other beating between the fourth-order harmonics and the optical carrier. Simulation results show that the optical power of two sidebands and optical carrier depended on modulation index and bias voltage. Figs. 3.4(a) and (b) show simulated (marks) and calculated (lines) electrical power at $2f$ and $4f$ versus modulation index and bias voltage, respectively. It is seen that the calculated and simulated agree well.

Fig. 3.4(a) shows that RF power at $2f$ and $4f$ increases with the increase of modulation index, because optical power of optical carrier and second-order harmonics is enhanced by increasing modulation index. Since modulation index should be not larger than 1, we fixed the modulation index at m=1 and swept bias voltage, and results are shown in Fig. 3.4(b) which shows that the maximum RF power at $2f$ is achieved at $V_b = 1.4$ V and at $4f$ is achieved at $V_b = 1.65$ V. The results in Fig. 3.4(b) are really depending on the transfer function of the cascaded EAMs. If the transfer function is changed, the results may be totally different.

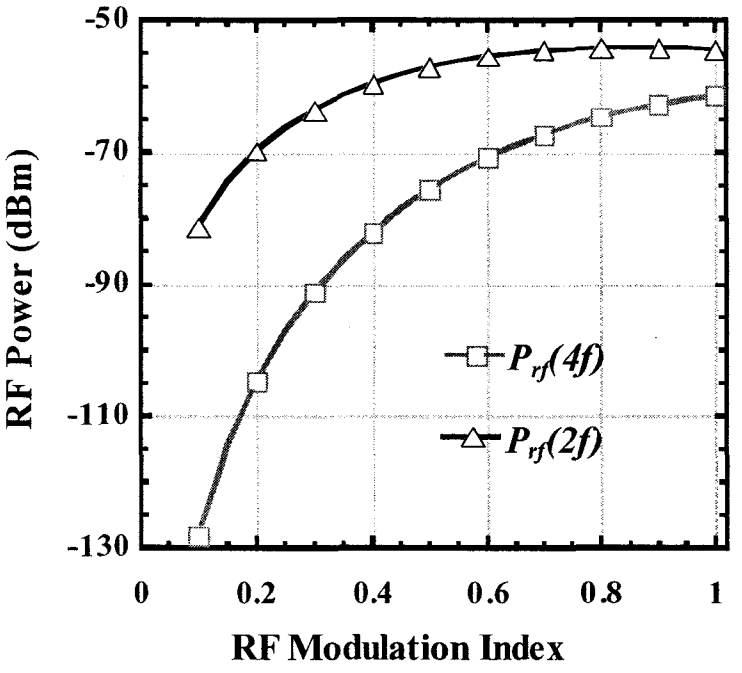

(a)

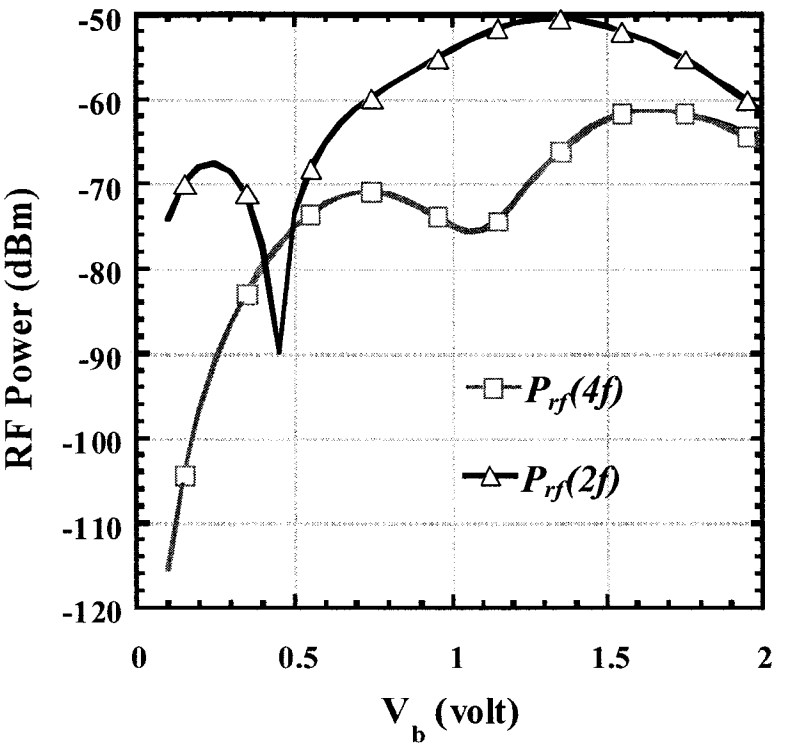

(b)

Figure 3.4 Performance of proposed OFM system using two cascaded EAMs with identical characteristics in both theory (lines) and simulation (marks) (a) RF power at $2f$ and $4f$ changed with modulation depth when $V_{b1} = V_{b2} = 1.7$ V; (b) RF power at $2f$ and $4f$ changed with bias when $m = 1$.

In back-to-back transmission, the electrical power at $2f$ and $4f$ is really depending on the modulation index and bias of the indicial two cascaded EAMs as shown in Fig. 3.4. The reason of these results is obviously seen from Eq. (3.6) which shows that the output power is determined by following parameters—modulation index, bias voltage and characteristics of the EAMs. In other words, if the characteristics of the EAMs were changed, the optimum modulation index and bias voltages would also be changed, and the performance of the whole system would be totally different too. So the choose of characteristics of the cascaded EAMs is another key issue to optimize the performance of

our system. It is possible that we can design EAMs to achieve the requirements of our system in the future research.

Fig. 3.5 shows the optical spectrum and electrical spectrum at m=1 and $V_b = 1.65$ V, and frequency of RF input f_{IF} is 10 GHz. From optical spectrum, it is clearly that only even order harmonics left and all odd order harmonics completely suppressed; and in the electrical field at -53.36 dB and -61.3 dB signal is generated at $2f$ and at $4f$, respectively.

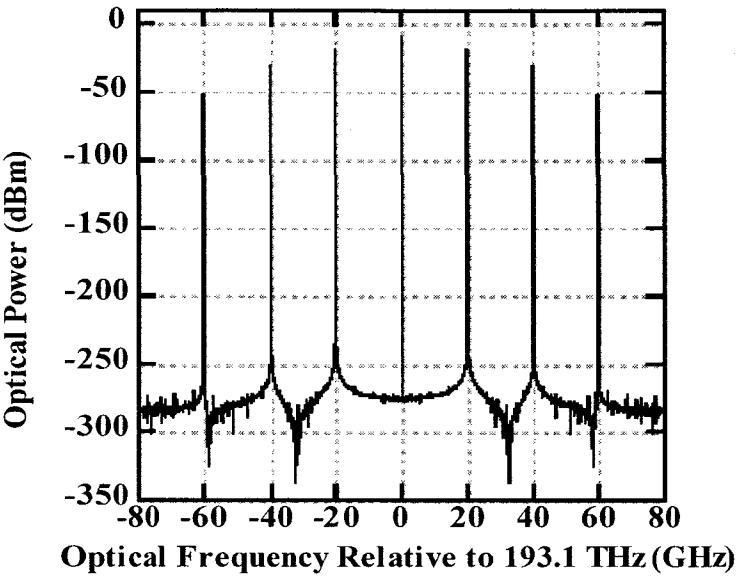

(a)

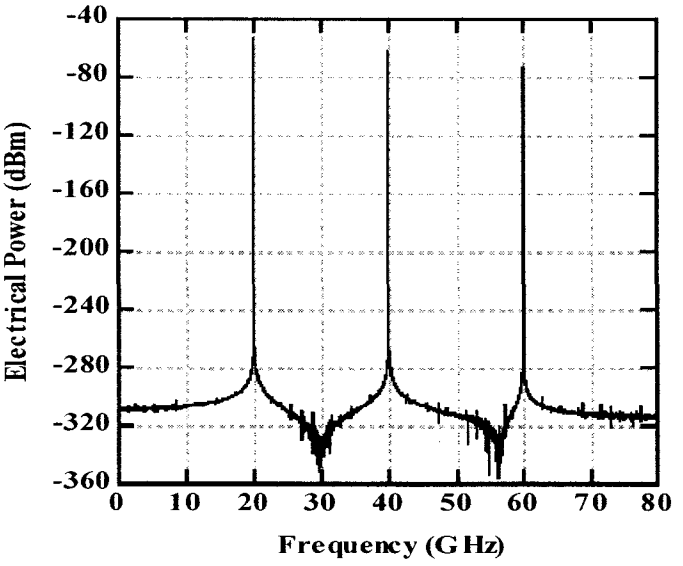

(b)

Figure 3.5 The spectrums of the system using two cascaded EAMs with identical characteristics (a) Optical spectrum (b) Electrical spectrum. m=1, $V_b = 1.65$ V and frequency of RF input f =10GHz.

3.4.1.2 Impact of Fiber Chromatic Dispersion

In Fig. 3.6, the impact of fiber chromatic dispersions, which induce power fading of the generated mm-wave signal, is investigated. It is supposed that the fiber have chromatic dispersion of $D = 16 \times 10^{-6} s/m^2$. Also, we compare the performance of system with and without using the optical filter in Fig. 3.6(a) and the bandwidth of optical filter is $B = 6f = 60$ GHz, which used to filter out the optical harmonics higher than second-order optical sidebands(at $\pm 2f$) such as fourth order and sixth order (at $\pm 4f$ and $\pm 6f$) optical sidebands. These optical components will experience different phase shift due to chromatic dispersion as they propagate through the optical fiber. At the photodetetor these components will beat each other and generate different RF currents at $2f$ and $4f$. For example, to generate RF currents at $2f$, 2nd order sidebands at $\pm 2f$ will beat with optical carrier and with 4th order sidebands at $\pm 4f$; to generate RF currents at $4f$, 2nd order sidebands at $\pm 2f$ will beat each other and with 6th order sidebands at $\pm 6f$, and 4th order sidebands at $\pm 4f$ will beat with the optical carrier. Because the different current will no longer be in phase when the fiber length changes there will periodically add constructively or destructively depending on the fiber length.

Fig. 3.6 (a) shows the impact of fiber dispersion on generated mm-wave signal at $4f$. The two dips of 3.5 km and 6 km (and repeat periodically at each 10km) come from two kinds of contribution that depends on the fiber length which are: one from beating between 2nd order sidebands at $\pm 2f$ and 6th order sidebands at $\pm 6f$, and the other from beating between 4th order sidebands at $\pm 4f$ and the optical carrier. By using optical filter to remove 4th and higher order optical sidebands the destructive interaction is removed and the dips disappeared at the expense of 9 dB loss compared to the constructive

interaction happening at 0 km (and repeat at each 10 km) in the case without optical filtering. Simulation results with the use of the filter perfectly match with the theory calculation.

Fig. 3.6 (b) shows the impact of fiber dispersion on generated signal at $2f$. It can be seen that there is not much difference between the performance with and without filter, because the main contribution to RF current at $2f$ is the beating between strong second-order optical sidebands and optical carrier, which is no difference whether by using the filter or not. As a result, a 20-km periodical constructive and destructive interaction happens with the dip of 10 km. Comparing Fig. 3.6 (a) and (b), it is seen that 20-km transmission is the best choice for both frequency doubling and quadrupling.

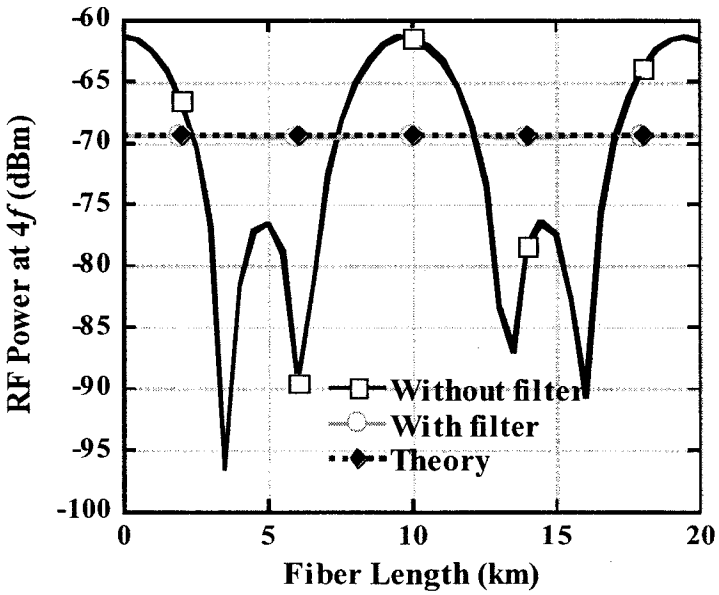

(a)

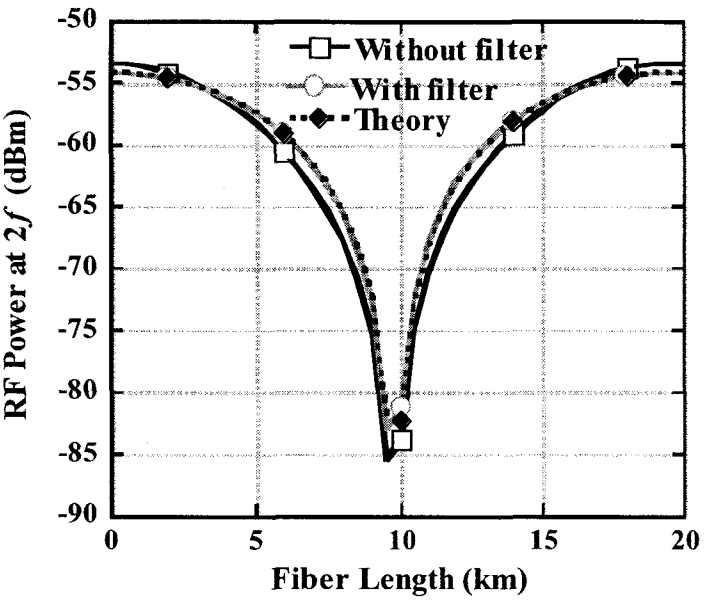

(b)

Figure 3.6 Performance of proposed OFM system using two cascaded EAMs with identical characteristics after signal transmitted over fiber: (a) electrical power at $4f$, (b) electrical power at $2f$, changes with fiber length with and without the optical filter ($B = 6f = 60$ GHz) while $V_b = 1.55$ V;

Case I is an ideal situation. In Case I, it is assumed that two cascaded EAMs have identical characteristics, and the applied bias voltage and RF voltage on the two EAMs are the same too. Moreover, phase shift between two EAMs should be exact 180 degree. However, in industry, it is hard to produce two EAMs with exactly same characteristics, which means that Case I is an ideal situation hardly to be realized. Furthermore, in real experimental environment, the existence of bias shifting and phase shifting may also influence the performance of the system, which will be investigated in Case II and Case III.

3.4.2 Case II: Use of Two Cascaded EAMs with Similar Characteristics

To simulate the unideal system, in this case, the two cascaded EAMs with similar characteristics are used in the simulation. It is assumed that the first EAM has the same parameter as we describe in previous section Eq. (3.53). The second EAM is different but similar with the first one. The characteristics of the second EAM is shown in Fig. 3.7 and parameters of the curve are:

$$\begin{bmatrix} b_0 \\ b_1 \\ b_2 \\ b_3 \\ b_4 \\ b_5 \\ b_6 \\ b_7 \end{bmatrix} = \begin{bmatrix} 0.0056 \\ -0.0920 \\ -0.0085 \\ 0.1028 \\ -0.0960 \\ 0.0160 \\ 0 \\ 0 \end{bmatrix}. \tag{3.54}$$

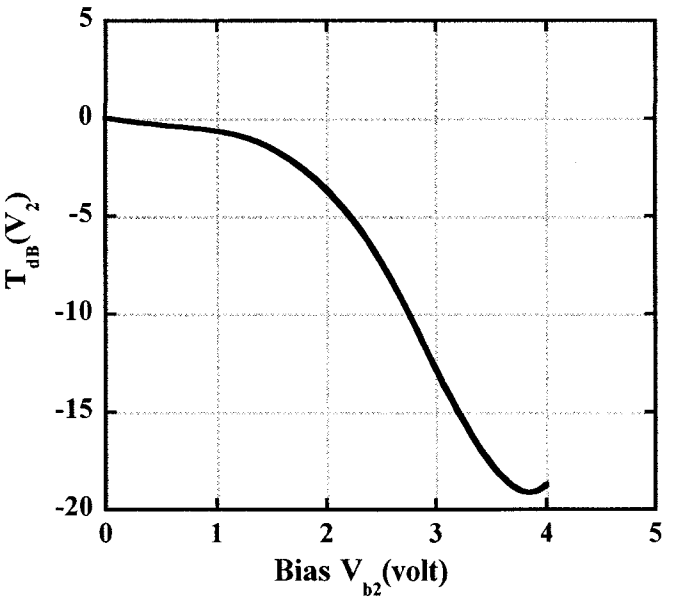

Figure 3.7 Characteristics of the second EAM used in simulation.

3.4.2.1 Impact of RF Modulation Index and Bias Voltage

In Section 3.3.2, we present the theoretical analysis of two cascaded EAMs with different characteristics. By assuming phase shift $\phi = 180^{\circ}$ and solving $\gamma_1 = 0$, where γ_1 is the parameter relating with first-order harmonics and depending on bias voltages V_{b1}, V_{b2} and RF modulation voltage V_0, we can get all the solution sets of these three variables (V_{b1}, V_{b2} and V_0) which satisfy $\gamma_1 = 0$ and resulting in suppression of the first-order optical sidebands. Parts of real roots of $\gamma_1 = 0$ are shown in Fig. 3.8, which shows that with the increasing of V_0, the number of solution groups is reduced. It is because $V_0 \le \min(V_b, V_{b\max} - V_b)$ must be satisfied to avoid clipping and as a result the range of bias voltages V_b becomes small when V_0 is high.

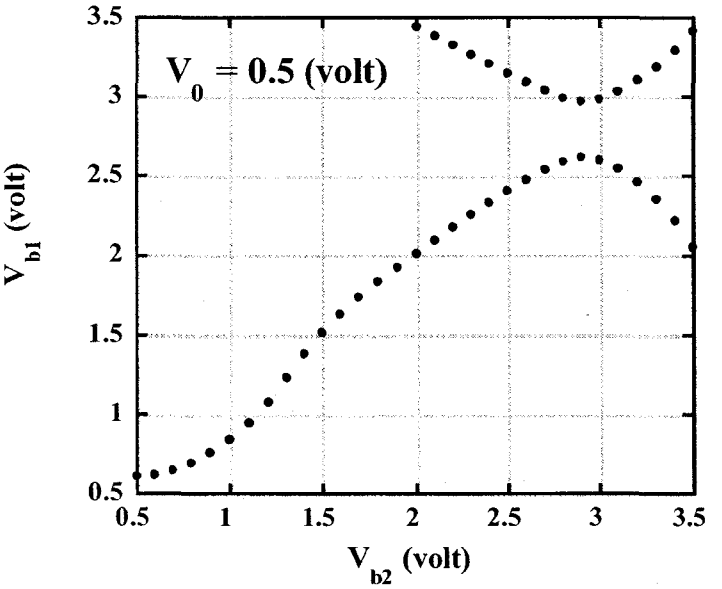

(a)

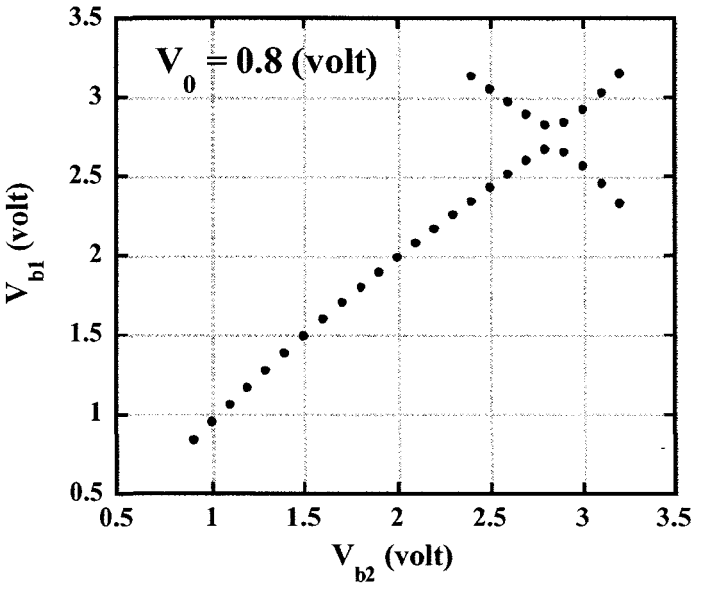
V0 = 0.8 (volt)
Vb1 (volt)
Vb2 (volt)
0.5
1
1.5
2
2.5
3
3.5

(b)

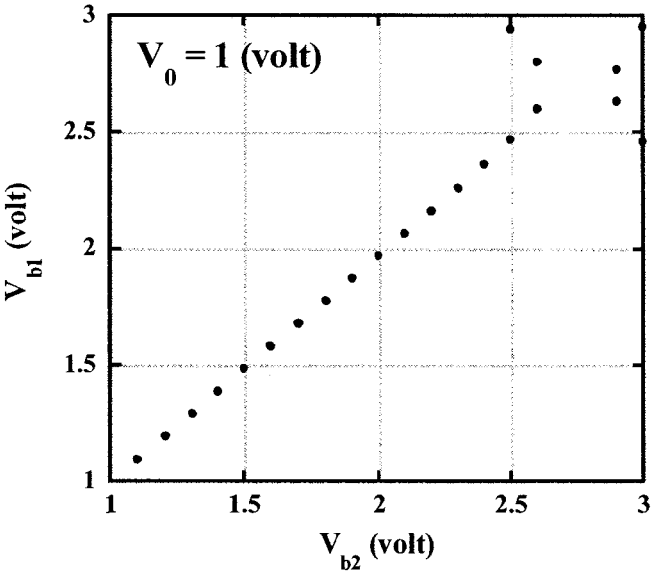
V0 = 1 (volt)
Vb1 (volt)
Vb2 (volt)
1
1.5
2
2.5
3

(c)

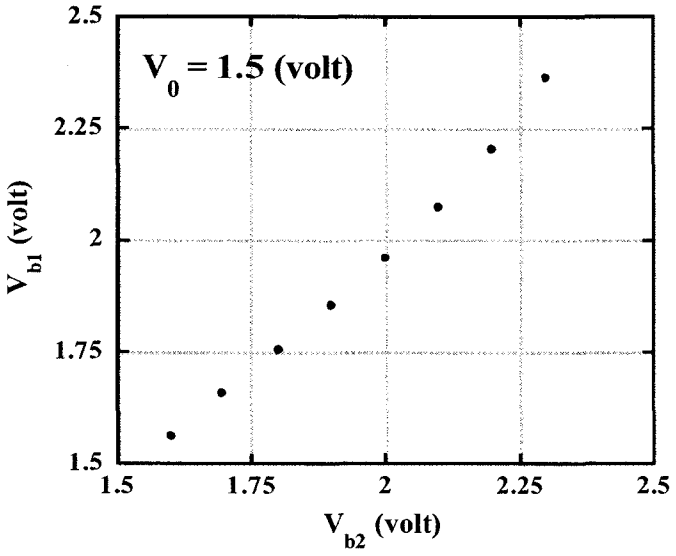

(d)

Figure 3.8 Values of V_{b1} and V_{b2} which satisfy that $\gamma_1 = 0$ to suppress the first order harmonic changed with V_0 in similar configuration system: (a) V_0=0.5 V (b) V_0=0.8 V (c) V_0=1 V and (d) V_0=1.5 V.

To find out which group of solution is the optimum one, all groups of solutions are put in the simulation system one by one to see which one can achieve the maximum ratio of optical power of second order harmonic comparing to that of first order harmonic. The simulation results are shown in Fig. 3.9. From the results, it is clear that almost all groups of solutions can achieve more than 30 dB suppressing of the first order harmonic, and the best one is 112 dB suppressing when, $V_{b1} = 1.3803$ V, $V_{b2} = 1.4$ V, and $V_0 = 0.5$ V. However, maybe this is not the optimum results, since we haven't listed out all the roots of the equation $\gamma_1 = 0$, and in fact, even if the bias voltages are not the roots of $\gamma_1 = 0$ but can achieve $\gamma_1 \cong 0$, the first-order harmonic can still be suppressed very well. Comparing to OFM techniques based on MZMs which have to be biased at the minimum or maximum point [3-5], the proposed technique take advantage that many ranges of bias voltages can work out.

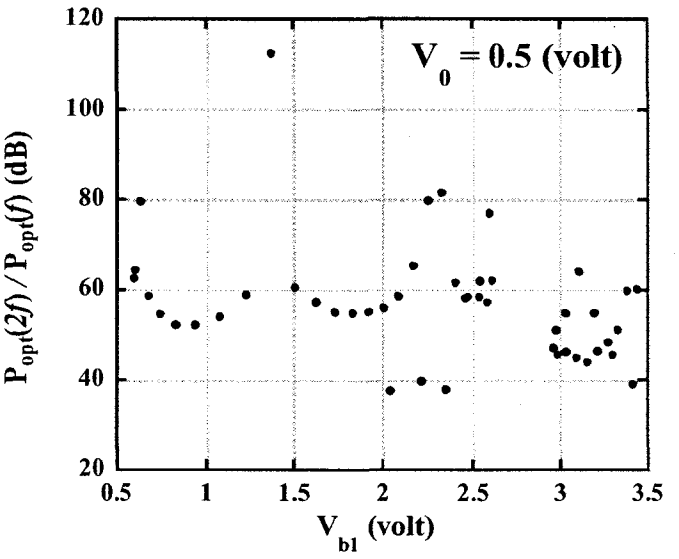

(a)

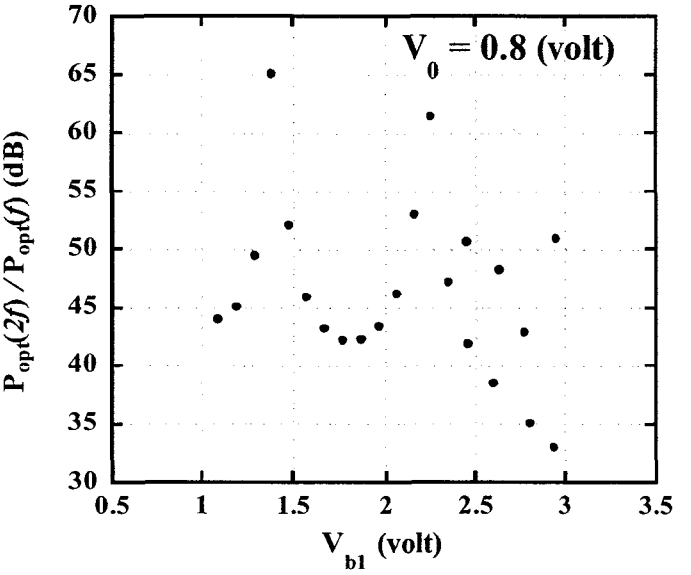
$V_0 = 0.8$ (volt)
$P_{opt}(2f) / P_{opt}(f)$ (dB)
V_{b1} (volt)
70
65
60
55
50
45
40
35
30
0.5
1
1.5
2
2.5
3
3.5

(b)

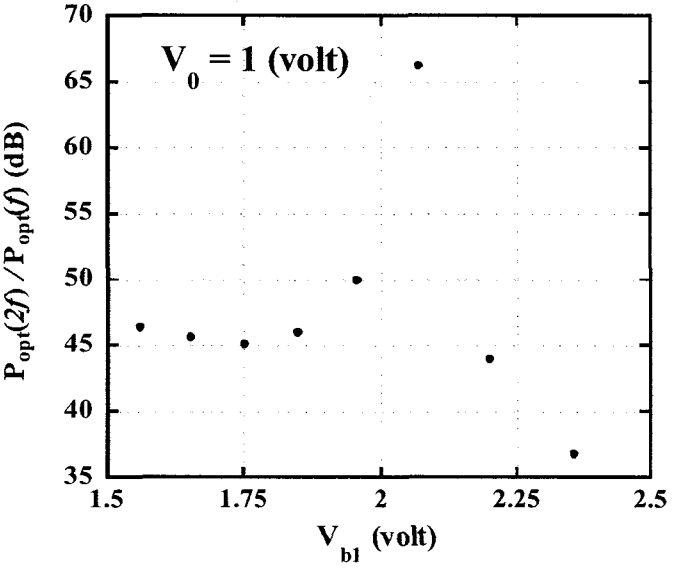
$V_0 = 1$ (volt)
$P_{opt}(2f) / P_{opt}(f)$ (dB)
V_{b1} (volt)
70
65
60
55
50
45
40
35
1.5
1.75
2
2.25
2.5

(c)

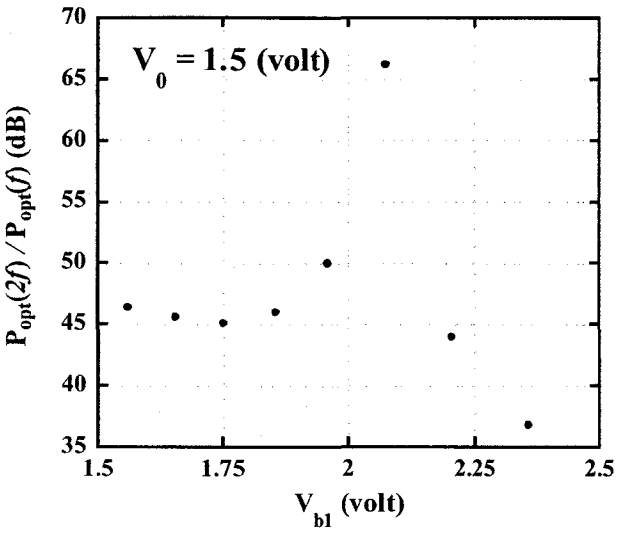

(d)

Figure 3.9 Power ratio of the second-order and first-order harmonics P_2 / P_1 for every group of solutions that make first order harmonic suppressed in similar configuration system: (a) V_0=0.5 V (b) V_0=0.8 V (c) V_0=1 V and (d) V_0=1.5 V.

3.4.2.2 Impact of Fiber Chromatic Dispersion

By choosing any group of solutions (V_{b1}, V_{b2} and V_0) is used in the simulation system, first-order harmonic is suppressed in the simulation result. In order to investigate impact of fiber chromatic dispersion on the system, one group of the solutions is chosen as follows: $V_{b1} = 1.1629$ V, $V_{b2} = 1.2$ V and $V_0 = 0.8$ V An optical filter with bandwidth of $B = 5f = 50$ GHz is still used in the system to filter out optical sidebands higher than second-order optical sidebands. Simulation results are shown in Fig. 3.10. From Fig. 3.10(a), we can see that there is 45 dB suppression of first order-harmonic related to second-order harmonic, and Fig. 3.10(b) shows that with the filter, the generated mm-wave signal at $4f$ is almost immune to fiber dispersion.

In this case, the situation is different from the case of the two cascaded EAM with identical characteristics. By comparing Fig. 3.10(a) with Fig. 3.5(a), it is obvious that odd-order sidebands are suppressed very well but still exit in Fig. 3.10(a), while in Fig. 3.5(a), odd-order sidebands are perfectly suppressed even without using an optical filter. As a result, in the system of two cascade EAMs with similar characteristics, odd-order components will also have contribution to generate RF current at $4f$, besides even-order components. For example, the beating between 1st order sideband at $-f$ and 3rd order sideband at $3f$, and the beating between 1st order sideband at f and 3rd order sideband at $-3f$ will also generate RF current at $4f$. This also explains why this system is not completely immune to fiber chromatic dispersion even when the optical filter is used as shown in Fig 3.10(b). It is also seen that theoretical result is 1 dB higher than simulation result, which is due to part of second-order sidebands filtered out by filter in the simulation. Fig. 3.10 (c) shows that the impact of fiber dispersion on signal at $2f$ has almost the same result as in Case I with a dip of 10 km.

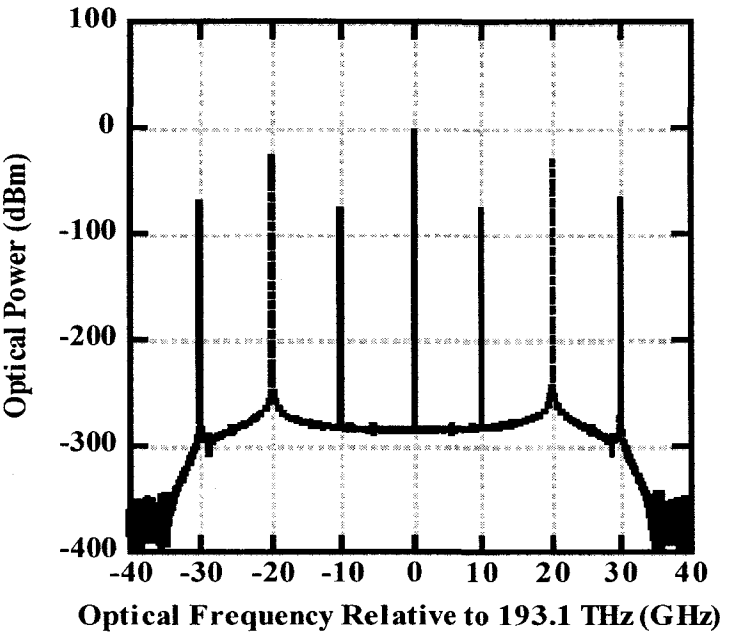
100
0
-100
-200
-300
-400
Optical Power (dBm)
-40 -30 -20 -10 0 10 20 30 40
Optical Frequency Relative to 193.1 THz (GHz)

(a)

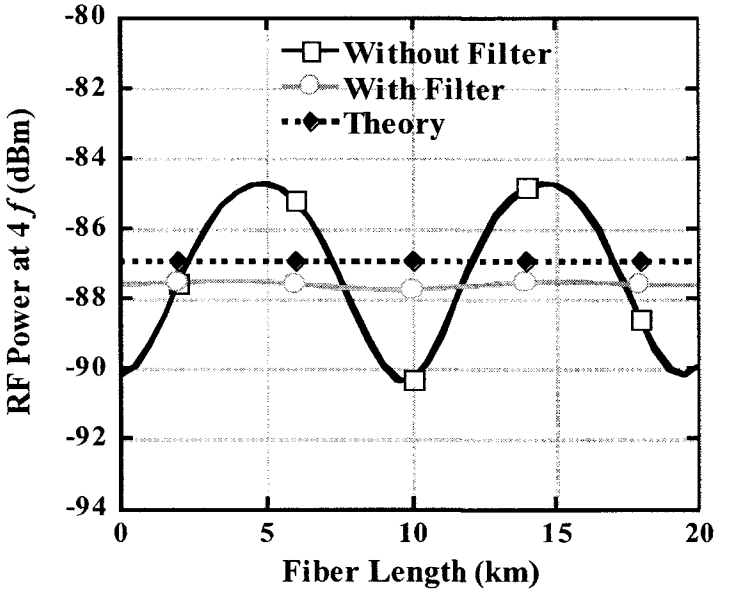
-80
-82
-84
-86
-88
-90
-92
-94
RF Power at 4 f (dBm)
Without Filter
With Filter
Theory
0 5 10 15 20
Fiber Length (km)

(b)

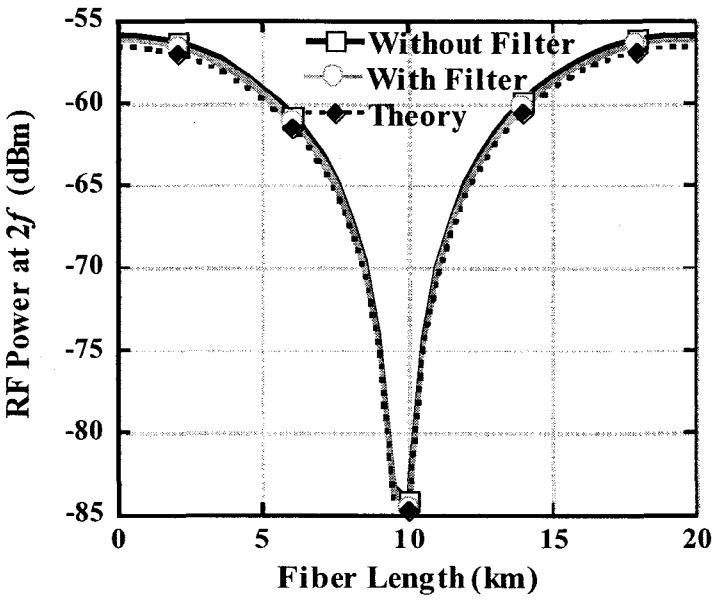

(c)

Figure 3.10 Simulation results of two-similar-EAM system: (a) Optical spectrum of signal after passing filter with $B = 5f = 50$ GHz; (b) electrical power at $4f$ changes with fiber length; (c) electrical power at $2f$ changes with fiber length.

3.4.2.3 Impact of Phase Shifting

The shifting problem may happen on phase shift. So the system sensitivity based on phase shift ($\Delta\phi$) between the two cascaded EAMs is investigated. In Fig. 3.12, we change $\Delta\phi$ from -10° to 10°, and the power ratio of second-order to the first-order harmonic changed with $\Delta\phi$. It is clear that the optical ration $P_{opt}(2f)/P_{opt}(f)$ decreases with the increase of $\Delta\phi$, but RF power at $2f$ and $4f$ does not change with phase shift, which means that our system is immune to phase shifting at frequency doubling and quadrupling. The reason is because the small change in phase shift didn't influence the optical power at second-order sidebands and optical carrier which have major contribution to the current at $2f$ and $4f$. But first-order optical sidebands are increasing

with the amount of $\Delta\phi$, which may increases the level of noise. However, there is still more than 10 dB suppression of first-order sidebands with 10 degree phase shifting when RF driving voltage V_0 is higher than 1 V.

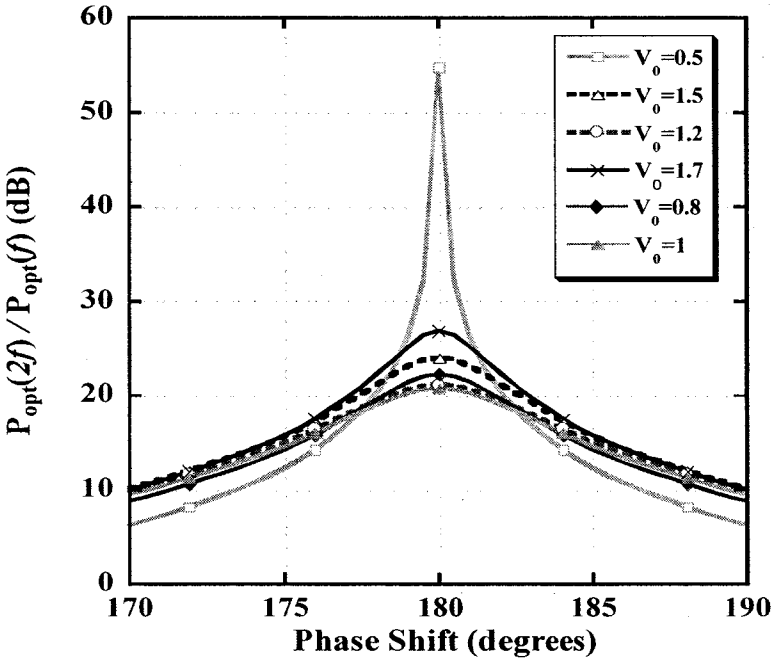

(a)

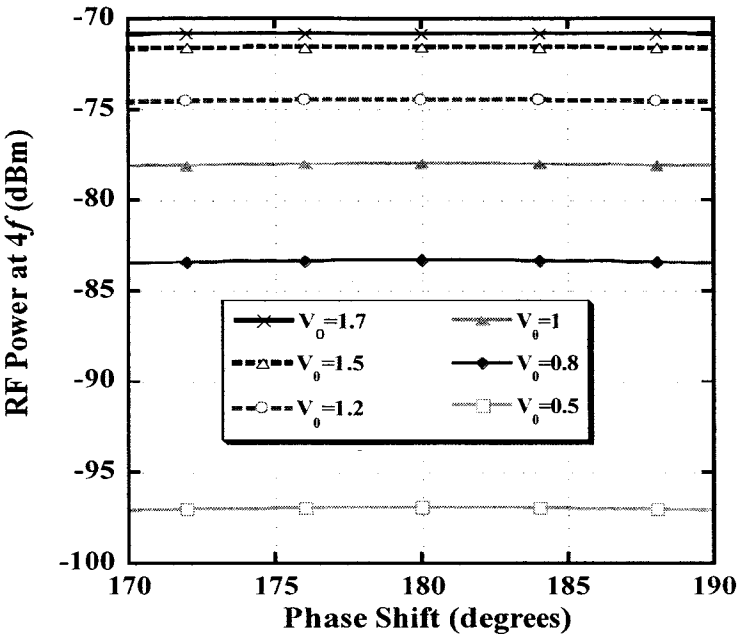

(b)

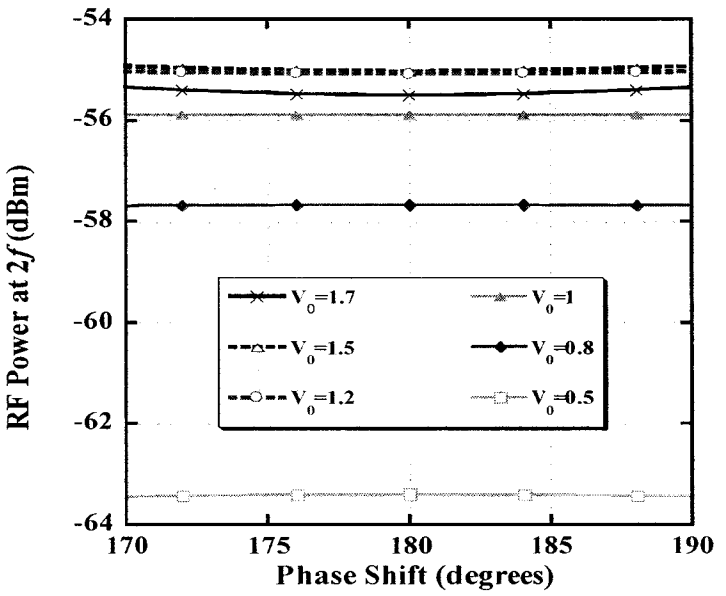

(c)

Figure 3.11 (a) Power ratio of the second-order to first-order harmonics versus phase shift (a) RF Power at $4f$ versus phase shift and (c) RF Power at $2f$ versus phase shift in similar configuration system, where V_{b1}=1.7369 V and V_{b2}=1.7 V.

3.4.2.4 Impact of Bias Shifting

In real experimental system, the values of V_{b1}, V_{b2} and V_0 would be changed due to the drifting problem which leads to the result that the value of bias voltages may not exactly the same as we want. So to verify sensitivity of the proposed system, variable ΔV changing from -1 to +1 V is added to both V_{b1} and V_{b2} in the simulation system. As examples, a set of solutions is chosen from Fig. 3.7 and simulation results are shown in Fig. 3.12. From the results, we can see that even if the bias voltages suffering a shift between -0.8 and 0.8 V, we still can get more than 20 dB suppression of the first order harmonic. This is because the suppression of the first-harmonics works in a range of the bias voltages, not only some special values. As a result, the system is really robust to the bias drifting.

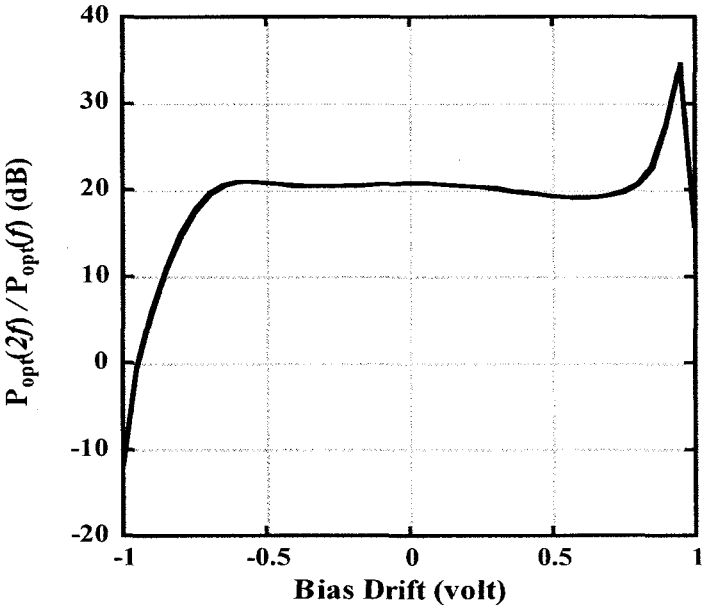

Figure 3.12 Power ratio of the second-order to the first-order harmonics versus the bias voltage for similar configuration system, where V_{b1} =1.7369 V, V_{b2} =1.7 V, and V_0 =1 V.

3.4.3 Case III: Use of Two Cascaded EAMs with Different Characteristics

In order to have better predication of mm-wave generation using two cascaded EAMs for frequency doubling and quadrupling, we consider two commercially available EAMs that will be used latter in the experimental proof of concept. Therefore, we first measured the transfer characteristic of an electro-absorption modulator integrated laser (EML) (1544. 14 nm) and an individual EAM. The measured normalized transfer characteristics are shown in Fig. 3.13 (a) and (b) for the EML and EAM. The coefficients, extracted by curve fitting according to Eq. (3.2), are listed in Table 3.1.

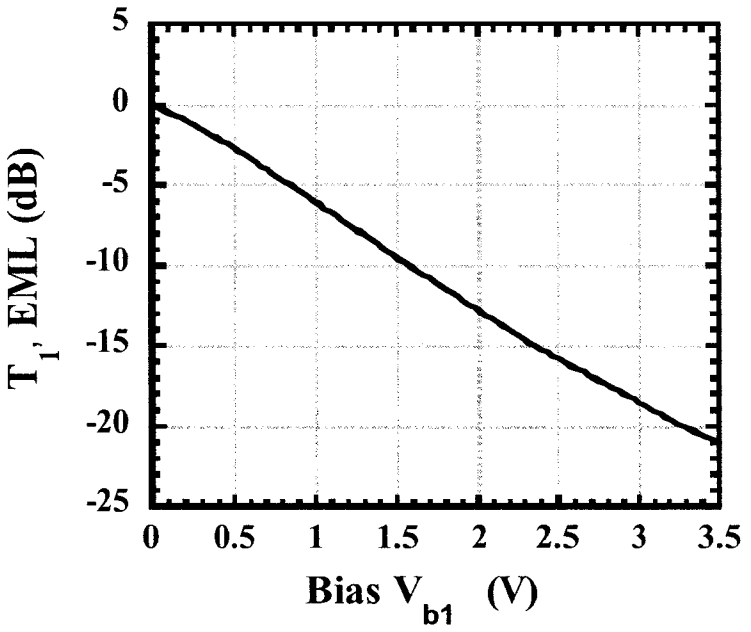

(a)

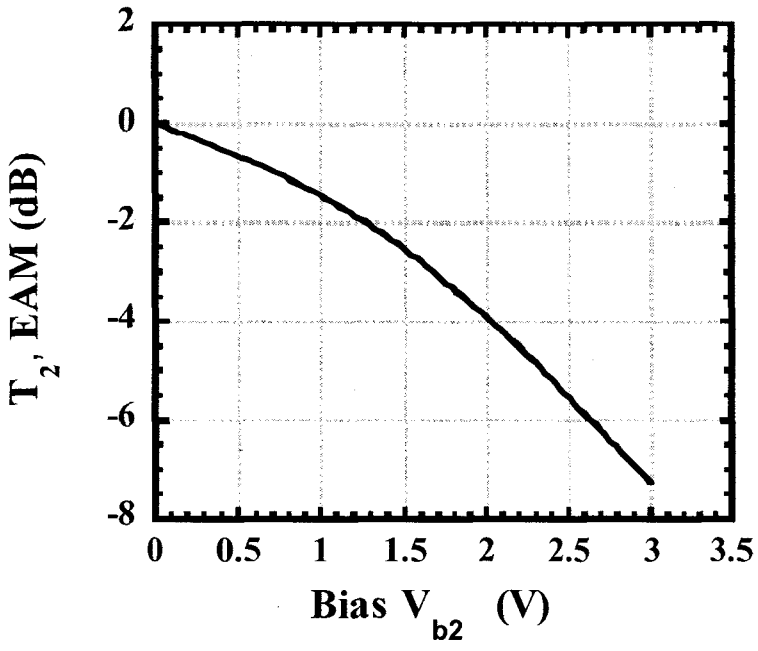

(b)

Figure 3.13 Measured transfer characteristics of (a) EML and (b) EAM.

Table 3.1. Extracted coeffients of two EAM transfer characteristics

k	0	1	2	3
a_k	-0.0021	-1.0597	-0.3731	-0.0757
b_k	-0.0018	-0.2013	-0.5115	1.0376
k	4	5	6	7
a_k	0.1879	0.0779	0.0137	-0.0009
b_k	-1.0817	0.5480	-0.1351	0.0130

3.4.3.1 The Optimum Phase Shift

We used our developed theoretical analysis in Section 3.3.2 to compute the optimum phase shift to minimize the first order optical sidebands (at $\pm f$) and maximize the second order optical sidebands (at $\pm 2f$) for given V_0, V_{b1} and V_{b2} of the two cascaded EAMs. We consider P_{in}=1mW, f = 6.1 GHz, V_0 = 0.5 and 1 V, and V_{b1} = 1 and V_{b2} = 3 V. Then, the optical power ratio of the second order sideband at $\pm 2f$ to the first, third and forth order

sidebands at $\pm f$, $\pm 3f$, and $\pm 4f$, respectively, can be calculated using Eq. (3.39) and simulated using VPI Transmission Maker [48]. Fig. 3.34 (a) and (b) shows the calculated (lines) and simulated results (marks) versus phase shift ϕ for V_0 = 0.5 and 1 V, respectively. It is clearly seen that a good agreement between the theory and simulation is obtained, and also 180° phase shift is found optimum that results in a maximum suppression of 18.3(18.2) dB and 39.5(21.8) dB of the first- and third order optical sidebands below the second order optical sidebands for V_0 = 0.5(1) V. Conversely, the fourth order optical sidebands are suppressed by 21(8.5) dB for V_0 = 0.5(1) V. This suggests that such a configuration is better for frequency doubling and quadrupling. In addition, with the increase of RF signal voltage the optical power of the fourth and third order sidebands are significantly increased.

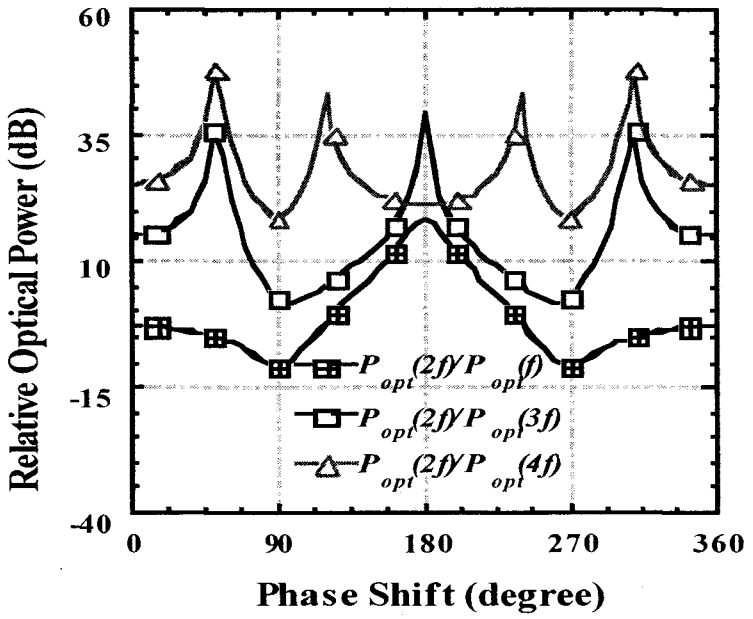

(a)

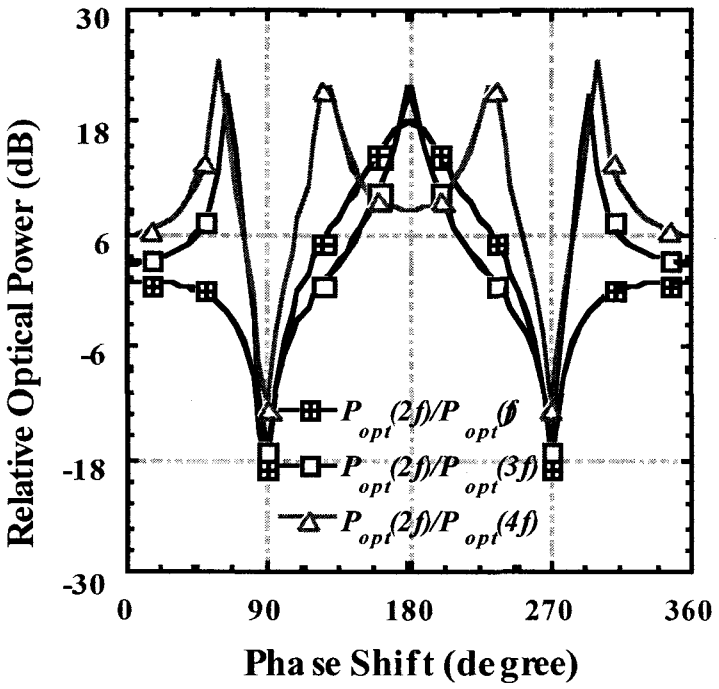

(b)

Firgure 3.14 Calculated (lines) and simulated (marks) ratio of optical power at $2f$ to optical power at f, $3f$ and $4f$ versus phase shift in different configuration system for V_0 of (a) 0.5 V and (b) 1 V. V_{b1} =1 V and V_{b2}=3 V.

3.4.3.2 The Impact of RF Modulation Voltage

To study the impact of RF modulation voltage, we set the phase shift to 180°, V_{b1}=1 V and V_{b2}=3 V, and then vary V_0. Fig. 3.15(a) shows the calculated (lines) (using Eq. (3.39)) and simulated (marks) optical power ratio of the second order sideband at $2f$ to first, third and fourth order sideband at f, $3f$ and $4f$, respectively, versus RF modulation voltage. It is shown from Fig. 3.15(a) that maximum suppression of 24.4 and 55.6 dB of first and third order optical sideband occurs at RF modulation voltage of 0.75 and 0.65 V, respectively, whereas the fourth order optical sideband increases monotonically with the RF modulation voltage. When V_0 is ~0.55 V all the first, third, and fourth order optical

sidebands are suppressed by more than 19.4 dB in power level below the second order optical sidebands. In this way, in-band distortions due to the contribution from beating between the undesired optical sidebands are reduced accordingly, and high purity mm-wave with frequency doubling and quadrupling can be realized. Fig. 3.15(b) shows the calculated (lines) (using Eq. (3.44)) and simulated (marks) RF power ratio of the generated signal at $2f$ (frequency doubling) and $4f$ (frequency quadrupling) to undesired component at f and $3f$, respectively, versus RF modulation voltage. For frequency doubling, the undesired RF component located at f can be suppressed by more than 22.7 dBc below the generated RF signal at $2f$ when V_0=0.7 V as shown in Fig. 3.15(b). On the other hand, for frequency quadrupling the undesired RF component at $3f$ is more than 47.9 dBc suppressed below the desired RF signal at $4f$ when V_0=0.5 V. Fig. 3.15(b) shows that the optimum RF modulation voltage is different for frequency doubling and quadrupling.

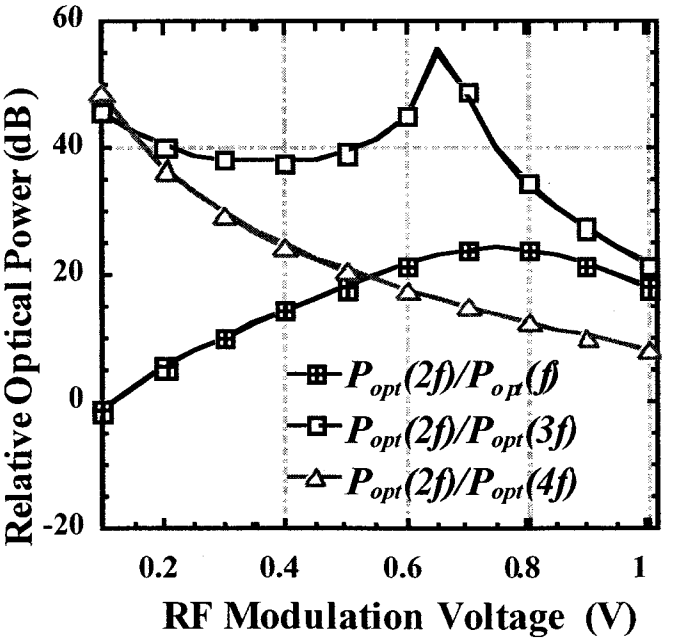

(a)

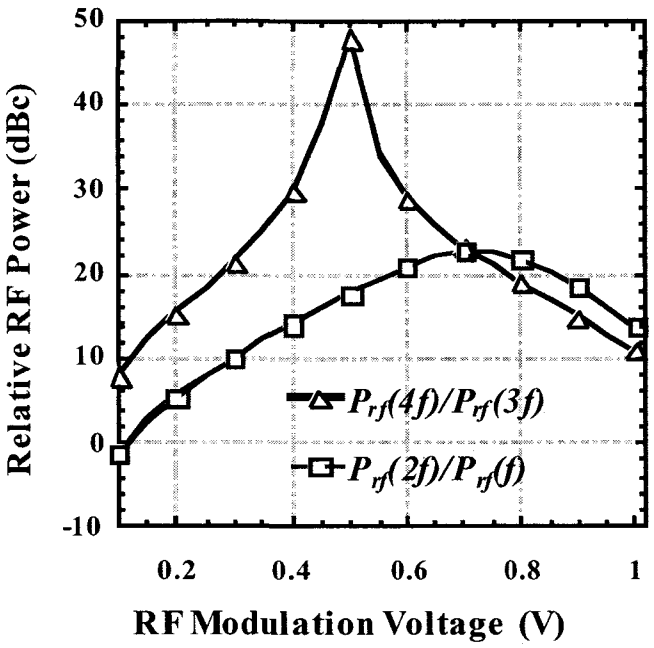

(b)

Figure 3.15 Calculated (lines) and simulated (marks) ratio of (a) optical power at $2f$ to that at f, $3f$ and $4f$ and (b) RF power at $2f$ and $4f$ to that at f and $3f$, respectively, versus RF modulation voltage in different configuration system. ϕ=180 degree, V_{b1} =1 V and V_{b2}=3 V.

3.4.3.3 The Impact of Bias Voltage

To investigate the impact of bias voltage, we set V_0= 0.5 V and V_{b1}=1 V, and sweep V_{b2} from 0 V to 3 V. Fig. 3.16 (a) and (b) shows the calculated (lines) and simulated (marks) relative optical and RF power versus bias voltage V_{b2}. It is shown that 50.8 and 39.5 dB maximum suppression of the first and third order optical sidebands can be achieved by setting V_{b2} to 1.2 and 3 V, respectively. The fourth order optical sideband is more than 21 dB suppressed blow second order sideband over the whole variation range of V_{b2} (0~3 V). Fig. 3.16 (b) shows that 38.9 and 47.9 dBc maximum suppression of the undesired RF component at f and $3f$, below the desired generated RF component at $2f$ and $4f$, can be achieved at V_{b2} = 1.2 V and 3V, respectively. At V_{b2} = 3 V the undesired RF component at f is suppressed by more than 17.7 dBc below the desired RF component at $2f$, whereas

at V_{b2} =1.2 V the undesired RF component at $3f$ is 10.9 dBc higher than the desired RF component at $4f$. This suggests that V_{b2} =1.2 and 3 V is optimum and results in high purity mm-wave generation by frequency doubling and quadrupling, respectively.

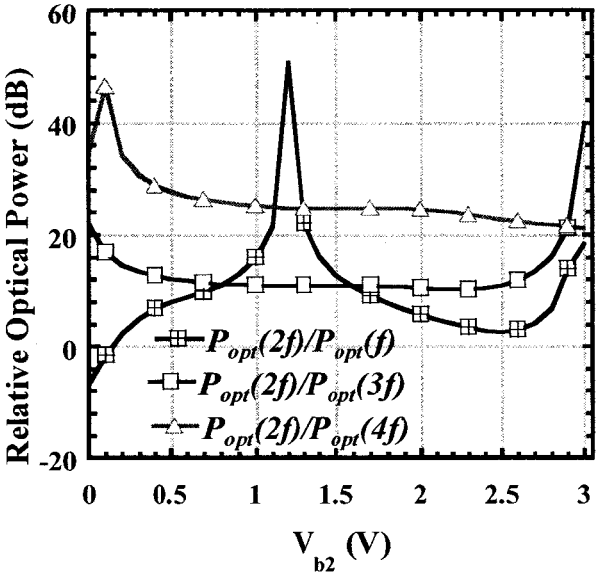

(a)

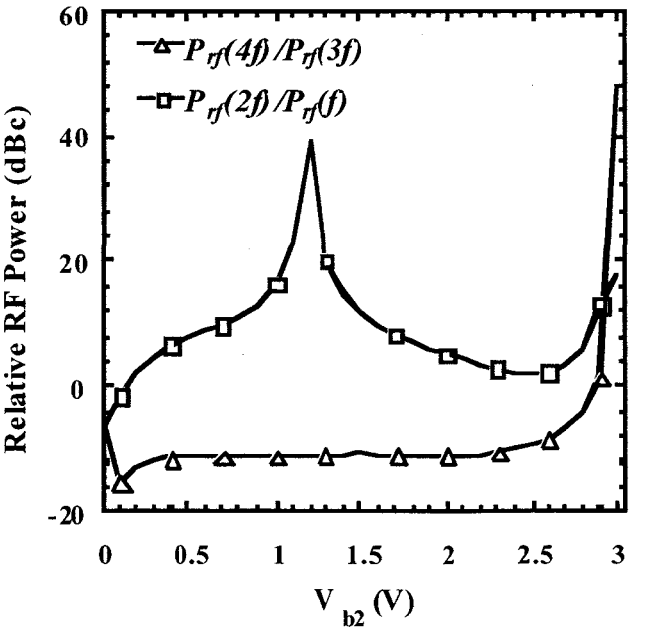

(b)

Figure 3.16 Calculated (lines) and simulated (marks) ratio of (a) optical power at $2f$ to that at f, $3f$ and $4f$, and (b) RF power at $2f$ and $4f$ to that at f and $3f$, versus bias voltage V_{b2} in different configuration system. ϕ = 180 degree, V_{b1} =1 V and V_0 =0.5 V.

3.4.3.4 Impact of Fiber Chromatic Dispersion

To investigate the impact of fiber chromatic dispersion on the system using two cascaded EAMs with different characteristics, Fig. 3.17 shows RF power at f, $2f$, $3f$ and $4f$ versus fiber length from 0 km to 20 km. To effectively investigate power fading caused by chromatic dispersion, we assume that other kinds of dispersions equal to 0. An optical filter with $5f$ bandwidth was used. The same as Case I and Case II, generated signal at $4f$ is almost immune to fiber chromatic dispersion. Comparing to signal at $4f$, signals at f, $2f$ and $3f$ suffer from power fading in different degree and period. The reason of periodical power fading is already discussed in Case I.

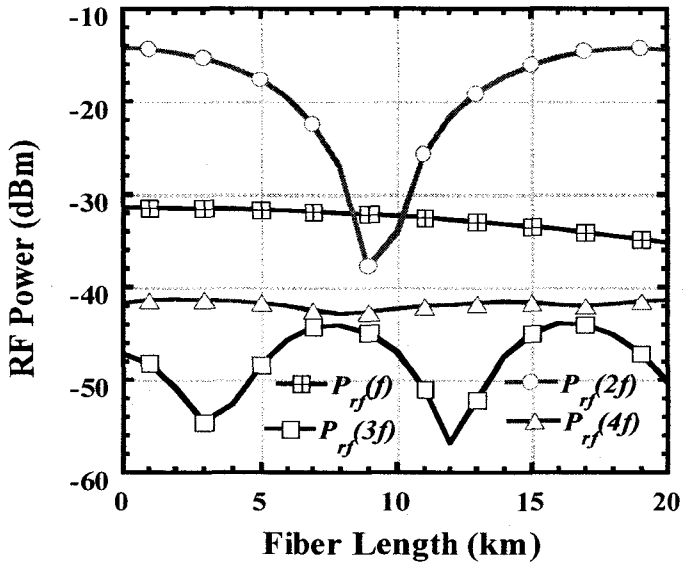

Figure 3.17 Simulated RF power at f, $2f$ and $3f$ and $4f$, versus fiber length in different configuration system. ϕ = 180 degree, V_0 = 0.5 V and V_{b1} =1 V and V_{b2}=3 V, Bandwidth of optical filter B = $5f$.

3.4.3.5 Impact of Phase Shifting and Bias Drifting

The same as in Case II, phase shifting and bias drifting should be investigated. The results are shown in Fig. 3.18 and Fig. 3.19 respectively. It is seen that RF power at $2f$ and $4f$ does not change with small (10 degree) phase shifting, because second-order optical sidebands and optical carrier (which is mainly contribution to currents at $2f$ and $4f$) don't change with small phase shifting either as discussed in Case II.

For bias drifting, as shown in Fig. 3.19, the suppression of the first-order sideband is influenced by bias drift. Fortunately, there is a flat range from 0 to 0.5 V drifting where suppression of first-order sideband is kept higher that 15 dB, which means that the system is robust to bias drifting.

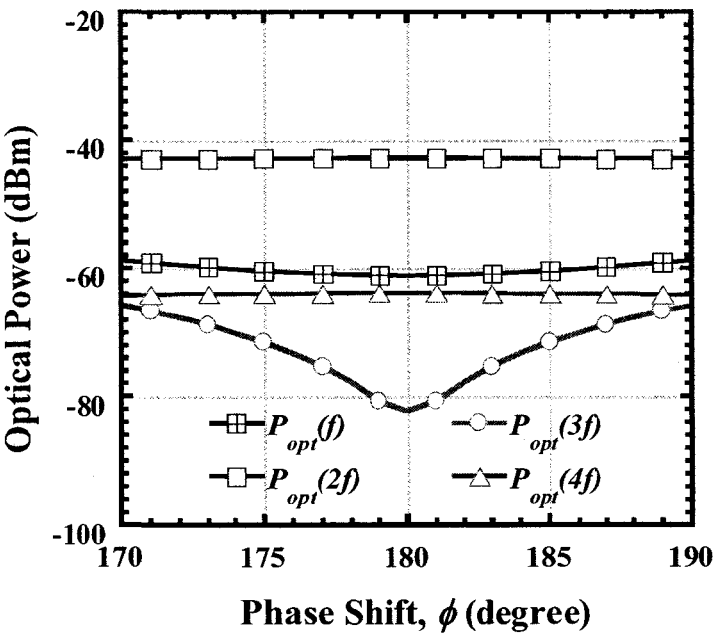

(a)

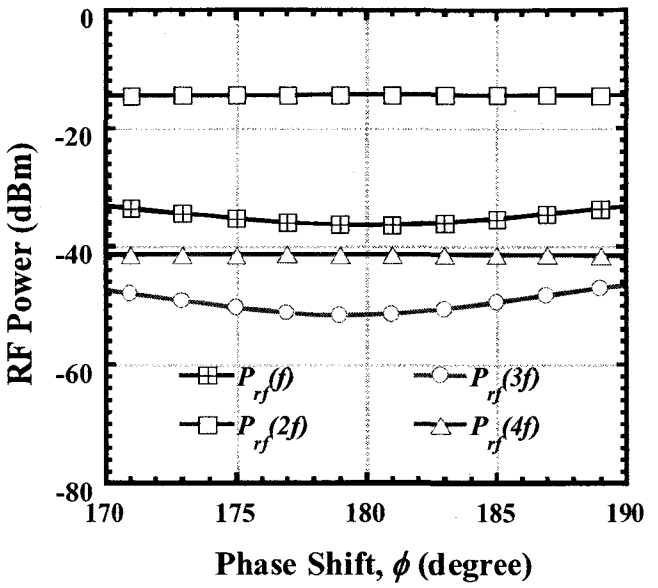

(b)

Figure 3.18 Simulated (a) optical power and (b) RF power at f, $2f$ and $3f$ and $4f$, versus 10 degree phase shifting in different configuration system, V_0 = 0.5 V and V_{b1} =1 V and V_{b2}=3 V, bandwidth of optical filter B = $5f$.

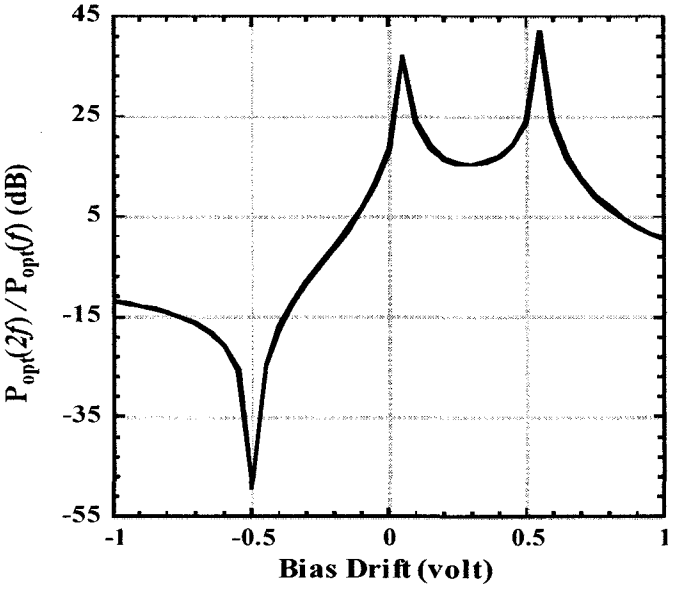

Figure 3.19 Optical power ratio of the second-order to the first-order harmonics versus the bias voltage in different configuration system. ϕ = 180 degree, V_0 = 0.5 V and V_{b1} =1 V and V_{b2}=3 V, bandwidth of optical filter B = $5f$.

3.5 Summary

In this chapter, theoretical analysis and the simulation results of the two-cascaded-EAM OFM systems are discussed. A comparison of the two cascaded-EAM systems and MZM systems is also shown in Table 3.2.

Overall, performance of the system of cascaded EAMs with identical/similar characteristics is much better than that of the system of cascaded EAMs with different characteristics, no matter from the robustness or the performance of the system. However, when two different EAMs are used, we can consider using a low cost EML as the first EAM and cascaded with an isolate EAM. As a result, the cost of the system is largely reduced since EMLs are very cheap (around five hundred dollars for one) compared with isolate EAMs (usually costing thousands of dollars).

Table 3.2 Comparison of the three cascaded-EAM systems and MZM systems

Techniques	Advantages	Disadvantages
Cascaded EAMs with the same characteristics	▪ Prefect suppression of odd-order harmonics; ▪ Immune to bias drifting and phase shifting; ▪ Robust System performance; ▪ Easy for optimization.	▪ Higher cost at the CS; ▪ Suffering from fiber chromatic dispersion. ▪ Hard to realize.
Cascaded EAMs with the similar characteristics	▪ High suppression of first-order harmonics; ▪ Immune to phase shifting; ▪ Robust to bias drifting;	▪ Higher cost at the CS; ▪ Suffering from fiber chromatic dispersion.
Cascaded EAMs with different characteristics	▪ Lower cost at the CS when cheap EML is used; ▪ Immune to phase shifting; ▪ Robust to bias drifting.	▪ Suffering from fiber chromatic dispersion.
Techniques using MZMs	▪ Simpler structure of the system at the CS when only one MZM is used; ▪ MZM not easy to be broken because of wider operating voltage.	▪ Working at the minimum or maximum point causing bias drifting problem; ▪ Suffering from fiber chromatic dispersion.

Chapter 4

Experimental Verification

4.1 Introduction

In the previous Chapter, the theory of the OFM technique using two cascaded EAMs is stated and verified by simulations. To further prove the proposed theory, an experimental verification using two cascaded EAMs with different characteristics will be introduced in this chapter.

This chapter is organized as follows. Experimental setup is given in Section 4.2, experimental results and discussion is presented in Section 4.3 and and the conclusions are drawn in Section 4.4.

4.2 Experimental Setup

Experimental setup for mm-wave generation using the proposed technique is shown in Fig. 4.1. A photograph of the experimental setup is shown in Fig. 4.2 that implement the block diagram of Fig. 4.1. In the experiment, a low cost EML (from JDSU) was cascaded with an individual EAM (from OKI). The laser source of the EML was biased at current of 90 mA and temperature was set to 25 ^{o}C to emit light at wavelength of 1544.146 nm. The total RF input power to the two cascaded EAMs was 7 dBm (V_0~0.5 V) at 6.1 GHz. The modulated signal was amplified, by an erbium doped fiber amplifier (EDFA), to 4.0 mW before it was transmitted through a 20 km of fiber with dispersion of 17 ps/nm/km

and an attenuation of ~0.25 dB/km. To reduce amplified spontaneous emission noise (ASE) the optical signal was filtered by a tunable filter of 0.55nm bandwidth. After photodetection, by a PIN diode of 35GHz bandwidth and 0.62 A/W DC responsivity, the generated RF signal was amplified by an LNA of 22 dB gain and noise figure of 2.6 dB. The measured characteristic transfer functions of the EML and EAM are given in Fig. 3.13 (a) and (b) respectively.

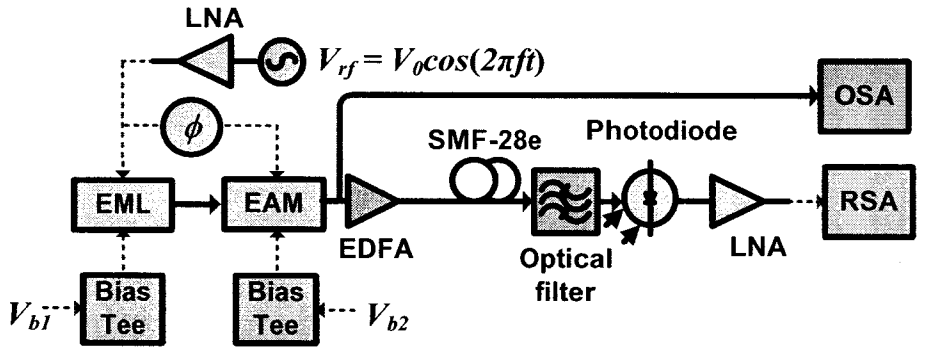

Figure 4.1 Experimental setup for mm-wave generation using the proposed technique.

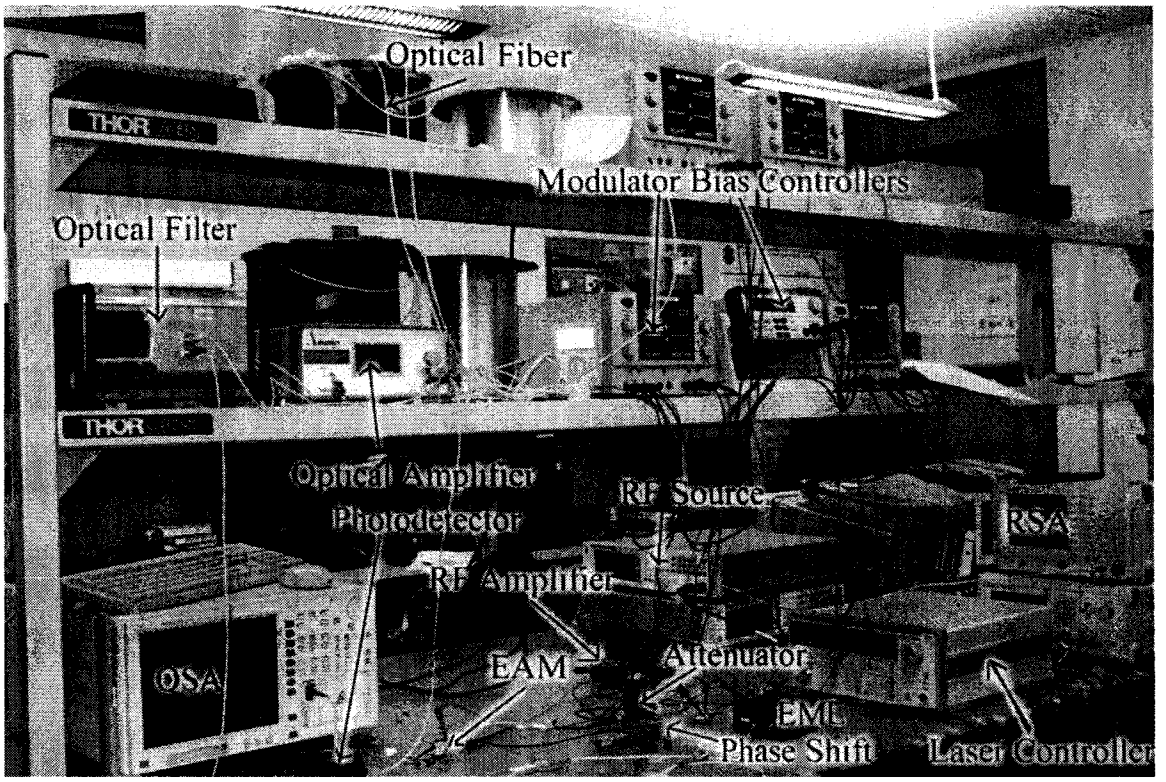

Figure 4.2 Photograph of experimental setup for mm-wave generation using the proposed technique.

4.3 Experimental Results and Discussion

By adjusting bias voltages of the two EAMs, optimum suppression of the first-order optical sidebands was achieved at bias voltage of the EML V_{b1}=~1 V and of the EAM V_{b2}=~3 V. It is found that the power of the second-order optical sidebands was enhanced with the increase of the input RF signal power. Furthermore, more suppression of the first-order optical sidebands can be achieved when the phase shift between the two cascaded EAMs was close to 180°. Fig. 4.3 (a) and (b) shows the measured optical before the EDFA and RF spectrum after the LNA using an optical and RF spectrum analyzer (OSA and RSA), respectively. For comparison, we also simulate the optical and RF

spectrum shown in Fig. 4.4 (a) and (b), respectively. The simulation set-up and system's parameters are identical to the ones used for experiment shown in Fig. 4.1.

Fig. 4.3(a) shows that the first-order optical sidebands are suppressed by ~12 dB below the second-order optical sidebands. However, this result is not as good as the expected of ~17.3 dB as shown in the simulated optical spectrum of Fig. 4.4 (a). One of the reasons is due to the imprecise manual tuning of bias voltage, phase shift and some voltage unbalance between the driving signals of the two EAMs as shown from the asymmetry of the optical spectrum. It is seen, from Fig. 4.3 (b), that the generated RF power at f (6.1 GHz), $2f$ (12.2 GHz), $3f$ (18.3 GHz) and $4f$ (24.4 GHz) is -33.880, -14.480, -50.670 and -44.36 dBm, which is in good agreement with the simulated RF power (see Fig. 4.4(b)) of -35, -14.2, -51 and -41dBm, respectively. This is due to the suppression of first and third-order optical sidebands and enhancement of the second-order optical sidebands. The RF power at 6.1 and 18.3 GHz is minimized while the RF power at 12.2 and 24.4 GHz is maximized. The generated RF signal at 24.4 GHz presents a signal to noise ratio of more than 25 dB. This suggests that the proposed technique is efficient for mm-wave generation using frequency doubling or quadrupling.

Compare the experimental results with the technique using MZM [7], our technique can generate much better doubling signal than technique in [7]. For frequency quadrupling, MZM can get higher quadrupling signal when it biases at MATB, and our system can achieve better quadrupling signal than the system of MZM working at MITB and QB.

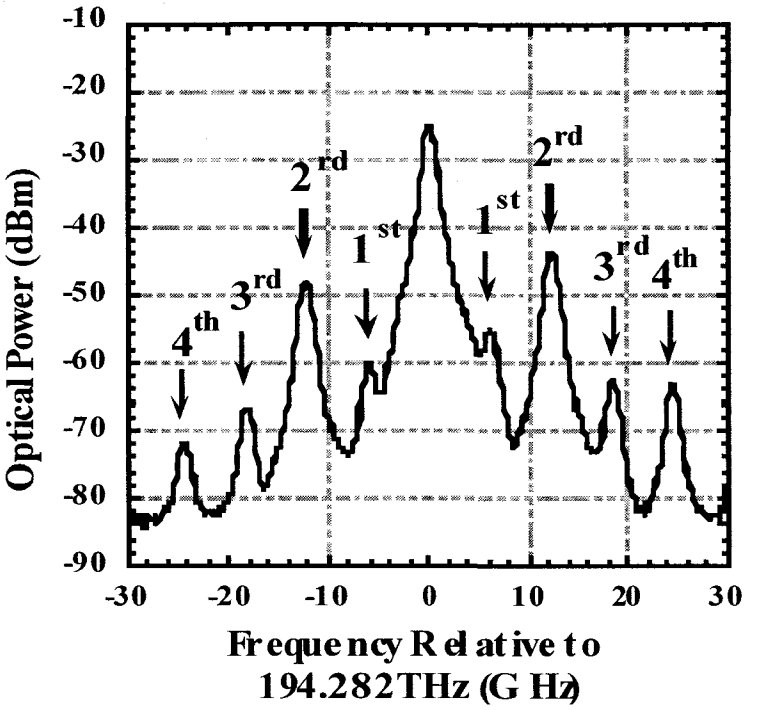

(a)

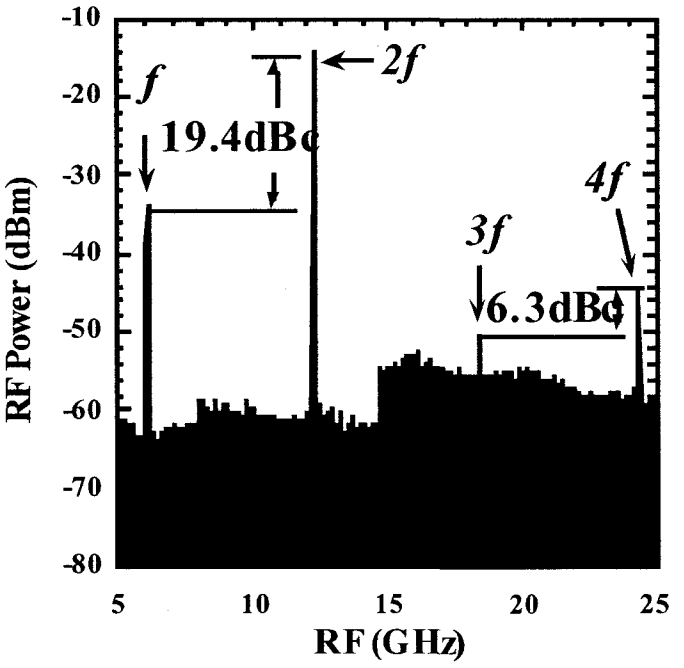

(b)

Figure 4.3 Measured (a) optical and (b) RF spectrum (resolution 100 kHz).

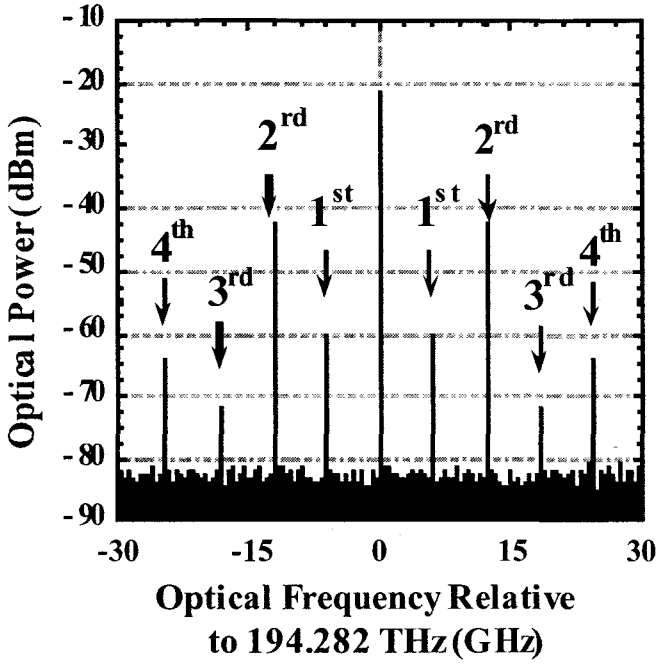

(a)

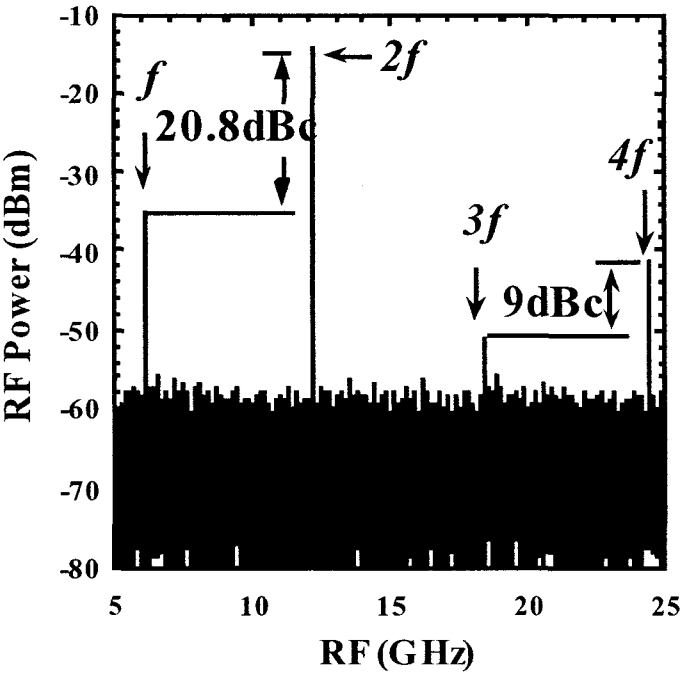

(b)

Figure 4.4 Simulated (a) optical and (b) RF spectrum. $\phi = 180^{o}$, $V_0 = 0.5$ V, $V_{b1}=1$ V and $V_{b2}=3$ V.

4.5 Summary

In this chapter, an experimental verification of the proposed technique is discussed. In this experiment, to generate mm-wave signal, EML was cascaded with an isolate EAM. 12dB suppression of first-order harmonic relative to second-order harmonic is achieved by adjusting phase shift, modulation index and bias voltages of the cascaded EAMs. This result is worse than the simulation result mainly due to the imprecise manual tuning of bias voltage, phase shift and some voltage unbalance between the driving signals of the two EAMs. A -14.480 dBm doubling signal and a -44.36 dBm quadrupling signal were generated while noise level was reasonable.

Chapter 5

Conclusion

5.1 Concluding Remarks

In this thesis, we have proposed and investigated a novel OFM technique for frequency doubling and quadrupling. This OFM technique, using two cascaded EAMs driven by a low frequency oscillator, can be used to generate mm-wave signals. By using two cascaded EAMs with identical characteristics, odd-order harmonics is suppressed and second-order harmonic is maximized; while two cascaded EAMs with different characteristics is used, the suppression of first-harmonic is achieved and second-order harmonic is maximized. So up-conversion efficiency of mm-wave frequency can be obtained with less impact of nonlinear distortion.

For the system of two cascaded EAMs with the same characteristics, the advantage of the system is that the odd-order harmonics is completely suppressed if the two EAMs are applied the same bias voltage and driven by the same RF input signal, which means that the high quality and high pure mm-wave signals can be generated with any level of RF input power and bias voltage in the working range compared with techniques using MZM modulator in which MZMs have to work at only the minimum or maximum point. Because of prefect suppression of the odd-order harmonics, we can simply achieve the optimum working point by sweeping bias voltage and input RF power to reach the highest second-order harmonics. Furthermore, it is possible to use this technique to generate $8f$ even higher mm-wave signal because it is found out that at some

work point forth-order or higher-even-order harmonics are really good while the second-order harmonics are suppressed relative to the higher-even-order harmonics. However, because of the 180 degree phase shift, the system suffers terrible fiber dispersion effects in transmissions of some lengths of fiber, and in these cases, optical filter should be used to filter out optical harmonics higher than second order.

For the system of two cascaded EAMs with different characteristics, the first-order harmonic is still suppressed pretty well when it is biased at some points. However, it really depends on the transfer functions of the two cascaded EAMs. If the transfer functions of EAMs are changed, the optimum point may also change. So it is very important to choose proper EAMs with certain characteristics to get better performance. It is found that the optimum phase shift is 180 degree. As the system of cascaded EAMs with identical characteristics, the system suffers chromatic-dispersion-induced power fading too.

The proposed techniques have many benefits. Firstly, in the system of cascaded EAMs with identical characteristics, odd-order optical harmonics are completely suppressed. For the system using cascaded EAMs with similar characteristics, more than 40 dB suppression of first-order harmonic relative to second-order harmonic can still be achieved. As a result, these techniques are cost-effective since the high quality and high pure optical mm-wave signal is generated at the CS, transmitted over low-loss fiber link, and converted to electrical mm-wave signal using a low-cost photodetector at the simple BS.

Secondly, another advantage of the proposed systems, compared with the systems using MZM as external modulator, is that the proposed systems are very robust to bias

drifting problem. In frequency quadrupling techniques based on MZM [3-5], to suppress even-order or odd-order optical sidebands, MZM is biased at the minimum or maximum point of transfer function, resulting in the bias drifting problem. While, in the techniques using two-cascaded EAMs, a range of modulator bias voltages can be chosen, rather than just one or two working point. As a result, even bias drifting happens, good suppression of odd-order or first-order harmonics can still be achieved.

Furthermore, when a low-cost EML cascaded with an isolate EAM, the cost of the CS is also reduced and the structure of the system is simpler. This technique is already verified by experiments. In the experiment, the low RF signal at 6.1 GHz was modulated by the cascaded EML and EAM. We got more than 12 dB suppression of the first-order harmonic relative to the second-order harmonic, which is lower than results got from theory and simulation the imprecise manual tuning of bias voltage and phase shift. -14.480 dBm doubling signal and -44.36 dBm quadrupling signal is generated at 12.2 GHz and 24.4 GHz respectively which is close to our predicted results.

However, as many other OFM techniques using external modulators, the proposed system suffers fiber chromatic dispersion effects. To deal with this problem, an optical filter is used to filter out third- and higher-order optical harmonics when signals are transmitted over a fiber, so generated quadrupling signal is almost immune to fiber dispersion. Simulations based on VPI Transmission Maker have verified the proposed theories pretty well.

5.2 Future Works

It is the first time that two-cascaded-EAMs structure is used to generate mm-wave signals. However, this is just only a start but not the end. There are still many jobs to be done for this research.

Firstly, some experiments haven't been done because of limited experiment components. The system using two cascaded EAMs with identical characteristics will be verified by experiments once we can get two EAMs exactly the same or with similar characteristics. The experiment of UWB transmission using the proposed system will be finished in continuing research too.

Secondly, the optimization of the system should be discussed in the further jobs. In this thesis, we only considered optimizing the system by sweeping the RF modulation index and bias voltages of the two EAMs while the transfer functions of the EAMs are fixed. In fact, it is possible that we can design EAMs with the optimum transfer functions to improve the system performance. Furthermore, methods used to deal with drifting problems in the proposed system should also be investigated in future.

Thirdly, Bi-directional transmission over fiber is another important issue that needs to be investigated in future. The issues of up conversion and down conversion should be addressed simultaneously for more reasonable resource distribution and cost efficiency.

5.3 List of Publications

L. Wu, B. Hraimel, X. Zhang, M. Mohamed, K. Wu et al., "Photonic generation of millimeter-waves using two cascaded electro-absorption modulators in radio-over-fiber systems," *Proceedings of IEEE Topic meeting on Microwave Photonics 2010*, Montreal, Canada.

C. Sui, B. Hraimel, X. Zhang, L. Wu, K. Wu et al., "Performance of MB-OFDM ultra-wideband signals over fiber transmission using a low cost electro-absorption modulator integrated laser," (*Submitted to IEEE/OSA Journal of Lightwave Technology,2010*)

References

[1] X. Zhang, B. Liu, J. Yao, K. Wu, and R. Kashyap, "A novel millimeter-wave-band radio-over-fiber system with dense wavelength-division multiplexing bus architecture," *IEEE Trans. Microwave Theory Tech.*, vol 54, no. 2, Feb. 2006.

[2] Z. Xu, X. Zhang, and J. Yu, "Frequency upconversion of multiple RF signals using optical carrier suppression for radio over fiber downlinks," *Optics Express*, vol.15, no.10, Dec. 2007.

[3] M. Mohamed, X. Zhang, B. Hraimel and K. Wu, "Analysis of frequency quadrupling using a single Mach-Zehnder modulator for millimeter-wave generation and distribution over fiber systems," *Opt. Express*, vol.16, no.14, Jul. 2008.

[4] L. Xu, C. Li, C. W. Chow, and Hon Ki Tsang, "Optical mm-wave signal generation by frequency quadrupling using an optical modulator and a silicon microresonator filter," *IEEE Photon. Tech. Lett.*, vol. 21, no. 4, Feb. 2009.

[5] C. Lin, P. Shih, J. Chen, etc., "Optical millimeter-wave up-conversion employing frequency quadruplihng without optical filtering," *IEEE Trans. Microwave Theory Tech.* vol. 57, no. 8, Aug. 2009.

[6] J. Li, Y. Liang, and K. K. Wong, "Millimter-wave UWB signal generation via frequency up-conversion using fiber optical parametric amplifier," *IEEE Photon. Tech. Lett*, vol. 21, no. 17, Sep. 2009.

[7] M. Mohamed, B. Hraimel, X. Zhang, and K. Wu, "Efficient photonic generation of millimeter-waves using optical frequency multiplication in radio over fiber systems," *Proceedings of IEEE Topic meeting on Microwave Photonics 2007*, paper Th.-4.20, Victoria, Canada.

[8] Abuelma'att, M. T. "Large-signal performance of the serially cascaded electroabsorption modulator," *Fiber and integrated Optics*. vol.24, no.2, 2005.

[9] J. Seo, C. Choi, Y. Kang, etc., "SOA–EAM frequency up/down-converters for 60-GHz bi-directional radio-on-fiber systems," *IEEE Trans. Microwave Theory Tech.* vol. 54, no. 2, Feb. 2006.

[10] L. Chen, Y. Shao, X. Lei, etc., "A novel radio-over-fiber system with wavelength reuse for upstream data connection," *IEEE Photon. Tech. Lett.*, vol. 19, no. 6, Mar. 15, 2007.

[11] J. Ma, X. Xint, C. Yut, ect., "Millimeter-wave optical subcarrier generation by using an external modulator and optical carrier suppression," *9th International Conference on Transparent Optical Networks 2007 (ICTON'07)*, Jul. 2007.

[12] T. Kuri, K. Kitayama, and Y. Takahashi, "A single light-source configuration for full-duplex 60-GHz-band radio-on-fiber system," *IEEE Trans. Microwave Theory Tech.*, vol. 51, no. 2, Feb. 2003.

[13] M. Memon, G. Mezosi, B. Li, etc., "Generation and modulation of tunable mm-wave optical signals using semiconductor ring laser," *IEEE Photon. Tech. Lett.*, vol. 21, no. 11, pp. 733-735, Jun. 1, 2009

[14] C. Hong, M. Li, C. Zhang, etc., "Millimeter-wave frequency tripling based on four-wave mixing in sideband injection locking DFB lasers," *International Conference on Microwave and Millimeter Wave Technology, 2008 (ICMMT'08)*, vol. 2, pp. 876-877, April 2008.

[15] J. Yu, J. Gu, X. Liu, Z. Jia, and G. Chang, "Seamless integration of an 8×2.5 Gb/s WDM-PON and radio-over-fiber using all-optical up-conversion based on Raman-assisted FWM," *IEEE Photon. Technol. Lett. 17 (2005)*, pp. 1986–1988.

[16] J. Yao, "Microwave photonics," *J. Lightwave Technol.*, vol. 27, no. 3, Feb. 1, 2009.

[17] S. Sohn and S. Han, "Linear optical modulation in a serially cascaded electroabsorption modulator," *Microwave. Opt. Technol. Lett.*, vol. 27, no. 6, Dec. 20, 2000.

[18] M. Mohamed, B. Hraimel, X. Zhang, ect., "Frequency quadrupler for millimeter-wave multiband OFDM ultrawideband wirless signals and distribution over fiber systems," *J. Opt. Commun. Netw.*, vol. 1, no. 5, Oct. 2009.

[19] ECMA-368, High rate ultra wideband PHY and MAC standard, ECMA International, Geneva, 2nd edition, Dec. 2007.

[20] M.N. Sakib, B. Hraimel, X. Zhang and etc., "Impact of optical transmission on multiband OFDM ultra-wideband wireless system with fiber distribution," *J. Lightwave Technol.*, vol. 27, no. 18, Sep. 15, 2009

[21] B. Hraimel, X. Zhang, M. Mohamed and K. Wu, "Precompensated optical double-sideband subcarrier modulation immune to fiber chromatic-dispersion-induced radio frequency power fading," *J. Opt. Netw.*, vol. 1, Issue 4, pp. 331-342.

[22] A.M.J. Koonen, M. García Larrodé, A. Ng'oma and etc., "Perspectives of radio over fiber technologies," *Optical Fiber communication/National Fiber Optic Engineers Conference*, 2008, pp. 1-3

[23] D. Opatic, "Radio over fiber technology for wireless access," Ericsson.com

[24] M. Mohamed, "Photonics generation and distribution of millimeter-wave signals using optical frequency multiplication for radio over fiber systems," Ph.D. Thesis, Concordia University, 2009

[25] U. Gliese, S. Norskov, and T. N. Nielsen, "Chromatic dispersion in fiber-optic microwave and millimeter-wave links," *IEEE Trans. Micro. Thy. Tech.*, vol. 44, pp. 1716-1724, 1996.

[26] R. Hofstetter, H. Schmuck, and R. Heidemann, "Dispersion effects in optical millimeter-wave systems using self-heterodyne method for transport and generation," *IEEE Trans. Micro. Thy. Tech.*, vol. 43, pp. 2263-2269, 1995.

[27] A. Ng'oma, "Radio-over-fibre technology for broadband wireless communication systems," Ph.D. Thesis, the Eindhoven University of Technology, 2005

[28] D. Wake, and K. Beachman, "A novel switched fibre distributed antenna system," *Proceedings of European Conference on Optical Communications (ECOC'04)*, vol. 5, 2004, pp. 132 – 135.

[29] D. K. Mynbaev and L. L. Scheiner, "Fiber optic communications technology," Prentice Hall, New Jersey, 2001.

[30] C. Liu, A. Seeds, J. Chadha, P. Stavrinou, etc. "Bi-directional transmission of broadband 5.2GHz wireless signals over fiber using a multiple-quantum-well asymetric fabry-perot modulator/photodetector", *Proceedings of the Optical Fiber Communications (OFC) Conference. 2003*, Vol. 2, pp. 738 – 740.

[31] L. Goldberg, R. D. Esman, and K. J. Williams, "Generation and control of microwave signals by optical techniques," *Optoelectronics, IEE Proceedings J,* vol. 139, pp. 288-295, 1992.

[32] A. Stöhr, R. Heinzelmann, A.Malcoci and D. Jäger, "Optical heterodyne millimeter-wave generation using 1.55-μm traveling-wave photodetectors," *IEEE Trans. Micro. Thy. Tech.*, Vol. 49, No. 10, Oct. 2001

[33] S. Kobayashi and T. Kimura, "Optical phase modulation in an injection locked AlGaAs semiconductor laser," *Electron. Lett.*, vol. 18, pp. 210-211, 1982

[34] R. C. Steele, "Optical phase-locked loop using semiconductor laser diodes," *Electron. Lett.*, vol. 19, pp. 69-71, 1983

[35] Y. Katayama and B. Gaucher, "One-minute introduction to mm-wave technology and applications", IBM Research

[36] Federal Communications Commission Office of Engineering and Technology, "Millimeter wave propagation: spectrum management implications" July 1997.

[37] J. J. O'Reilly, P. M. Lane, R. Heidemann, and R. Hofstetter, "Optical generation of very narrowlinewidth millimeterwave signals," *Electron. Lett.*, vol. 28, no. 25, pp. 2309–2311, 1992.

[38] J. J. O'Reilly and P. M. Lane, "Fiber-supported optical generation and delivery of 60 GHz signals," *Electron. Lett.*, vol. 30, no. 16, pp. 1329–1330, 1994.

[39] J. O'Reilly and P. Lane, "Remote delivery of video services using mm-waves and optics," *J. Lightwave Technol.*, vol. 12, pp. 369-375, 1994.

[40] J. J. O'Reilly, P. M. Lane, and M. Capstick, "Optical generation and delivery of modulated mm-waves for mobile communications," in *Analogue Optical Fibre Communications*, B. Wilson, Z. Ghassemlooy, and I. Darwazeh, Eds. London: The Institute of Electrical Engineers, 1995.

[41] W. Jiang, C. Lin, H. Huang, and etc., "Experimental demonstration of a novel filterless frequency quadrupling technique for colorless WDM millimeter-wave up-conversion systems," *Conference on Optical Fiber Communicatio*n, pp.1-3, 2009.

[42] G. Qi, J. P. Yao, J. Seregelyi, C. Bélisle, and S. Paquet, "Optical generation and distribution of continuously tunable millimeter-wave signals using an optical phase modulator," *J. Lightw. Technol.*, vol. 23, no. 9, pp. 2687–2695, Sep. 2005.

[43] Z. Jia, J. Yu, D. Boivin, M. Haris, and G. K. Chang, "Bidirectional ROF links using optically up-converted DPSK for downstream and remodulated OOK for upstream," *IEEE Photon. Technol. Lett.*, vol. 19, pp. 653-655, 2007.

[44] A. J. Cooper, "Fiber/Radio for the provision of cordless/mobile telephony services in the access network," *Electron. Lett.*, vol. 26, no. 24, pp. 2054-2056, Nov. 1990.

[45] M. N. Sakib, B. Hraimel, X. Zhang and etc., "Impact of optical transmission on multiband OFDM ultra-wideband wireless system with fiber distribution," *J. Lightw. Technol.*, vol. 27, iss. 18, pp. 4112-4123, 2009

[46] B. Kalantari-Sabet, M. Mjeku, N. J. Gomes and etc., "Performance impairments in single-mode radio-over-fiber systems due to MAC constraints," *J. Lightw. Technol.*, vol. 26, no. 15, Aug. 1, 2008

[47] http://www.fiberoptics4sale.com.

[48] http://www.vpiphotonics.com, April 2009.